



Activity Report
2017

| | | |
|------------|---|-----------|
| 1 | Introduction | 4 |
| 2 | ITER Project | 6 |
| 2.1 | <i>Activity for the development of Neutral Beam Injectors for ITER.....</i> | <i>6</i> |
| 2.1.1 | PRIMA | 8 |
| 2.1.2 | SPIDER..... | 13 |
| 2.1.3 | MITICA | 29 |
| 2.1.4 | Vacuum high voltage holding modeling and experiments..... | 42 |
| 2.1.5 | RF R&D..... | 43 |
| 2.1.6 | Development and test of Caesium Ovens | 46 |
| 2.1.7 | Host Activities..... | 47 |
| 2.2 | <i>ITER Modelling.....</i> | <i>50</i> |
| 2.2.1 | M3D code validation on JET data | 51 |
| 2.2.2 | Magnetic topology reconstruction | 53 |
| 2.3 | <i>ITER Diagnostics</i> | <i>54</i> |
| 2.3.1 | ITER core Thomson scattering..... | 54 |
| 2.3.2 | Diagnostic systems Engineering Services | 55 |
| 3 | EUROfusion Programme | 58 |
| 3.1 | <i>RFX-mod: experimental, modeling activities and upgrades.....</i> | <i>58</i> |
| 3.1.1 | Introduction..... | 58 |
| 3.1.2 | Helical states..... | 59 |
| 3.1.3 | Transport studies..... | 60 |
| 3.1.4 | Fast particle dynamics studies..... | 61 |
| 3.1.5 | MHD and magnetic equilibrium active control | 62 |
| 3.1.6 | Plasma-wall interaction | 63 |
| 3.1.7 | Edge physics, new analysis and developments | 64 |
| 3.1.8 | Plasma-beam interaction studies..... | 65 |
| 3.1.9 | Electrical model of RFP applied to the design of vacuum components in RFX-mod2 65 | |
| 3.1.10 | Diagnostic upgrades | 66 |
| 3.1.11 | Design of machine modifications | 68 |
| 3.1.12 | RFP as neutron source for a fusion-fission hybrid..... | 71 |
| 3.2 | <i>MST1 and ITER Physics Work Packages(Valisa 15p).....</i> | <i>74</i> |
| 3.2.1 | MST1- Medium-Size Tokamak Campaigns | 75 |
| 3.2.2 | JET1 - JET Campaigns | 80 |
| 3.2.3 | Task 17-02. Development and integration of a real-time state observer for plasma state monitoring..... | 80 |
| 3.2.4 | WPS1/2 - Preparation and Exploitation of W7-X Campaigns/Stellarator optimization | 84 |
| 3.2.5 | WPISA - Infrastructure support activities..... | 87 |
| 3.2.6 | WPSA - Preparation of exploitation of JT-60SA..... | 87 |
| 3.3 | <i>ITER NBI Physics activities and accompanying program</i> | <i>90</i> |

| | | |
|------------|---|------------|
| 3.3.1 | Operation of NIO1 | 90 |
| 3.3.2 | Development of alternative ion source (Enabling Research)..... | 91 |
| 3.3.3 | Magnetic configuration | 93 |
| 3.3.4 | Pressures, flux and final configuration | 94 |
| 3.3.5 | Numerical simulation including space charge compensation | 96 |
| 3.3.6 | Plasma characterization by Energy Analyzer on NIO1..... | 98 |
| 3.3.7 | International collaborations | 99 |
| 3.4 | <i>PPPT Projects</i> | 101 |
| 3.4.1 | WPHCD - Heating and Current Drive systems | 101 |
| 3.4.2 | WPDC – Diagnostic and Control | 102 |
| 3.4.3 | WPPMI - Plant Level System Engineering, Design Integration and Physics Integration Plant Electrical System Design..... | 103 |
| 3.4.4 | WPMAG - Magnet system | 105 |
| 3.4.5 | WPTFV Tritium, Fuelling and Vacuum | 106 |
| 3.4.6 | WPSES - Socio Economic Studies..... | 107 |
| 4 | Broader Approach | 109 |
| 4.1 | <i>Contribution to the JT-60SA tokamak</i> | 109 |
| 4.1.1 | Power supply system for in-vessel sector coils for RWM control | 109 |
| 4.2 | <i>Remote participation</i> | 112 |
| 5 | Industrial Collaborations | 112 |
| 5.1 | <i>Model for the electrostatic design a new VCB prototype</i> | 112 |
| 5.2 | <i>Biomedical plasma applications</i> | 113 |
| 6 | Education, Training and Information to the public | 115 |
| 6.1 | <i>Education and Training</i> | 115 |
| 6.1.1 | International Doctorate in Fusion Science and Engineering | 115 |
| 6.1.2 | Other education and training activities..... | 116 |
| 6.2 | <i>Information to the public</i> | 117 |
| 6.2.1 | Production of information content | 117 |
| 6.2.2 | Outreach and communication initiatives. | 118 |
| 6.2.3 | Events and media coverage..... | 119 |

1 Introduction

The 2017 activities developed along the guidelines of the Activity Programme of Consorzio RFX, evaluated by Scientific-Technical Committee on 10 November 2016, was approved by the Consorzio RFX partners in the meeting on 29 November 2016. This introduction briefly highlights the main achievements of the year, while a more complete presentation is found in following chapters.

The main milestones reached in 2017 are:

- The commissioning of SPIDER started with test on individual and integrated subsystems, despite the late delivery of the Beam Source in late October 2017.
- All the JADA in-kind contribution for MITICA has been delivered and approximately 90% of the installation activities have been completed. The one year delay in the delivery of the MITICA vessel had a significant impact on the completion of the PS and TL installations and on the start of commissioning.
- The PRIMA infrastructures have been almost completed and in particular the MV connection to the 400 kV power substation.
- The RFX-mod2 design has been finalized in most of the details and a proposal to obtain funds under the POR-FESR European scheme for regional development support has been submitted in November 2017.
- The Broader Approach activities entailed the test of the prototype PS to feed the RWM coils in JT-60SA, an essential step before starting the series production of the 18 PS. In addition, the Consorzio RFX has answered the Call for Interest issued by EUROfusion to host the European REC (Remote Experimentation Center) to operate JT-60SA.
- The participation to the preparation of the ITER operation continued both through direct ITER activities and with contributions to the EUROfusion activities of the ITER department. Extensive participation to both experimental, modelling and data analysis activities on JET and on the other MST devices also continued.
- The physics activities on the RFP configuration, inclusive of aspects of direct relevance to tokamaks and stellarators, progressed significantly in several theoretical and modelling areas, such as studies on helical states, transport, fast particle dynamics, MHD magnetic equilibria and active control, plasma-wall interaction and beam-plasma interaction, as well as in the development of diagnostics.

- Good progress was also achieved in the contribution to the development of the DEMO project under PPPT in four main areas: NBI design, Power Supplies, diagnostics and Socio Economical Studies.
- The education and public information activities continued to have an important role, primarily by hosting many students during internships, bachelor and master thesis. The important direct education activity on the European PhD on Fusion Science and Engineering entailed the agreement of a new collaborative scheme involving Padova University and Ghent University (Belgium). The public information activities have seen this year important steps such as recording the development of PRIMA and SPIDER installations in collaboration with F4E and IO, actively participating in the call for funding for RFX-mod2, organizing public events and developing traditional and innovative communication tools.
- Technology transfers to other scientific and technology fields resulting from R&D on high voltage holding in vacuum and on cold plasma source prosecuted with significant external interest.
- In 2017, 125 papers have been published in International Journals, including 47 papers submitted by partner laboratories. There have been participations to 30 National and International Workshops and Conferences. 70 Abstract have been submitted to 17 Workshops and Conferences and 50 Articles submitted to 13 International Conferences will be published on Proceedings or Journal Special Issues.
- Scientific and Technology supporting activities to most of the above mentioned activities have been widely performed and are described in the report.

2 ITER Project

2.1 Activity for the development of Neutral Beam Injectors for ITER

The activities for the development of the Neutral Beam Test Facility (NBTF), including those of the third parties, are done in the framework of the existing agreements among ITER, F4E and Consorzio RFX ¹.

The main activities performed in 2017 by NBTF Team and third parties were:

- *Construction supervision* for the completion of PRIMA buildings and auxiliaries, including the plant commissioning, to be ready to host the experimental plants.
- *Design* of controls, diagnostics, protection and safety systems. The activity includes the preparation of the documentation for the call for tenders.
- *R&D activities* for experimental qualification of critical items finalised to the confirmation of the design choices. The activities have been performed with the support of the HV Test Facility (HVPTF), RF and Caesium Test Stands.
- *Technical follow up* of procurement contracts from the call for tender phase, issued by F4E, up to the installation, including factory and site acceptance tests.
- *Interface management* among buildings/plants/components to guarantee the coherence of the overall design. To guarantee proper integration between experimental plants and PRIMA buildings, a full 3D integrated CAD model was developed and continuously updated.
- *Management* of the contract for the installation of JADA components and of the overall installation activities on-site.
- *Procurement* by Consorzio RFX of plants or components for the Facility, e.g. HV Bushing supporting structure (HVBSS).

During 2017 there was a considerable commitment of human resources to follow-up procurements, in particular SPIDER Beam Source, MITICA VV and Cooling plant, to prepare and perform activities on SPIDER BS after delivery on-site, to perform the integrated commissioning of SPIDER PS's and auxiliary plant, to support different suppliers in on-site activities and plant integrations including JADA and INDA.

Finally, work has been entailed by third Framework Contract which assigned to Consorzio RFX the assembly and completion activities: the HV Bushing Support

¹ V. Toigo, et al. "The PRIMA Test Facility: SPIDER and MITICA test-beds for ITER neutral beam injectors" New J. Phys. 19 (2017) 085004, <https://doi.org/10.1088/1367-2630/aa78e8>

Structure (HVBSS) has been procured and installed and several activities to recover defects present on the SPIDER Beam Dump (BD) before his installation on the SPIDER VV were performed.

The assembly activities of the SPIDER BS at Fives Nordon premises in Nancy had been stopped in 2016 as consequence of several ongoing issues on parts to be assembled. Strong effort was spent in 2017 by NBTf Team to follow-up all the recovery, assembly and test activities in supplier and sub-supplier premises. On 26th October SPIDER BS was delivered on-site and taken in charge by NBTf Team to perform all activities to correctly install it inside the vacuum vessel: all inspections, pressure, leak and electrical tests were performed. The installation inside the VV will follow in January 2018.

As regards the SPIDER PS, during 2017 most of the systems have been completed with Site Acceptance Test (SAT): the High Voltage Deck and Transmission Line, the Ion Source and Extraction Grid Power Supply. While the supply by INDA of the Acceleration Grid PS (AGPS) suffered various difficulties of both administrative and organizational nature, so that installation activities took much longer than expected.

Auxiliary plant systems including Vacuum and Gas Injection system, Cooling plant system and Medium Voltage grid necessary to operate SPIDER have been completed and tested. Also the control (CODAS) and protection (PIS) plant systems are ready for SPIDER operation. In July 2017 the integrated commissioning activity gradually started on the basis of the availability of the various plants. Unfortunately, due to a flooding that involved part of the premises of the cooling system, the integration of the cooling system with CODAS and Interlock has been interrupted and now we are studying a temporary solution to start the experimental phase even if the cooling system will not be completely available.

The MITICA realization progressed. All the procurement contracts are already active or launched. Procurement of PS's and other auxiliary plants progressed, with many of them completely manufactured and installed. An important issue has been the large delay in the construction of the BS Vessel (BSV) which resulted in the postponement of the installation of the Japanese components. Hence also the 1MV insulation tests, expected to start in Q4 2017, are postponed to Q2 2018. Moreover, difficulties are being encountered in the awarding of the BS supply contract which could result in a delay in the delivery of this component.

Finally, great progress has been made in the implementation of the RF HV Test Stand (RFHVTS) and CAesium Test Stand (CATS).

The detailed status of the project and the main achievements in the year are described in the following sections.



Fig. 2.1.1 Aerial view of the NBTF buildings

2.1.1 **PRIMA**

2.1.1.1 *Buildings and auxiliaries*

The NBTF building construction, including conventional auxiliary plants finished in 2015, see Fig. 2.1.1. In 2017 also the formal closure of the contract was done. Further supplies of auxiliary plant systems have been done under different contracts; in particular:

- completion of auxiliaries of buildings hosting MITICA PS's and MITICA bunker;
- special sealed and insulating closures of the penetrations of the MITICA HV transmission line in buildings (Fig. 2.1.2).



Fig. 2.1.2 Special sealed and insulating closures of the MITICA HV Transmission Line

Finally, activities of adaptation of the buildings and auxiliaries have been done to integrate experimental plants to the site; a significant example is the special concrete basements supporting MITICA HVD1 mechanical structure.

2.1.1.2 *Cooling Plant for SPIDER and MITICA*

The on-site assembly of SPIDER Cooling Plant was completed during Q1 2017 and NBTF Team gave continuous technical support with follow-up activities aiming to verify the correct installation, to help the supplier's operators if needed and to solve the problems due to integration issues and compatibility with all the other on-going activities and plants on PRIMA site.

Overall CAD views of pipes, pumps, heat exchangers, air coolers and cooling towers inside and on the roof of Building 2 are shown in Fig. 2.1.3. Pictures of pipes installed inside the MITICA Neutron Shield are presented in Fig. 2.1.3 and Fig. 2.1.5.

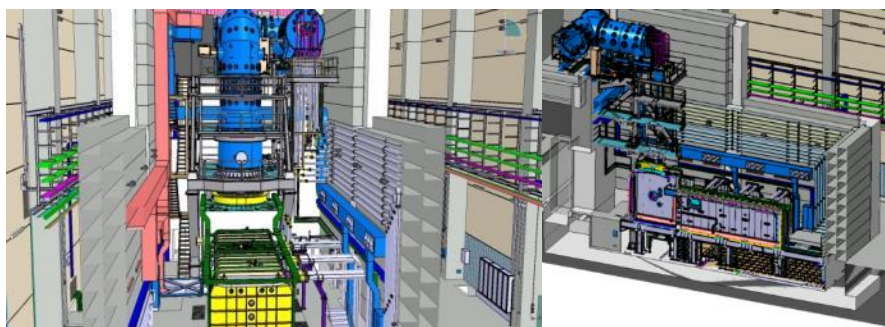


Fig. 2.1.3 CAD layout of MITICA Cooling Plant Unit inside the MITICA Neutron Shield

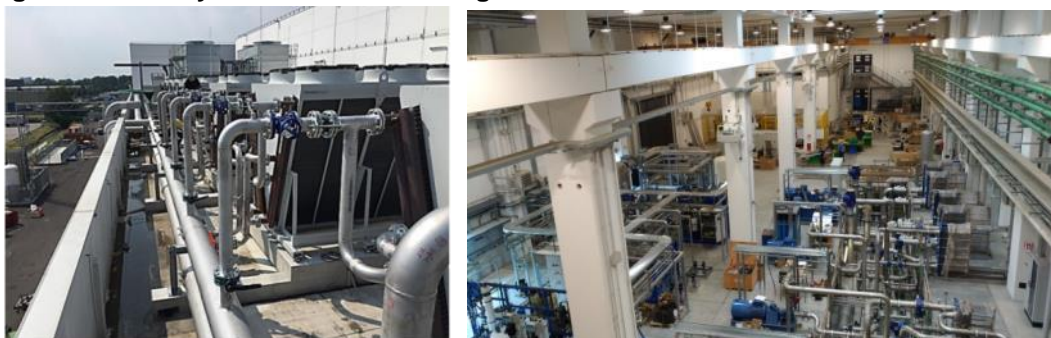


Fig. 2.1.4 Cooling Plant equipment installed on the roof and inside Building 2

The commissioning and site acceptance tests of the SPIDER Plant Unit were carried out starting from pressure tests on primary, secondary e tertiary circuits.

Power supply, monitoring and control equipment were set up and completed to allow the complete commissioning and acceptance tests of SPIDER and Shared Plant Units carried out during 2017.

In parallel the detailed design of MITICA Plant Unit was completed by the supplier with continuous support and verification by NBTF Team.

The full 3D CAD model of cooling circuits was continuously updated by NBTF Team to allow careful integration checks and to give support to the supplier in the preparation of the detailed drawings of the cooling circuits



Fig. 2.1.5 Installation of cooling pipes inside the MITICA Neutron Shield

2.1.1.3 Vacuum, gas injection and gas storage for SPIDER and MITICA

During 2017 the procurement of the Gas and Vacuum System (GVS), see Fig. 2.1.6, continued up to the completion of the installation and the site acceptance tests of the gas storage and distribution plant (GSD-Shared Plant Unit, which serves both



Fig. 2.1.6 SPIDER GVS: pumping system inside the bioshield (left), gas injection cabinet GIS-A (middle), cryo control system HMI window (right).

SPIDER and MITICA) and of the SPIDER Plant Unit (which includes the vacuum system, the gas injection system and their control system). The NBTf team has carried out the technical follow-up during the installation and the site acceptance tests. The latter finished in September due to an issue on the cryopumps. Just after the conclusion of the site acceptance tests the “one-to-one” commissioning of the GVS with the Central Interlock System and CODAS was performed and concluded mid of November with overall positive results also concerning the performances of the cryopumps.

In parallel to the SPIDER related activities, the review of the MITICA gas injection and vacuum system design has been performed, freezing the information necessary for the integration of the GVS with buildings conventional and experimental plants. The installation of the MITICA GVS Plant Unit should start early in 2018.

2.1.1.4 Medium voltage

The NBTf experiments require a dedicated power distribution system to deliver power from the existing 400/21.6 kV substation to SPIDER and MITICA.

Main components are medium voltage distribution boards and medium voltage lines and associated civil infrastructure. They have been procured by two different procurement contracts.

The procurement contract of the medium voltage lines, launched in September 2016, it took place essentially throughout the year 2017 and concluded in December with the administrative and technical testing of the plant. Also the contract for the medium voltage distribution board, signed at the end of 2015, has been concluded with the delivery and the commissioning of the three MV Distribution Boards, see Fig. 2.1.7. NBTf Team provides to integrate to integrate the two systems between them.



Fig. 2.1.7 – MITICA MV Distribution Board

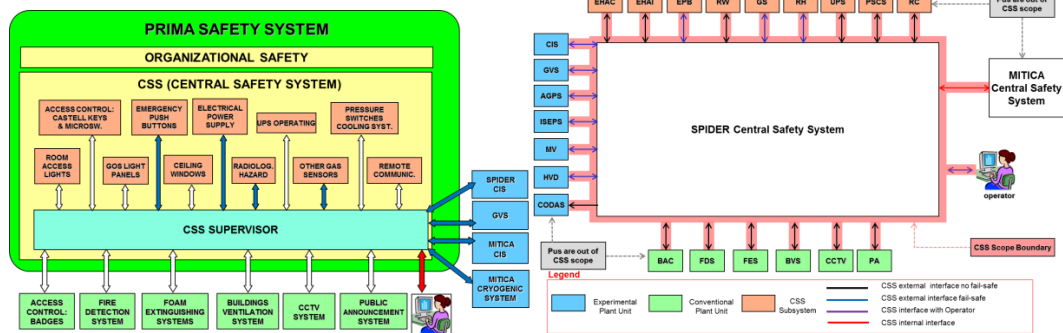


Fig. 2.1.8 Safety scheme for PRIMA (left) and SPIDER CSS with interfaces (right)

The SPIDER DB was made available again in spring and used for the commissioning of the SPIDER PS's. MITICA DB has been ready by the end of the year and in time for MITICA's PS's commissioning expected at the beginning of 2018.

2.1.1.5 PRIMA Safety

The PRIMA safety Fig. 2.1.8 is the set of measures, procedures, tools, hardware, software and risk analyses that, as a whole, are devoted to prevent dangerous event in the NBTF facility². During 2017 the technical specifications for the Central Safety System (CSS), the system implementing the safety functions, as well as monitoring of the whole site safety, has been completed³. The call for tender for the procurement of the SPIDER

² see RFX_SPIDER_TN_342_rev2

³ see RFX_SPIDER_TS_028_rev3



Fig. 2.1.9 – Various phases during SPIDER BS assembly at the factory

part of Central Safety System (CSS) has been launched and the contract has been awarded in July 2017. The contract follow up is in the phase of Detailed Design analysis. In parallel the implementation of the SGSA (Sistema Gestione della Sicurezza Antincendio – System for the Management of the Fire Safety) has been defined and a draft version has been sent to the Fire Brigade Responsible Officer. The risks analysis for MITICA part of CSS has also started together with the definition of the actions aimed at mitigating the identified risks.

The interfaces between the MITICA part of the safety system, the SPIDER part of CSS, the conventional plants and experimental plants have been defined: further analyses will be necessary in the near future to integrate the upcoming plant procurements (as the cryoplant) for which only a preliminary design of the interfaces has been developed in 2017

2.1.2 **SPIDER**

2.1.2.1 *SPIDER Beam Source*

The contract for the supply of the SPIDER Beam Source (BS) was signed in 2012. In 2017 a huge effort was required to the Team to recover the criticalities emerged in the procurement of some components (cooling pipes and grids) and the completion of the assembly at the factory, alignment of the accelerator included. The NBTF Team was heavily involved in meetings, inspections to verify the manufacturing progress and to witness intermediate and final tests at the factory, according to the control plans. Significant contributions were given during several phases of the dimensional checks and alignment procedure (Fig. 2.1.9).

The source was delivered in October 2017 (Fig. 2.1.10), still with outstanding issues, such as a leak in a GG segment that will require a replacement. On-site activities started, including site acceptance tests and preparations for installation in the VV, the latter having been moved from the procurement contract to being in charge of RFX. Many tools were procured to carry out these activities, such as a clean room and several fixtures and auxiliary handling tools. The procurement of the Beam Source handling tool was completed successfully the beginning of 2017.

2.1.2.2 *SPIDER Beam Dump*

The SPIDER Beam Dump delivered at PRIMA site in 2015 required adjustments of the

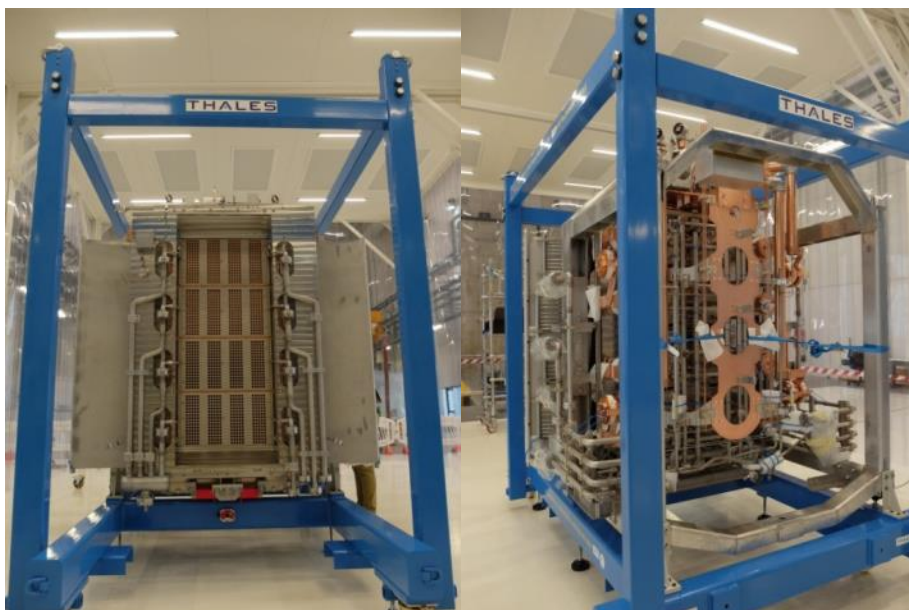


Fig. 2.1.10 – SPIDER BS delivered on site, located inside the clean room

hypervapotron positions located on one of the two panels, in order to close some gaps that could cause beam shinethrough, see Fig. 2.1.11. A technical solution was agreed in 2016 by ITER Organization and NBTF Team by which the hypervapotrons are fixed and their position adjusted with proper combs engaging the inlet/outlet cooling pipes.



Fig. 2.1.11 Detail of a typical shinethrough between adjacent hypervapotron elements of SPIDER Beam Dump

The Beam Dump was then transported in Building 1 assembly room at PRIMA site, and

fixed to a temporary support structure to test the IO+NBTF solution, see Fig. 2.1.12.

Combs and clamps to correct the positions of HTEs were installed in Q1 2017, but some shine-through remained.

The finally agreed action to solve the issue was the installation of some instrumented Cu plates on the back side of the hypervapotrons to intercept any possible power due to local beam shinethrough. Procurement and installation of the instrumented Cu plates (plates, thermocouples, electronics, flanges, etc.) have been carried out by NBTF Team.

The complete set of sensors necessary for calorimetric measurements was fully installed on the Beam Dump by NBTF Team: 120 embedded TCs plus 60 calorimetry TCs were installed and cabled up to the vacuum vessel ports, see Fig. 2.1.14. MoS₂ coating spray was applied on the front surface to allow proper surface temperature monitoring with thermo-cameras.

Original electrical isolation problems were fixed, final pressure tests and leak tests were carried out before moving the Beam Dump from the assembly area to the SPIDER

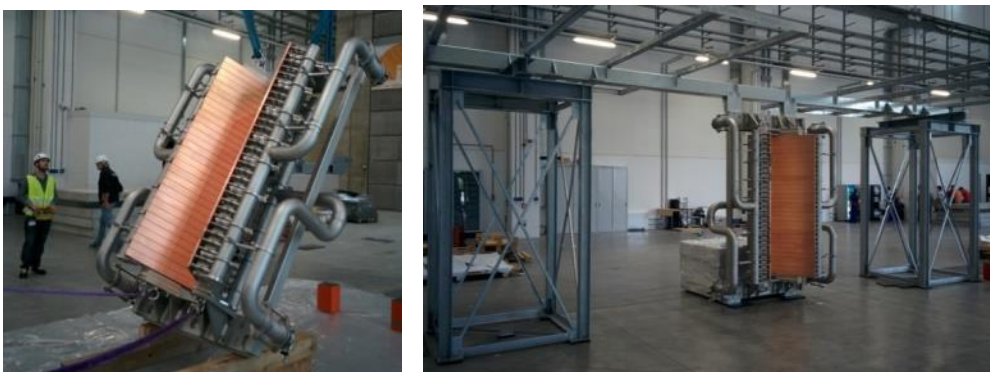


Fig. 2.1.12 Pictures of the Beam Dump during installation and recovery activities inside Building 1.

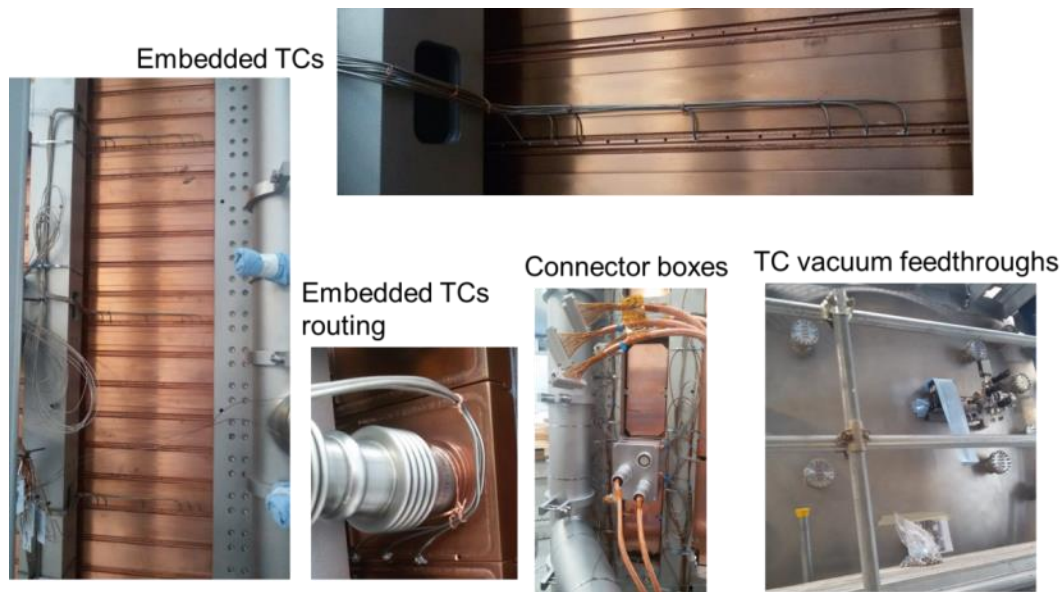


Fig. 2.1.14 Views of thermocouples (sensors, cabling and feedthroughs) installed on the SPIDER Beam Dump

Vacuum Vessel. All these assembly, repair and tests activities on-site have been carried out involving a specific NBTF team composed by expert engineers, physicists and technicians.

In view of the installation of the SPIDER Beam Dump (SBD) on the vessel front lid and of STRIKE inside the vessel, on-site preparatory activities have been performed, such as the vessel venting and the transportation of the front lid out of the bioshield. In August 2017 the provisional handover of the SBD has been signed, both from IO to F4E and

from F4E to Consorzio RFX, and the installation of the SBD on the front lid started, see Fig. 2.1.13. Some misalignment issues were found when fixing the cooling manifolds to the Lid hydraulic connections: excessive distortions of bellows, not compatible with installation limits, should have been applied.

For this reason new bellows and specific tools for alignment corrections were designed and procured. The completion of Beam Dump installation

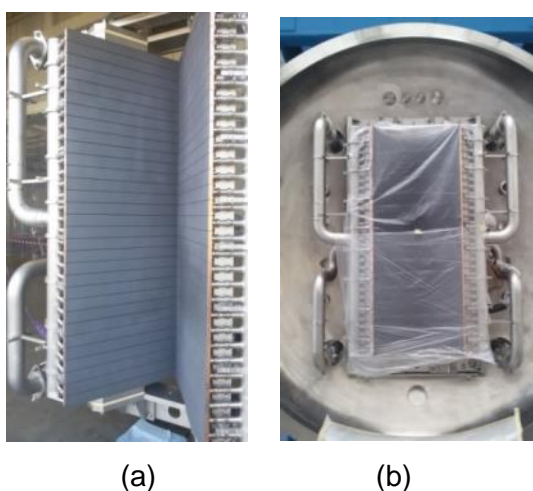


Fig. 2.1.13 The SPIDER Beam Dump under installation at PRIMA Site: view of the Beam Dump panels (a) and Beam Dump fixing to the Vacuum Vessel front lid (b)

inside the Vacuum Vessel is foreseen by the end of 2017.

2.1.2.3 SPIDER power supplies

SPIDER PS includes the Ion Source Power Supply (ISEPS), hosted in the High Voltage Deck (HVD) a Faraday air insulated with respect to ground for -100 kV, and the Acceleration Grid Power Supply (AGPS). The system is completed by the Transmission Line that connects the HVD to the BS through the HV Bushing installed on the Vacuum Vessel (VV). A 3D view of the SPIDER layout is shown in Fig. 2.1.15. AGPS is procured by INDA, while all the other SPIDER PS and the other plants are procured by F4E. In 2017, most part of SPIDER Power Supply (PS) has been realized, commissioned and accepted. The PS not yet completed is the AGPS.

Ion Source and Extraction Power Supply system

The commissioning and SAT of the Ion Source and Extraction Power Supplies was completed in 2016 and only a small activity has been performed at the beginning of 2017 to verify all the associated technical documentation. Hence the SPIDER system was formally accepted by F4E and Transferred for Use (TfU) to the Consorzio RFX. This is the first example of an official TfU of a system from F4E to the Consorzio RFX and it allowed us to check the administrative procedures to be applied.

Voltage Deck and Transmission Line

Both HVD, hosting ISEPS the ISEPS system and the associated diagnostics, and the High Voltage Transmission Line (TL), tht carries the power and signal conductors from the ISEPS to the Ion Source, had been finished and accepted in 2016. In 2017 the TL has been tested in order to verify that there were no thermal problems due to defects on

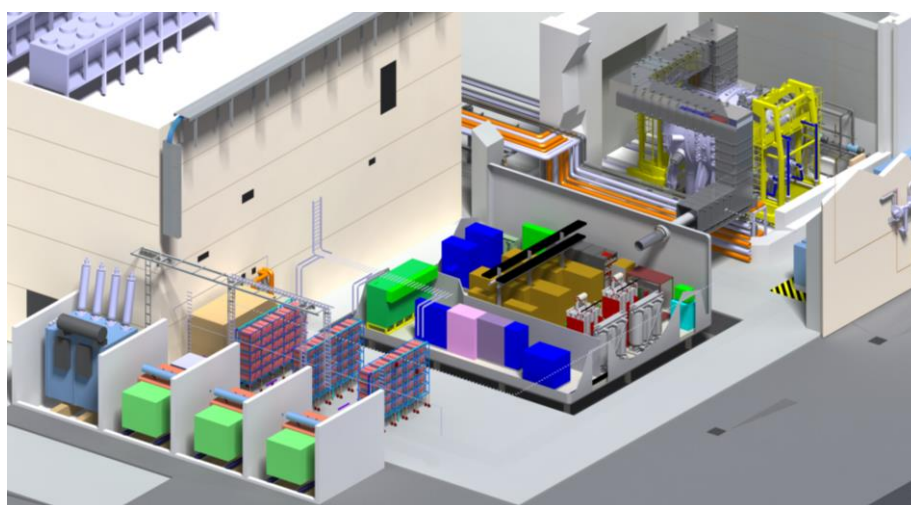


Fig. 2.1.15 - 3D view of SPIDER power supply system

the internal connections. During the test a nominal current values, up to 5.6kA, have been circulated on the high current conductors and reproducing the nominal cycle conditions (1hour on/3 hours off). Overtemperatures were of some °C and in all case within the limits foreseen by the simulations. This test has been performed involving TL, ISPES system to feed the current, and the cooling system, thus representing a first case of plant integration.

Acceleration Grid Power Supply (AGPS)

Installation activities of the SPIDER AGPS provided by the Indian Domestic Agency (INDA started in July 2016, see Fig. 2.1.16. In spite of the scheduled few months of installation, at the end of 2016 the installation had not yet been completed. Moreover, some manufacturing and installation issues were detected that did not allow starting the commissioning phase. The main issues encountered were: lack of a adequate fire barrier in correspondence to the cable feedthroughs interfacing outdoor multi-winding transformers and indoor power modules; weakness of some cooling pipes; defects of the multi-winding transformers such small oil leakage, rust on bolts, supports bars and other components; some wiring of the control cabinets executed not according to IEC standard.

Regarding the problem of having feedthroughs with homologated flame retardants, NBTF Team has supported INDA both by identifying the suitable material and carrying out tests in its laboratory. NBTF Team has also continued to assist INDA in the interface with the installation company to limit the accumulated. Nevertheless, due to administrative difficulties, INDA has delayed the allocation of the additional contracts to carry out the above described additional activities. On-site activities actually resumed in September. The transformer defects have been solved, the cooling pipes replaced and the flame-retardant seals installed. After having restored the transformers and verified the correct documentation associated with these machines, NBTF Team authorized the no-load test of the transformers. Unfortunately, in the last part of 2017 there has been a further delay



Fig. 2.1.16 - General overview of SPIDER AGPS

in the activity of rewiring some parts of the control cubicles. As long as this has not been solved and adequate certification has been produced, the commissioning of the system cannot begin. Presently it is expected that the recovery activity will resume in mid-January 2018, immediately followed by commissioning. This is still compatible with the experimental plan of SPIDER since in the first experimental phase it is not necessary to operate the accelerator and, consequently, the AGPS. This system is currently the most critical one for the SPIDER operation.

2.1.2.4 SPIDER & MITICA diagnostics

A significant advancement in the procurement of SPIDER diagnostics has been achieved in 2017 under the F4E procurement contract OFC-531-01, which assigns to the NBTF diagnostic team the full assembly, integration and commissioning of a first set of diagnostics needed to start operation. The set comprises vacuum windows, thermocouples, emission and laser spectroscopy, electrostatic probes, visible and IR imaging, components of other diagnostics that need R&D (instrumented calorimeter STRIKE, neutron, tomography), and includes the tiles for STRIKE (diagnostic calorimeter) planned for delivery in April 2018. In 2017 all orders for components have been issued and most parts have been delivered, so that assembly could progress and installation started.^{4,5}

The current status is the following:

- beam source and beam dump thermocouples are installed and cabled up to the acquisition cubicles, they will be tested as soon as beam source and beam dump are installed in the vacuum vessel; conditioning electronics with optimized performance and reduced cost have been developed and installed: they will be particularly important in MITICA where more than 1000 thermocouples are used;
- vacuum windows are ready to be installed on the vessel;

⁴ R.Pasqualotto et al., "Progress on development of SPIDER diagnostics", : AIP Conference Proceedings 1869, 030020 (2017)

⁵ R.Pasqualotto et al., "A suite of diagnostics to validate and optimize the prototype ITER neutral beam injector", JINST 12, C10009 (2017)

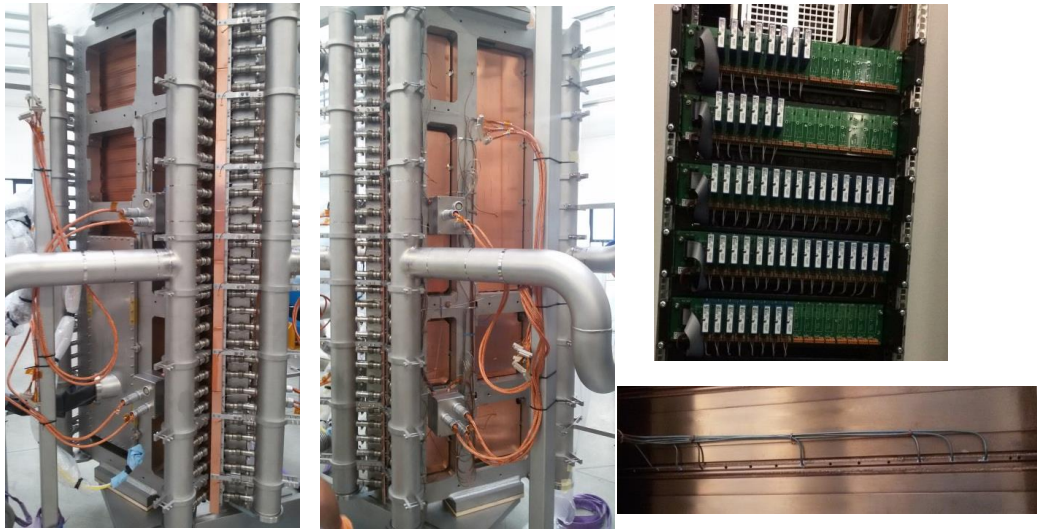


Fig. 2.1.17 Back side of the two beam dump panels. The cabling of the 180 thermocouples can be seen, together with the vacuum box of the neutron imaging detector (left); detail of the installation of embedded thermocouples from the rear side of the hypervapotrons for detection of the horizontal beam profile (bottom right); electronics in the acquisition cubicle (top right)

- all components of emission spectroscopy are in house and individually tested, in particular the spectrometers are fully characterized and we are waiting for installation of the optical fibres and collimating heads to align the system and test the full measurement chain; custom electronics for a set of filtered photodiodes has been developed and a prototype is now under test;
- laser absorption spectroscopy is ready for operation and it has been temporarily installed on the caesium test bed to measure the caesium density;
- electrostatic probes custom electronics has been designed, successfully prototyped and is now being manufactured;
- visible and imaging cameras are procured, tested on the NIO1 facility and are ready for installation;
- the neutron diagnostic has been completed in-vessel, with procurement of the GEM detector and the vacuum box and their installation on the beam dump;
- the visible tomography camera has been developed and tested extensively in NIO1;
- the in-vacuum mechanical structure of the instrumented calorimeter STRIKE has been manufactured and installed in the vessel and the custom CFC-1D tiles have been ordered following a deep qualification program on a set of prototypes.

Some of these diagnostics installed for test on NIO1 have significantly contributed to the scientific exploitation of the facility, proving their performance and reliability.

Development of MITICA diagnostics and of the remaining part of SPIDER systems progressed under the F4E NBTf Work Programme, in particular the design of the thermal and electrical sensors embedded in the beam line components of MITICA.

A second procurement contract with F4E (OFC.531-02) started in September 2017 to

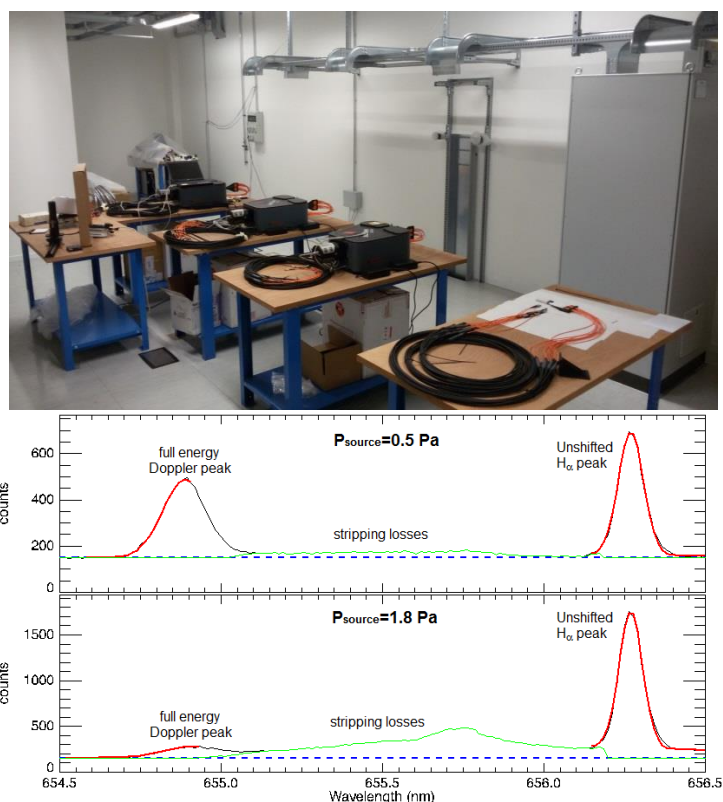


Fig. 2.1.18 SPIDER optical diagnostic room with three imaging spectrometers and connected fibre bundles (top); beam emission spectroscopy spectra measured on NIO1 with one of these spectrometers (bottom)

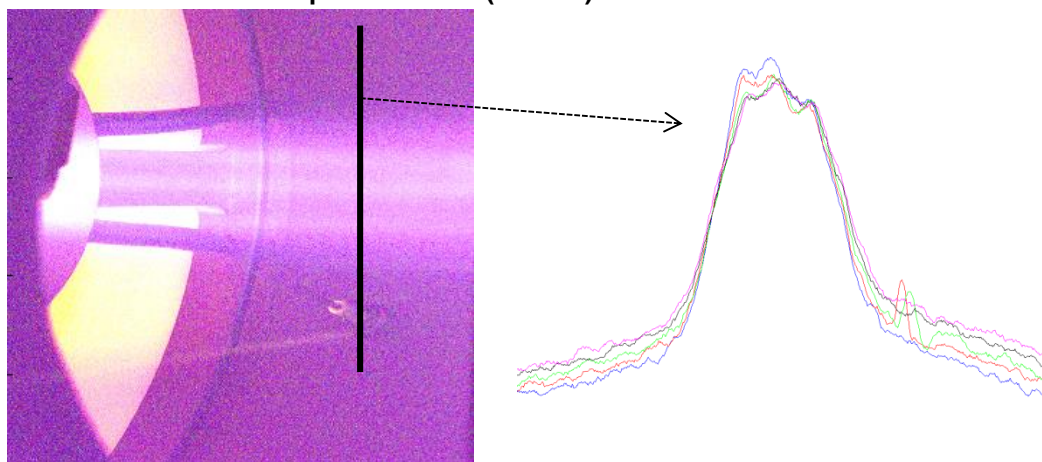


Fig. 2.1.19 H α radiation from interaction of the beam with the background gas in NIO1, imaged by the visible camera procured for SPIDER (left) and beam profiles across the beam (right): the three beamlets can be discriminated

cover the remaining SPIDER diagnostics (cavity ring down spectroscopy, tomography and completion of STRIKE and neutron imaging) and some prototypes of embedded diagnostics for MITICA (thermocouples and Langmuir probes).

2.1.2.5 SPIDER and MITICA Instrumentation and control systems

In 2017 NBTF Team has carried out the activities on the instrumentation and control systems of SPIDER and MITICA under the framework contract F4E-OFC-280 and the WP2017, respectively.

SPIDER Control and Data Acquisition System (CODAS)

SPIDER CODAS has made a substantial step forward thanks to the integrated commissioning that marked the transition to a control system able to effectively interact with plant systems, to control and monitor them, acquiring, storing and displaying actual plant system data in a flexible and reliable way. Section 2.1.2.6 reports the progress achieved in the SPIDER integrated commissioning.

During the half of 2017 most of the efforts were devoted to preparing the SPIDER PS plant system, the PRIMA plant system (including gas and vacuum and cooling), and the SPIDER interlock plant system for the upcoming integrated commissioning phase. We prepared a specific set of human machine interface (HMI) panels to facilitate the execution of the commissioning tests. At the same time, we continued to develop the interface with the diagnostic systems, specifically with the thermocouples, the electrostatic probes and the visible and infrared cameras.

Furthermore, we carried out the definition, implementation, commissioning and operation of the control system of the Caesium Oven test-bed (see Section 2.1.6).

SPIDER Central Interlock System

During 2017, the interface with SPIDER ISEPS, gas and vacuum, and cooling plant units were verified. The whole system was extensively tested during the SPIDER integrated commissioning and it proved to be very flexible thanks to the software data-driven approach and in-built capability to deal with input/output signal through by-pass and forcing. Following the data driven-approach, protection tables allow configuring the system protection actions linking protection requests to protection commands. When the protection actions need to be changed, no PLC or FPGA software change is required. The protection tables can be filled via the dedicated graphical panel shown in Fig. 2.1.20.

| PU | Command sent from CIS to PU / Alarm from PU to CIS | BO-PS | BO-PS | SO-PS | SO-ISPD | SO-GISA | SO-CS | SO-CP | EN | FS-AGPS/ISEPS MVDB | CSS | CODAS Abort |
|-------|--|-------|-------|-------|---------|---------|-------|-------|----|--------------------|-----|-------------|
| CODAS | Fault | X | | | | | | | | | | |
| CODAS | Switch of received and executed | X | | | | | | | | | | |
| CODAS | Breakdown command received and executed | X | | | | | | | | | | |
| CODAS | Beam Of command received and executed | | X | | | | | | | | | |
| CODAS | Enable Command received and executed | X | | | | | | | | | | |
| CODAS | Heartbeat | | | | | | | | X | | | |
| ISEG | Protection tripped | X | | | | | | | | | | |
| ISEG | Breakdown Detected | | X | | | | | | | | | |
| ISEG | Beam Of Detected | | | X | | | | | | | | |
| ISEG | Switch Of command received and executed | X | | | | | | | | | | |
| ISEG | Breakdown command received and executed | X | | | | | | | | | | |
| ISEG | Enable command received and executed | X | | | | | | | | | | |
| ISEG | Local/Remote | | | | X | | | | | | | |
| ISEG | Heartbeat | X | | | | | | | | | | |
| ISRF | Protection Tripped | X | | | | | | | | | | |

Fig. 2.1.20 Graphical panel to configure the protection actions of SPIDER central interlock system. The rows and columns contain the protection requests and the protection actions, respectively. The panel works as an incidence matrix to connect protection requests with protection actions.

To improve reliability, once a protection table is set and then validated through ad-hoc tests, it cannot be changed without undergoing a whole system recommissioning. By-pass allows excluding input signals from the protection logics in a flexible and controlled way acting on the HMI panels. Every by-pass is marked on the HMI and registered as an operator command. The forcing allows asserting a digital input/output signal for debugging, thus drastically reducing the time necessary to test the plant unit signal interface. Fig. 2.1.21 shows the online processing of a set of SPIDER central interlock input signals, with the possibility to set the by-pass and forcing of each input signal.

SPIDER Central Safety System

In early 2017, NBTF Team completed the design and produced the technical specification of the SPIDER central safety system that coordinates the SPIDER safety actions. It has interface with a wide range of safety-related systems, either directly linked to the SPIDER operation, such as the gas and vacuum system, the 22 kV power distribution board, and the emergency push buttons, or linked to the NBTF buildings, such as the safety access control, the fire detection and extinguishing systems, the CCTV system. The system itself implements eight safety related functions, such as the closure of the laser shutter and of the nitrogen shut off valve. The system is required to comply with the IEC 61508/61511 technical standards on functional safety of

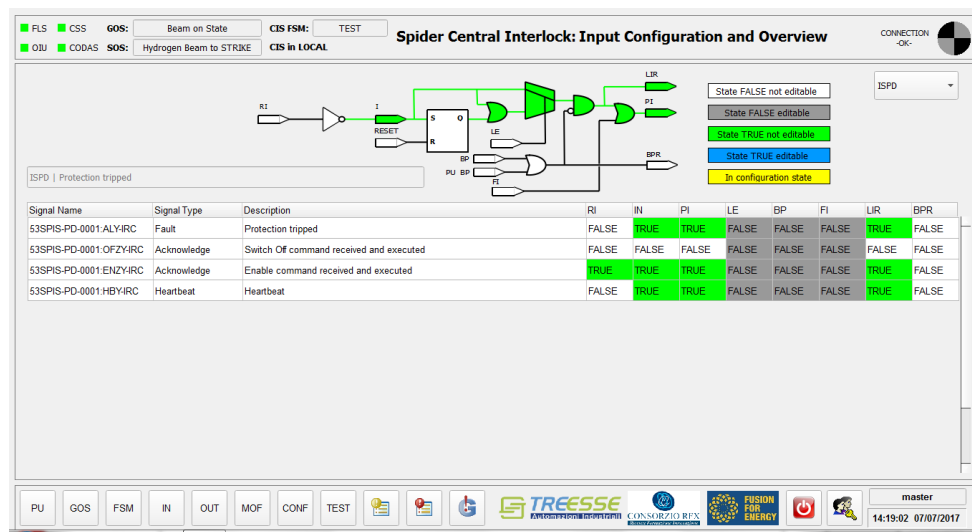


Fig. 2.1.21 SPIDER central interlock graphic panel showing the input signals from the power distribution board of ISEPS. The panel shows in real time the input signal processing. Each input signal can be by-passed or forced by acting on the panel (BP or FI cells set to FALSE/TRUE).

electrical/electronic/programmable safety-related systems and safety instrumented systems for the process industry sector, respectively.

By system analysis, NBTF Team defined the IEC 61508 safety integrity level (SIL) required for each safety-related function, being SIL3 the highest level to reach corresponding to a probability of failure on demand in the range 10^{-3} - 10^{-4} .

Due to the high SIL required, the SPIDER central safety system architecture relies on a redundant failsafe PLC (SIMATIC S7400FH) that is equipped with distributed failsafe I/O modules connected via a double Profibus ring. Fig. 2.1.22 shows the system hardware architecture. The integrator will program the safety related functions using a special programming tool (SIMATIC safety matrix). The supplier of the hardware components and software tools certifies the whole system up to SIL3. The HMI will use the WinCC OA SCADA (also qualified up to SIL3), in which the integrator will implement the transmission of safety related commands from SCADA to PLC through a doubly checked, secure channel. Fig. 2.1.23 shows the prototype of the overview panel of the SPIDER central safety system.

MITICA Control and Data Acquisition

In 2017, NBTF Team has addressed the design of MITICA central CODAS and the definition of the interface with the plant systems, especially with MITICA AGPS, ISEPS, cryogenic plant, gas and vacuum, and cooling.

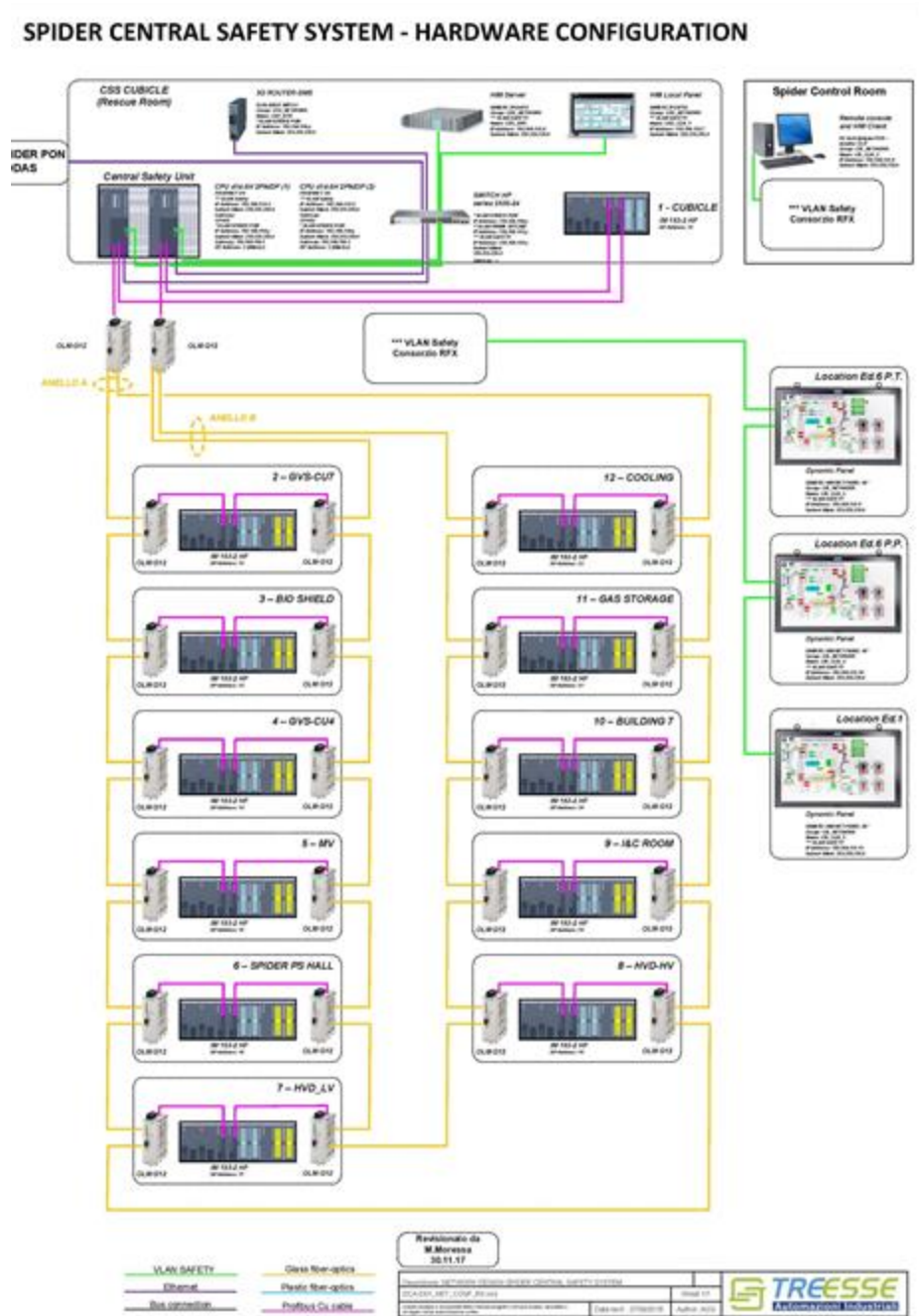


Fig. 2.1.22 System hardware architecture of the SPIDER central safety system.

As for the design of the MITICA central CODAS, NBTF Team worked on the definition of the MITICA global, common and plant system states, following the ITER schema for operating states. NBTF Team completed the implementation of the operating states by preparing a prototype implementing the relevant PLC and EPICS software.

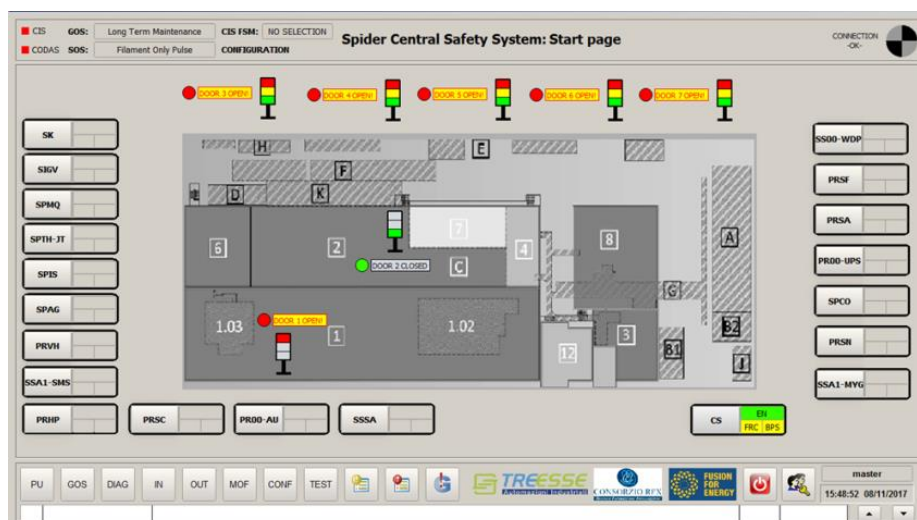


Fig. 2.1.23 Overview panel of the SPIDER central safety system.

Fig. 2.1.24 shows the mapping of MITICA plant system operating states over the common operating states. The MITICA control modes were also prepared starting from the correspondent SPIDER control modes.

With reference to the interface with the plant units, NBTF Team prepared the interface sheets of plant units included in the power supply plant system, including MITICA ISEPS, AGPS, GRPS, 22 kV power distribution board, and high voltage deck and transmission line. Moreover, we also defined the MITICA CODAS and interlock interface with the cryogenic plant.

MITICA Central Interlock System

Along with the CODAS interface sheets of the power supply plant system, the MITICA central interlock interface sheets were completed.

2.1.2.6 SPIDER Commissioning

The SPIDER integrated commissioning is the activity by which already-tested-and-accepted plant components are brought progressively to work together with the aim to achieve eventually the coordinated operation of the whole SPIDER experimental device. SPIDER integrated commissioning was a substantial activity that Consorzio RFX prepared and partially carried out in the first and last quarters of 2017, respectively.

The integrated commissioning and integrated test plan was prepared in Spring, submitted to F4E in June, reviewed by IO and F4E, and finally approved by F4E in early July 2017. It includes the NBTF Team organization to carry out the commissioning activity, identifying the roles of involved personnel, the overall commissioning procedures, the responsibilities, and the list commissioning campaigns to carry out (see

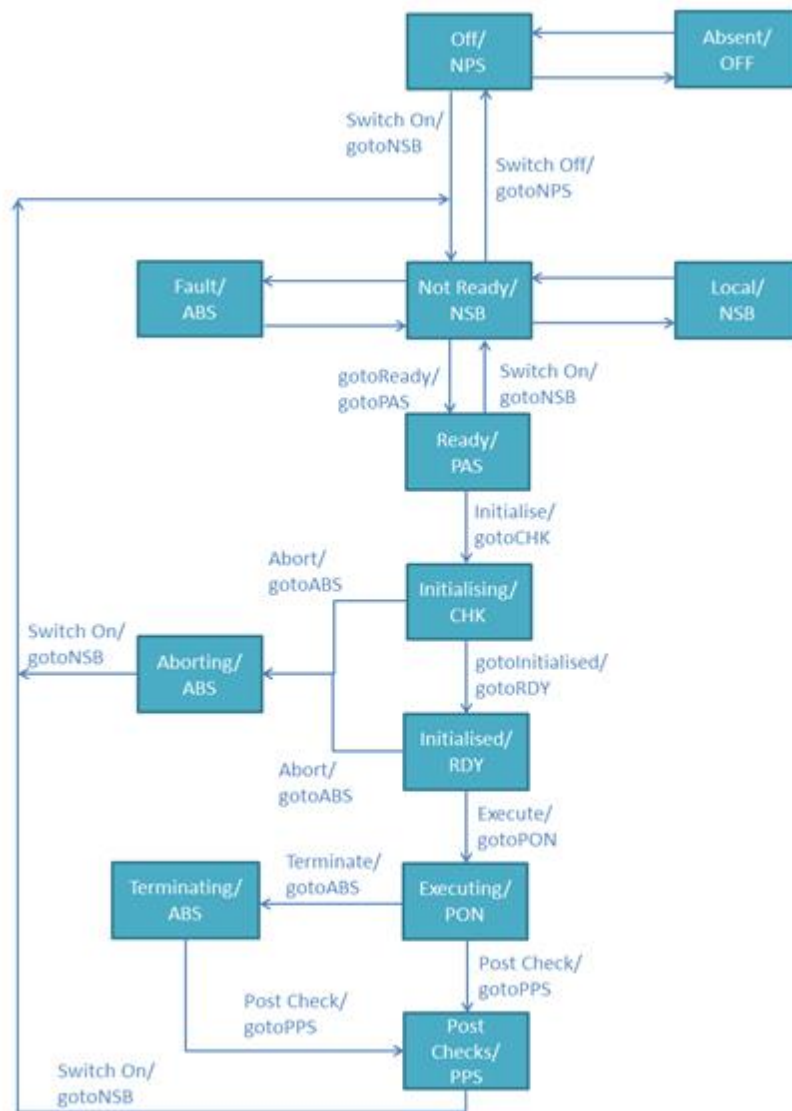


Fig. 2.1.24 Mapping of MITICA common and plant system operating states in MITICA CODAS.

Fig. 2.1.25). The document includes no technical details on the single commissioning campaigns, as a dedicated document is emitted for each campaign prior to the campaign itself containing all tests to execute, operating limits and constraints, measurements, and test passing criteria.

In 2017, Consorzio RFX executed four campaigns for the integration of:

- CODAS with the central interlock system;

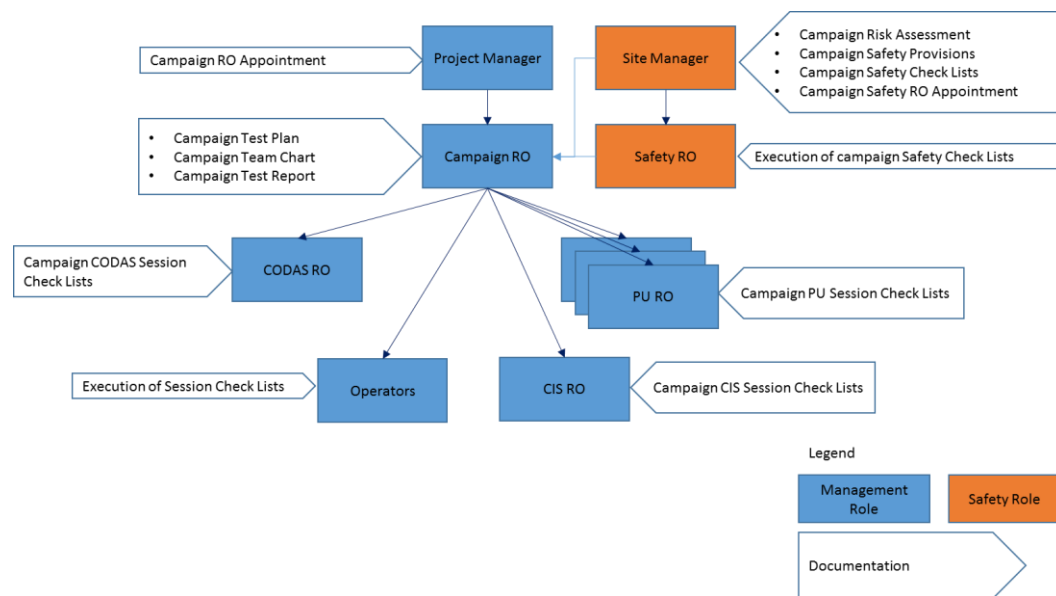


Fig. 2.1.25 The roles involved in the integrated commissioning activity, their interactions, and the documentation associated.

- SPIDER ISEPS with CODAS and the central interlock system
- SPIDER/Shared gas and vacuum system with CODAS and the central interlock system
- Thermal tests of the SPIDER transmission line

The interoperability of SPIDER CODAS and central interlock was the target of the first commissioning campaign.

The second and third campaigns aimed to achieve the remote operation of the ISEPs and GVS plant units, respectively, under central control by CODAS and the central interlock system. The last campaign aimed to check the thermal behavior of the transmission line at full performance.

The integrated commissioning was performed from a provisional remote control room located in the NBTf building 6 - first floor, equipped with the necessary PC-based consoles (Fig. 2.1.26). A web-based professional software tool (Bugzilla) was used to track all errors, such as erroneous system implementation, or unclear/missing interface definition, or missing requirements in the technical specification.

Campaign S-C1-A – SPIDER CODAS and Central Interlock system

Campaign S-C1-A was a 2-day campaign to check the signal and process variable interface of the two systems and to test the system interoperability. The campaign also verified the central interlock human machine interface (HMI) that runs under EPICS and can be displayed in the CODAS consoles. We executed a few simulated beam pulses to



Fig. 2.1.26 Provisional control room located in the NBTF building 6 – first floor.

make sure that CODAS can start the SPIDER beam or test and conditioning operations only if enabled by the SPIDER central interlock system and, vice versa, that if the central interlock system at any time disables CODAS, then CODAS promptly inhibits the continuation of SPIDER operations.

Campaign S-C1-B - SPIDER ISEPS, central interlock system, and CODAS

Campaign S-C1-B (8 weeks, from late June to mid-September), was a demanding campaign due to the complexity of SPIDER ISEPS that consists of 4 large subunits implementing the power distribution, extraction grid power supply, radio frequency power supply (4 units), and source support power supply (filament, bias, bias plate, and plasma grid filter power supply), respectively. Fig. 2.1.27 shows the voltage and current measurements of the extraction grid power supply taken during the system response to a breakdown event.

Campaign S-C1-C - SPIDER/Shared gas and vacuum system, central interlock system, and CODAS

Campaign S-C1-C lasted 5 weeks from mid-October to mid-November. It was devoted to the tuning of the gas injection procedure and to the performance tests of the gas pumping system under sustained gas injection. The campaign was very successful, showing that the gas pumping system can sustain the nominal pumping capacity for 3600s. Fig. 2.1.28 shows the pressure traces acquired from three different pressure gauges during a one-hour pulse with gas injection.

Campaign S-C1-D - SPIDER/Shared cooling system, central interlock system, and CODAS

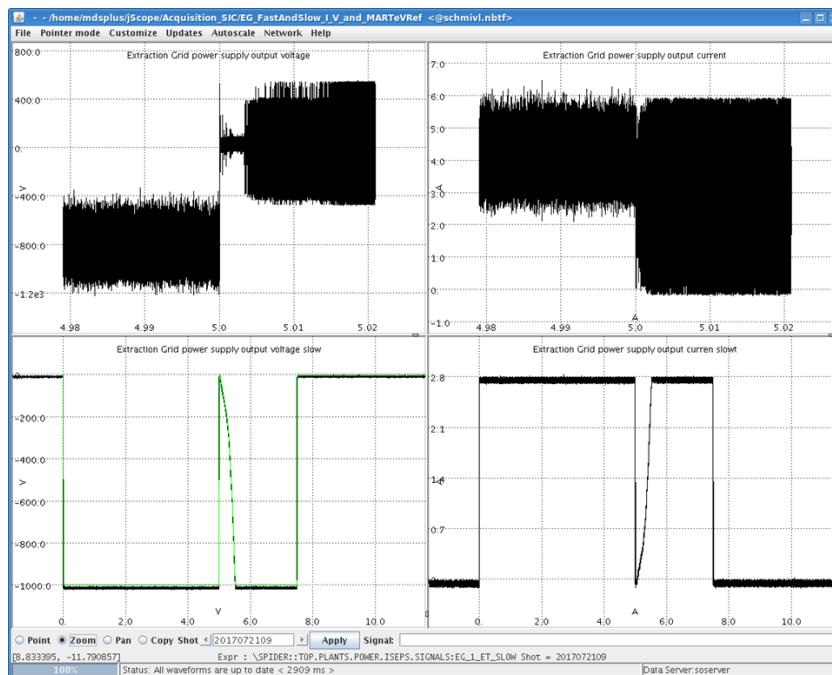


Fig. 2.1.27 Extraction grid voltage and current measurements during a simulated breakdown event done by short-circuiting the extraction grid power supply terminals. The lower waveforms are the voltage and current signals acquired at low sampling rate (10 kHz), whereas the upper ones are the same measurements at high sampling rate (1 MHz). The green-ink trace shown on the voltage panel is the CODAS time voltage reference which drives the extraction grid power generator.

NBTF Team prepared Campaign S-C1-D, issued the relevant test plan, and was ready to start the campaign. Unfortunately, the unexpected unavailability of the cooling plant prevented the campaign execution in 2017.

Campaign S-C4-A - Transmission line thermal tests

The NBTF Team tested the thermal behavior of the SPIDER transmission line by increasing the current in the conductors for the plasma grid filter, bias plate and bias up to nominal values. The conductors were short-circuited just inside the vacuum vessel. The test included three one-hour pulses with current in the wires, each followed by a 3-hour down time (25% duty cycle). The transmission line temperature was measured and its increase during the test was found to be less than a few degrees Celsius.

2.1.3 MITICA

2.1.3.1 MITICA Vacuum Vessel and HVB Support Structure

During 2017 the follow-up of the procurement of MITICA Vacuum Vessel continued with technical meetings at the supplier premises and review of technical documents submitted by the supplier in F4E-IDM. Technical support was given for manufacturing design

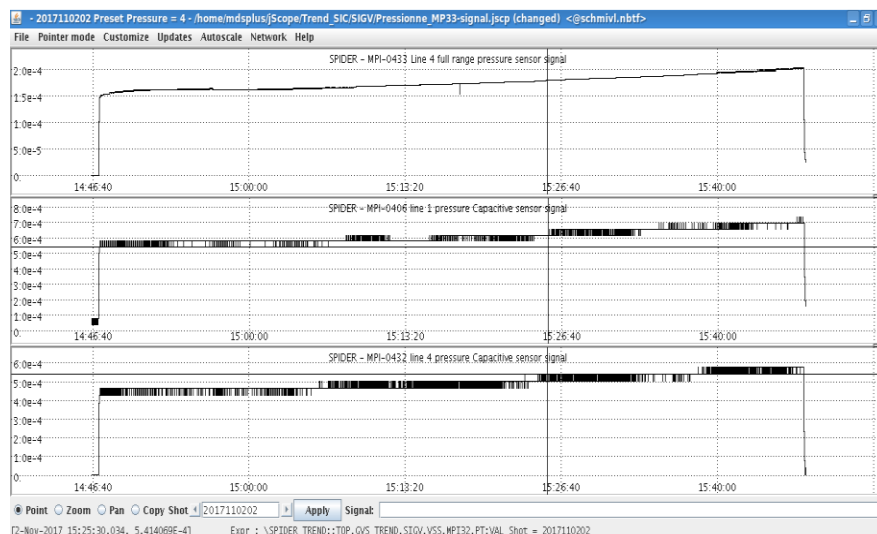


Fig. 2.1.28 Pressure in the SPIDER vacuum vessel during a one-hour gas injection pulse. The pressure measurements came from 3 different pressure gauges. 3 turbomolecular pumps (one was out of order) and 8 cryogenic pumps provided the pumping function. Gas injection was executed through valve SIGV-VG30001 with manual valve preset of 5 turns and gas injection pressure of 4 bar

decisions, discussing details and assessing proposals for the vessel support structure manufacturing and on-site installation.

Frequent on-site meetings and inspections were held to prepare and follow the on-site installation activities for the vacuum vessel support structure, also involving the metrology team at Consorzio RFX for precise positioning and controls of drilling jigs with respect to specific requirements and data targets inside MITICA Neutron Shield.

The schedule of the support structure installation has been discussed and optimized for integration with all the other MITICA installation activities.

The installation of the support structure was completed during 2017, as shown in Fig. 2.1.30. The Rear Lid Handling System was also completed and tested at the factory (see Fig. 2.1.29) and delivered on-site in 2017.

The construction of both Beam Source Vessel (BSV) and Beam Line Vessel (BLV) had put on hold by F4E at end 2016 due to issues of low strength and rigidity of the vessel as manufactured by the supplier. The matter was continuously discussed during the year among IO, F4E, NBTF Team and the supplier to agree the necessary recovery actions and to proceed with the procurement contract.



Fig. 2.1.30 Picture of the MITICA Vacuum Vessel Support structure as finally assembled inside the MITICA Neutron Shield.



Fig. 2.1.29 Tests of Rear Lid Handling System at supplier's workshop

A complete set of structural analyses and verifications were carried out by NBTF Team and external engineering consultants to support the proposals for BSV and BLV recovery. Dedicated meetings took place to discuss recovery strategies aimed at minimising the risk that excessive deformations of the vessel could reduce too much the allowance material on areas to be precisely machined in the following phases. As a preliminary action, an overall control of BSV dimensions was performed at the factory with the involvement of NBTF engineers and technicians of metrology team (see Fig. 2.1.31).

Finally a recovery strategy was agreed with the supplier and the manufacturing activities on BSV started again in December 2017. Further discussions and meetings will prosecute during Q1 2018 to agree a recovery strategy for the BLV and start again welding activities.

Completion of manufacturing and installation of BSV inside the MITICA Neutron Shield is presently foreseen in Q1 2019. This delay is the most critical issue on the time schedule

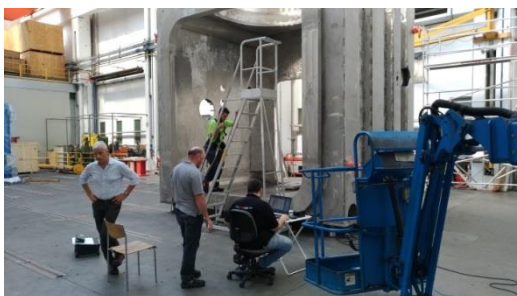


Fig. 2.1.31 Pictures of the Beam Source Vessel (metrology works) and Beam Line Vessels at supplier's workshop

for MITICA and is carefully monitored by the NBTF Team.

A very important milestone for MITICA schedule is about to be reached with the static test of the High Voltage Bushing Support Structure (HVBSS). Within the first specific contract of the NBTF Assembly framework contract (between Consorzio RFX and F4E), in which Consorzio RFX has to procure the HVBSS, the use of the High Voltage Bushing (HVB) as test-load allows to test the HVBSS and assess the procedure for the final installation of the HVB itself, thus verifying one of the most critical interfaces.

2.1.3.2 MITICA beam source

The design of the MITICA Beam Source, see Fig. 2.1.32, was completed and the tender was issued in 2015. The framework contracts for the procurement were signed by F4E in July 2016 and the NBTF Team in 2017 provided the entailed follow up support. The procurement strategy decided by F4E consists in a framework contract divided in three specific stages: stage 1 is the baseline design review, stage 2 is the MITICA Beam Source procurement and stage 3 is ITER Beam Source procurement. Stage 1 involved three companies in parallel, in charge of producing detailed and revised design, 3D CAD model, 2D drawings and the technical specifications. In this phase follow-up activities by NBTF Team were carried out with several meetings, both at suppliers' premises and in videoconference. A large effort was required throughout this contract to manage several technical queries raised in parallel by the 3 suppliers, with very tight time for discussions and responses.

Stage 1 was concluded in May 2017, with the receipt of all the deliverables by the 3 companies and the consequent review of all the documents by NBTF Team. In August a "mini-competition" among the 3 companies was reopened to get offers for Stage 2 (the actual manufacturing of MITICA BS) by the beginning of October. Only one offer out of 3 companies was received and it was judged technically not compliant, leading to the cancellation of the procedure. Now discussion among the stakeholders is ongoing to identify possible solutions.

2.1.3.3 MITICA Beam Line Components

During 2017 the process for CfT of MITICA Beam Line Components (BLCs) took place. The procurement contract is a two-stages contract, as for MITICA BS.

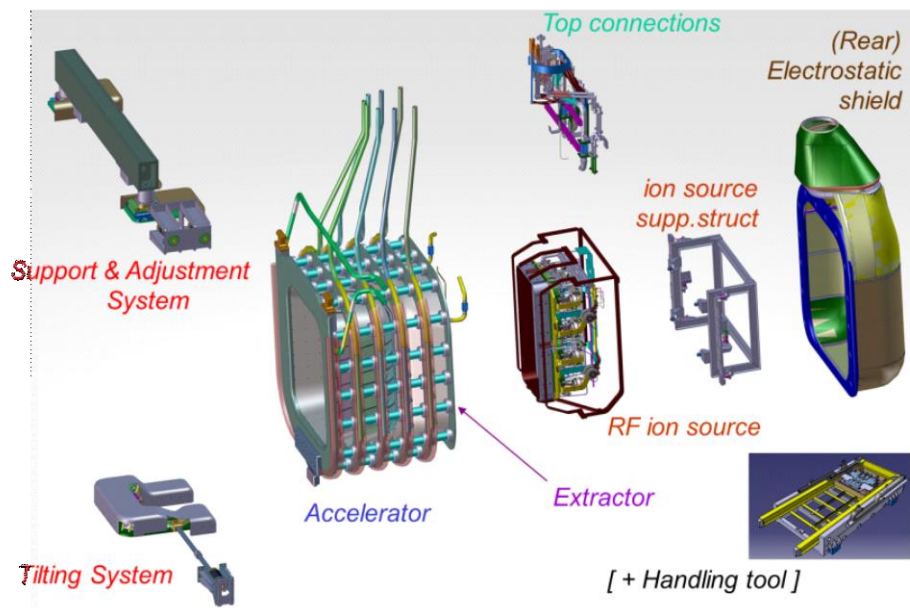


Fig. 2.1.32 Exploded view of the MITICA Beam Source under procurement.

- and tests of some prototypes (3 suppliers are awarded)
- Stage 2 for manufacturing and supply of the MITICA Beam Line Components with CfT restricted to the suppliers completing with positive result the Stage 1.

The CfT for Stage 1 was issued on 9th February 2017. Tenders evaluation started in May 2017 and the procurement contract for MITICA BLCs has been signed on 27th November 2017. Kick-off meetings with the three suppliers were held in December. NBTF Team guaranteed technical support during CfT phase (clarifications to bidders) and prepared a possible early purchase of CuCrZr alloy pipes and bars by F4E, for Stage 1 prototypes. Further work was spent to deal with various feedbacks by involved experts and engineering consultants. Final updates of CAD models and Technical Specification were done in 2017 to prepare the final version of documents and CAD models for Stage 1 procurement. Support was also given during the tender evaluation phase and for the initial follow-up phase at the end of 2017. The Stage 1 contract duration is 9 months, so the closing date is 26th August 2018. The following schedule is presently foreseen for Stage 2 procurement: launching of Call for Tender in Q1 2019, contract signature in Q3/Q4 2019 and duration 36 months.

• S
tag
e 1
for
Bas
elin
e
revi
ew
plu
s
ma
nuf
act
urin
g

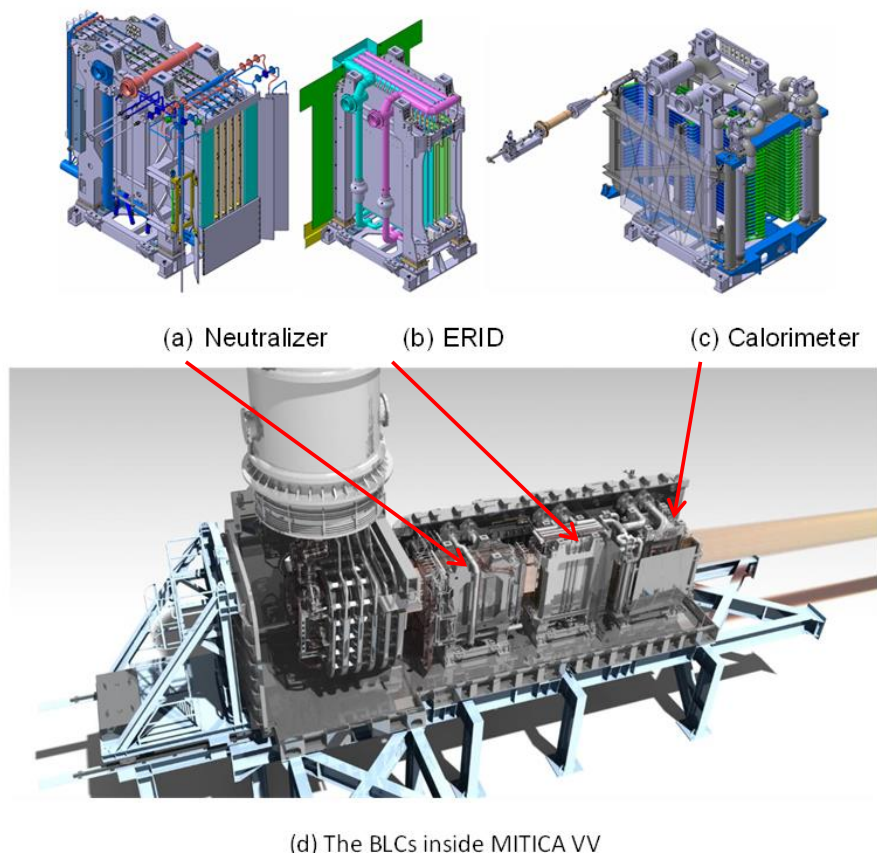


Fig. 2.1.33 Isometric views of the 3 MITICA Beam Line Components (a), (b), (c) and section view of the components installed inside the MITICA Vacuum Vessel (d)

2.1.3.4 MITICA Cryopumps

A specific procurement contract was launched in December 2016 by F4E for “The design, the prototyping and the manufacturing of Johnston Couplings for the MITICA Cryopump and Cryogenic Plant”. These are specifically customized connection elements between Cryopumps and Cryogenic Plant.

The contract for Johnston couplings was awarded to WEKA in January 2017 and closure is foreseen in Q1 2018. The Prototype Design Review meeting was held on 7th June at IO. Manufacturing was then completed and the factory tests positively carried out (see Fig. 2.1.34). Production and final tests of series parts is on-going. The technical follow-up of MITICA Johnston Couplings procurement (contract F4E-OPE-766) was carried out by NBTF Team providing technical support and taking part to meetings and documents review in F4E-IDM.

The MITICA Cryopump procurement is a complex procurement: subdivided in three Lots (Support Frame and Assembly, Expansion profiles, Charcoal coating) and two stages (negotiation/review and procurement), whose call for participation was issued in January 2017. Negotiation/review phase among F4E, IO, RFX and three bidders was completed mid July 2017. Reviewed specifications were issued by F4E in September 2017

(intermediate phase). Awarding of contract for procurement is scheduled in Q1 2018. During 2017 review of technical documents were performed by the NBTF Team and technical support was given for the Cryopump CfT negotiation phase, closing it with the final CfT documents preparation.

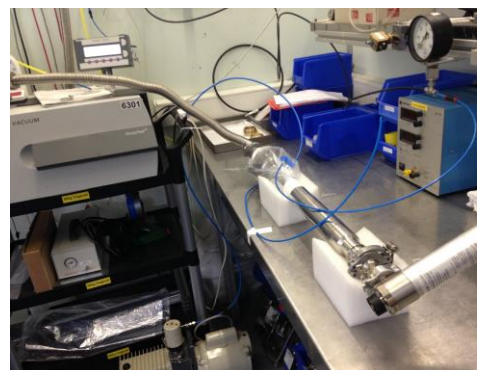


Fig. 2.1.34 – Johnstone Coupling prototype tests at WEKA workshop

2.1.3.5 MITICA Cryogenic Plant

The main functions of the Cryogenic Plant for MITICA experiment are:

- to produce supercritical Helium (ScHe) at 4.6 K and gaseous Helium (GHe) at 81 K and to feed these cryogens to the cryopump placed inside the MITICA Vacuum Vessel;
- to supply the needed refrigeration power to remove the heat loads on the Cryopump during different experimental scenarios, while maintaining the cryopump panels at the correct operational temperatures.

The procurement of MITICA Cryogenic Plant was launched by F4E in September 2016 after a negotiation phase with two bidders. Air Liquide Advanced Technologies (ALAT) was finally awarded this procurement.

The NBTF Team gave technical support to F4E for the technical follow-up of MITICA Cryogenic Plant procurement during 2017, with regular activities and meetings for technical discussions and documents review. Specific aspects regarding the plant integration on PRIMA site, HAZOP analyses and relevant main design choices have been addressed, discussing and transferring the information to the supplier. Electrical and control aspects were also faced since the beginning of this contract to allow a smooth and correct development of these parts, requiring several interactions with the

supplier and sub-suppliers during the design development phase. The Preliminary Design Review meeting was held in March 2017.

Integration issues such as space occupancy, compatibility of loads and assembly feasibility have been specifically discussed with the supplier and other involved experts and on-site responsible personnel. The Final Design Review meeting was held at F4E on 25th- 26th September 2017. The procurement will continue during 2018 with on-site installation activities foreseen to start in April 2018. Completion of assembly and on-site tests are foreseen in Q1 2019

2.1.3.6 MITICA power supply systems

The MITICA Power Supply, see Fig. 2.1.35, includes the following main subsystems:

- the Acceleration Grid Power Supply (AGPS) producing the 1MV dc voltage, in 5 stages, 200kV each, needed to accelerate the ions. AGPS is divided into two parts: the AGPS Conversion system (AGPS-CS), provided by F4E, and the AGPS DC Generator (AGPS-DCG), provided by JADA;
- HV SF₆ gas insulated Transmission Line (TL), 100m long, connecting ISEPS and AGPS PS to the loads inside the vacuum vessel;
- the Ion Source PS (ISEPS) to feed the Ion Source, similar to the one for SPIDER (see 2.1.2.3)
- the HVD1, a 1MV Faraday cage hosting the ISEPS system, and the HV Bushing connecting the HVD1 to the TL;
- 1MV insulating transformer feeding ISEPS;
- the Residual Ion Dump PS feeding the electric panel of the E-RID;
- the SF₆ Gas Handling and Storage Plant (GHSP) a special plant for SF₆ gas management.

The HV components, including step-up transformers and diode rectifiers of AGPS, TL and 1 MV insulating transformer of ISEPS, are provided by JADA (parts in blue in Fig. 2.1.35) all the other PS components, including HVD1 and HV Bushing connecting the HVD1 to the TL, by F4E.

In 2017, a significant advancement has been achieved on the procurement of the MITICA Power Supply (PS). In the following the progress made and the state of procurement is highlighted

Ion Source and Extraction Power Supply system (ISEPS)

In 2017, the activity progressed with the completion of the ISEPS design revision, based on the findings from the commissioning and acceptance tests of the ISEPS for SPIDER,

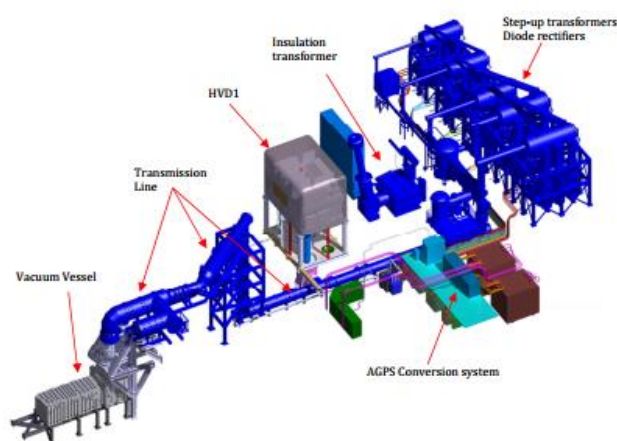


Fig. 2.1.35 - 3D view of the MITICA Power Supply system

and the start of the manufacturing phase. Components will be delivered on-site in September 2018 and installation phase will the start. Overall, activities have not progressed fast enough for on-site delivery to take place before the high-voltage components are already under test. Hence additional postponement of their installation.

Acceleration Grid Power Supply (AGPS)

The AGPS is a special conversion system feeding around 60 MW at -1MV dc to the acceleration grids. It has to interrupt the power delivery in tens of microseconds in case of grid breakdown, which is a condition expected to occur rather frequently during a pulse. The ITER AGPS reference scheme consists of an ac/dc stage feeding 5 three-phase inverters, each connected to a step-up transformer feeding a diode rectifier and a DC filter. The rectifiers are connected in series at the output side to obtain the nominal -1 MV dc acceleration voltage, with availability of the intermediate potentials.

Acceleration Grid Power Supply Conversion system (AGPS-CS)

The AGPS-CS includes 2 step-down transformers, the ac/dc converter and the dc/ac inverters and the control system. In 2017 the procurement activities progressed very well. After completion and approval of the detailed design, the manufacturing phase started. The step-down transformers were realized by a sub-supplier, tested in factory and delivered on site, see Fig. 2.1.36.

Conversion system realized and assembly in the supplier premises and in the period Q2 and Q3 a very close testing plan was followed and maintained until the completion of all the tests, the most significant of which is represented by the real simulation of the short circuit of a power component during full power operation.



Fig. 2.1.36 Step-down transformers

In September installation activities have been started. Also in this case, activities have progressed very well maintaining the installation schedule, see Fig. 2.1.37. Completion of this phase is foreseen by mid-January 2018, followed by the start of the commissioning phase. For the latter activity an important issue is the unavailability of the cooling plant necessary to cool the power components during commissioning activities. To solve this issue NBTF Team is working to set up a temporary skid able to satisfy the minimum cooling requirements.

Acceleration Grid Power Supply – DC Generator (AGPS-DCG)

The installation activities of JADA HV components, started in December 2015, prosecuted in 2016 and first half of 2017 without delays. All DCG components, the 1MV insulating transformer and 90% of TL, have been installed.

Afterwards, due to a significant delay of the availability of the BS Vessel, installation activities stopped for 5 months until December. Meanwhile, an alternative installation plan has been agreed and applied. This plan entails that the last piece of the TL, named TL3 bend, interfacing the BS Vessel through HVB will not be installed and TL will be closed by a special cup. Then the tanks containing the high voltage components will be

filled with SF6 gas, and the insulation tests will begin.

Also in 2017, support has been given by the NBTF Team to the installation of JADA components. The activities were performed under the supervision of QST laboratory of Naka and Hitachi experts, with specific contributions



Fig. 2.1.37 AGPS-CS installed on site

of the NBTF Team to finalize solutions for different issues encountered during operations.

High Voltage Deck and Transmission Line

The HVD1 is a large Faraday cage (12 m x 8 m x 10 m), air insulated to ground for -1 MV dc, that hosts the ISEPS system. The ISEPS outputs are connected to the TL via an air to SF₆ gas HV Bushing Assembly (HVBA), installed under the HVD1.

The design phase of the HVD1 and HVBA, closely monitored by the NBTF Team, was completed in June 2016, followed by the manufacturing phase. At the beginning of 2017 factory tests including 1MV insulation tests of the HVD1 mockup and of the HVBA were successfully completed.

The on-site activities began in May with the installation of the HVBA inside the TL pit (see Fig. 2.1.39), and ended in Fall with the functional tests of the auxiliary plant systems (see Fig. 2.1.40). Final acceptance tests will consist in the 1.3 MV insulation tests feasible only after connection of HVBA to TL by the Connecting Piece (CP). This activity is scheduled in Fall 2018.

The CP is a challenging interface between the HVBA and the TL not completely defined during the design of TL and HVBA. It consists of an external tank with bellows to be fixed to TL and HVBA flanges and a set of internal conductors enveloped in the HV screen. In

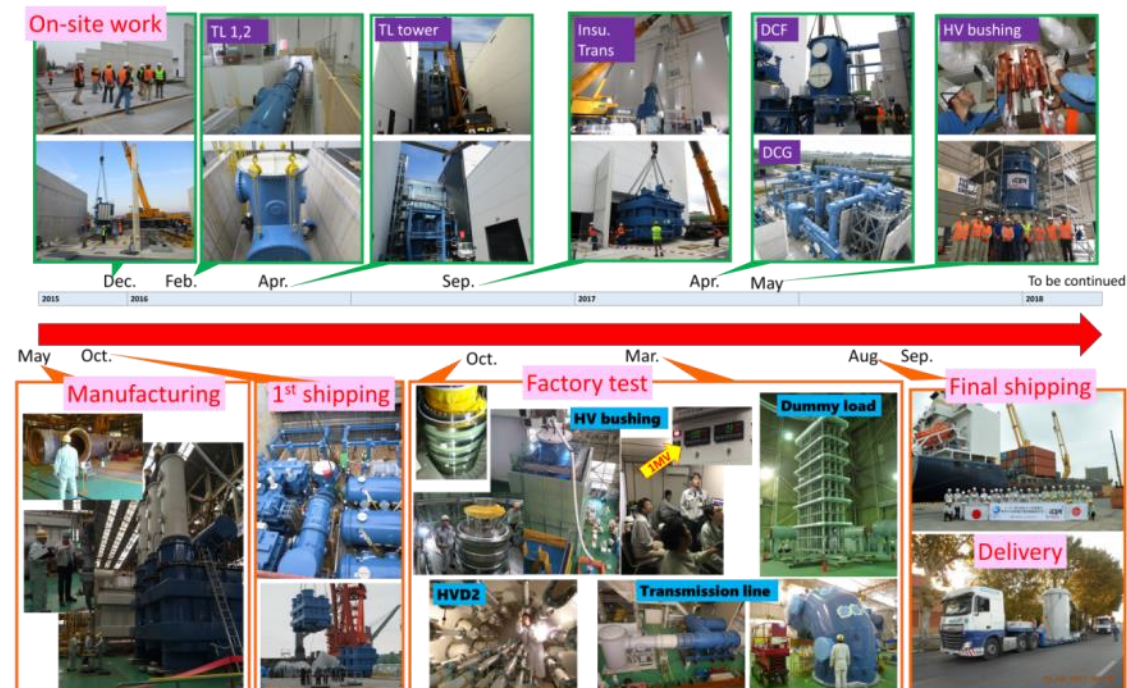


Fig. 2.1.38 Some significant milestones reached in NBTF Site during installation activities of the JADA components



Fig. 2.1.39 Installation of the HVBA inside the TL2 pit. Left: lifting of the HVBA before downloading in the pit. Right: HVBA inside pit with view of flanges interfacing the Connecting Piece

2017, a big effort was done by NBTF Team in order to correctly define all the aspects of the interface; in particular, an integrated mechanical model including TL and HVBA has been developed to calculate the stress transmitted through CP both in normal condition (effects of gas pressure, thermal expansion, weights, etc.) and in case of seismic events. On the basis of this model it has been demonstrated that forces transmitted in normal conditions can be sustained by the components without modifications, whereas, to sustain seismic events, a reinforcement structure must be installed. While JADA will install the CP, the NBTF Team will provide the additional components defined as a result of the study, included the reinforcement structure. The activity will terminate in 2018.

Ground related Power Supplies (GRPS)

In 2017, the follow-up of the contractual activities on GRPS prosecuted with 2 Progress Meetings and the revision of the technical documents released by the supplier. In particular, to answer the chits collected during the Design Review Meeting on the First Design Report held in December 2016, the supplier provided detailed seismic analyses on the RIDPS, a report on studies carried out for a specific fault condition in the RIDPS power modules and a report to demonstrate the proper working of RIDPS in no-load conditions. These documents satisfied the DRM panel (which includes a representative of the NBTF Team) and the chits were closed. The requirements and the scheme of the water cooling system have been discussed among the supplier, F4E and the NBTF Team, evaluating the need to increase the nominal pressure of the water, as required for



Fig. 2.1.40 Overview of the HV components inside High Voltage All. On left: 1MV bushing of insulating transformer. On right: HVD1 with temporary scaffolding necessary to access inside the Faraday cage.

the AGPS-CS (which is connected to the same circuit PC09). The increased pressure has been formalized by F4E with a Deviation Request, in which it is also specified the capability of RIDPS to self-protect in case of out-of-range water temperatures after long shutdown periods; this implies the adoption of an automatic bypass valve to avoid condensation. The impact of the Deviation Request is being evaluated by the supplier. In 2017 the technical specification of the RIDPS transformer has been provided by the supplier and reviewed by the DRM panel. A 3D CAD drawing of RIDPS has been also provided and it is being analysed by NBTf Team, focusing in particular on possible interference with AGPS-CS and other equipment installed in the same building.

SF₆ Gas Handling and Storage Plant (GHSP)

The SF₆ Gas Handling and Storage Plant (GHSP) is used to manage the SF₆ gas of the MITICA Plant. During 2017, the design of the SF₆ GHSP has been finalized. The components (storage tanks, pipes, storage area roof and Gas Handling Units) have been delivered to the MITICA Site and the plant has been installed. On-site pressure tests have been performed in order to ensure that the high pressure and low pressure piping was correctly welded. About 34 tons of SF₆ gas was delivered to the Site and temporarily stored in an external area, before final transfer to the seven storage tanks. In late 2017 the final acceptance test on-site has been performed by using the Gas Handling Units, individually and in parallel, to transfer the SF₆ gas from the storage tanks to a dummy

compartment placed on the mezzanine floor of Building 1. Various functions have been tested with satisfactory results. NBTF Team has been trained to use the GHSP and actively involved in the tests. The property of the system has been transferred to F4E and the plant is now being licensed by a notified body for the final transfer for use to RFX.



Fig. 2.1.41 Gas Handling Units

2.1.4 Vacuum high voltage holding modeling and experiments

During the WP 2017 five experimental campaigns, and more than 50 sessions, have been done at the High Voltage Padova Test Facility. Several sessions have been carried out adopting electrodes having not symmetric geometries (see Fig. 2.1.42).

A conditioning procedure to raise the voltage automatically has been implemented to obtain reproducible experimental results.

The study of the X-ray spectra emitted during the experimental sessions is a new method to investigate the nature of the physical phenomena during the high voltage conditioning in vacuum. Currents, X ray energy spectrum, voltages, and pressures have been routinely recorded during the year (see Fig. 2.1.43). An experimental campaign has been dedicated to test the effectiveness of some glow discharges treatments to improve the DC voltage holding in high vacuum. (see Fig. 2.1.44). The composition of the gas desorbed during the high voltage condition in high vacuum has been analysed routinely since February 17, an example is shown in Fig. 2.1.45.

The collaboration with QST laboratories has going ahead to benchmark the RFX Voltage Holding Predictive Model with the experimental results obtain by the Japanese HV test stand shown in Fig. 2.1.46.

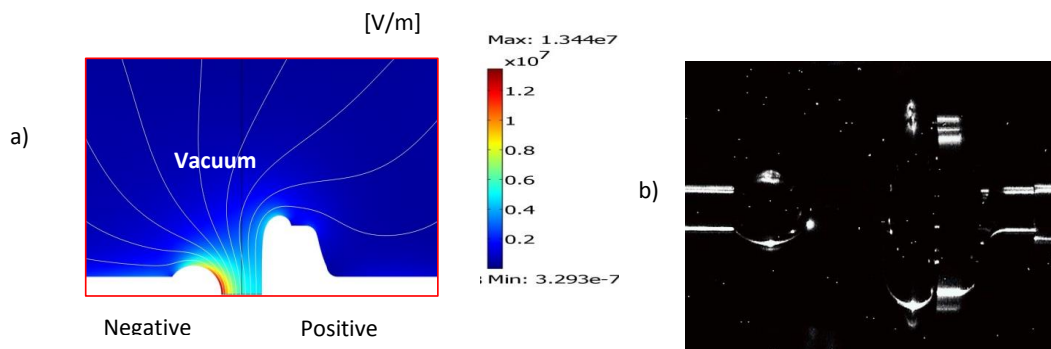


Fig. 2.1.42 a) Electrostatic field map of a Sphere-Plane configuration, vacuum gap length 30 mm, 200kVdc between electrodes b) picture of the electrodes under test during a micro discharge occurrence.

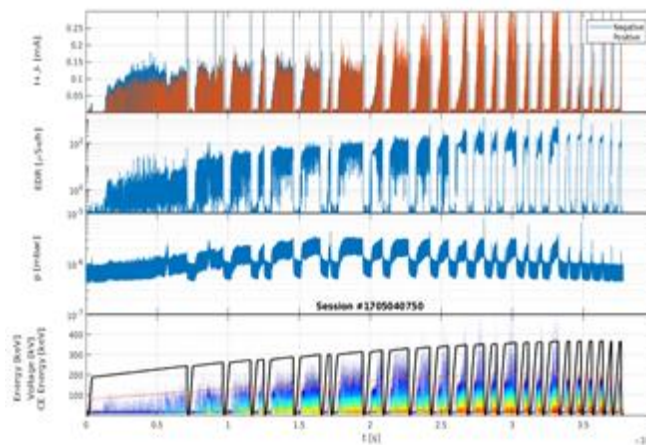


Fig. 2.1.43 Measured currents , X ray Equivalent Dose Rate , pressure , X ray spectrum and Voltage during session #1705040750

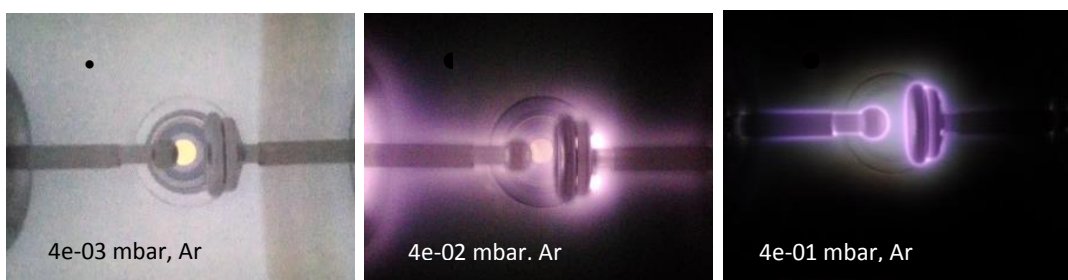


Fig. 2.1.44 RF glow discharge in Argon at different pressures, $f=40$ MHz, $P \approx 50$ W

2.1.5 RF R&D

In 2017 the main RF R&D activities were focused on the commissioning, first operation and further development of the High Voltage Radio Frequency Test Facility (HVRFTF): a simple, accessible and flexible test bed to characterize the dielectric strength in vacuum of the RF drivers of SPIDER and MITICA ion sources and address the issues related to

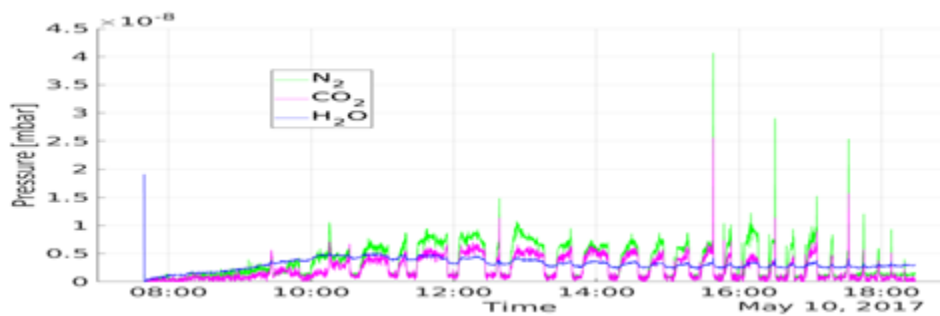


Fig. 2.1.45 RGA dominant signals in session# 1705050750 (same as Fig. 2.1.42)

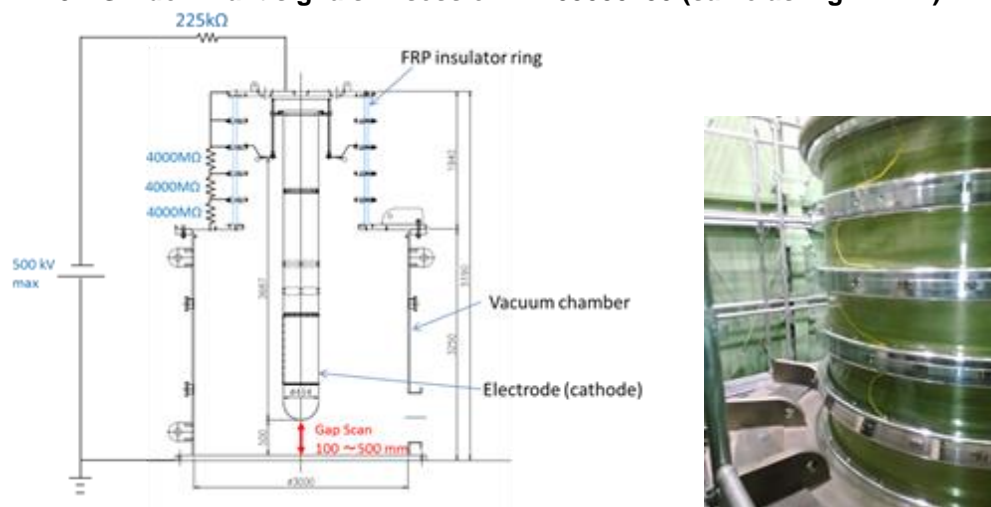


Fig. 2.1.46 New HV test facility installed at the QST laboratories in Naka, vertical cross section and picture of the HV bushing insulated by FRP rings

their voltage hold off when subjected to their operational radiofrequency E-fields and pressure.

Two test campaigns in Argon were carried out in 2017 on stainless steel Planar Circular Electrodes (PCE). Currently the HVRFTF is able to supply RF voltage of about 10 kV, producing E-fields up to 55 MV/m with a gap between the electrodes of 0.2 mm.

An issue arisen about the occurrence of a glow discharge between the high voltage electrode and the Vacuum Vessel at relatively high pressure was partially fixed with the adoption of a couple of insulating tubes placed around the electrodes (Fig. 2.1.48). The typical waveforms of a shot with a glow discharge are shown in the plots of Fig. 2.1.47.

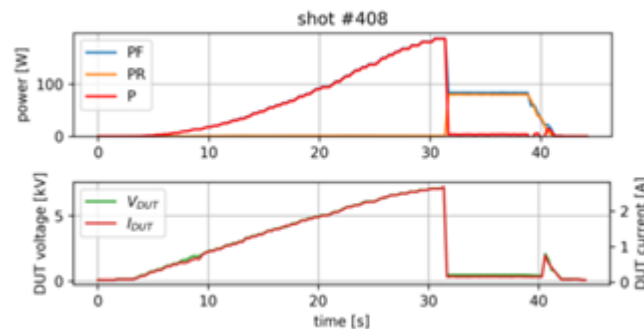


Fig. 2.1.47 Typical shot waveforms with breakdown at 32 s (some curves overlie).

No breakdown between the electrodes was detected by the data acquisition system, nevertheless some sparks were visible for short gaps (0.1 and 0.2 mm), see Fig. 2.1.49 a). After the test campaign the electrodes surface were visibly damaged see Fig. 2.1.49 b) and c).

In parallel to the experimental campaigns in 2017, analyses were carried out in order to identify suitable mockups of SPIDER and MITICA drivers to be tested on the HVRFTF. The PCE tested during the first campaigns in fact, have been useful for the validation of the test arrangement, but are not suitable to reproduce the E-field on the drivers.

Different configurations were considered as possible mockups and their E-fields were calculated by means of electrostatic analyses. The best configuration worked out for the scope is based on a couple of electrodes (one plane and one spherical) with a dielectric material in between. However, the studies have highlighted that a single sphere diameter is not sufficient to accurately cover the entire gap range of interest; in particular, the sphere diameter has to be increased in parallel to the gap increase. Nevertheless, 3

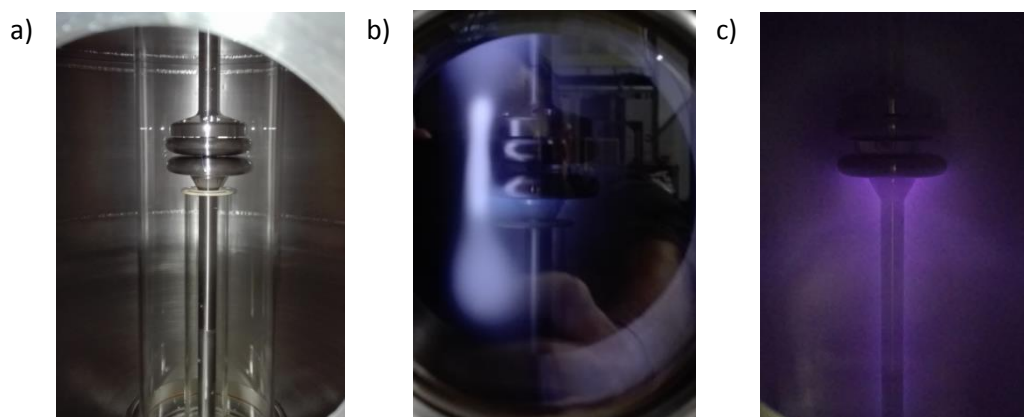


Fig. 2.1.48 Photos of the VV inside: a) PCE and tubes after installation (lighting from the outside), b) glow discharge around the bottom electrode and its support confined by the insulating tube with larger diameter, c) glow discharge without tubes, for comparison.

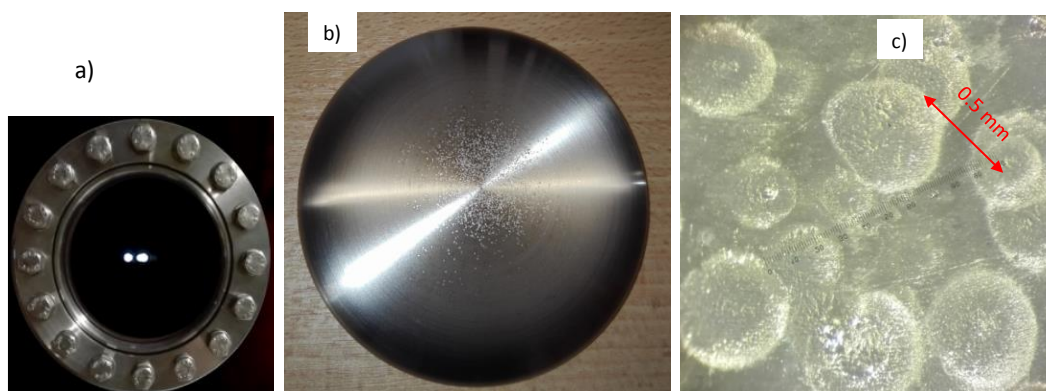


Fig. 2.1.49 a) Photo of sparks between the electrodes (frame extracted from video, the flange was added to figure out the position of the sparks); b) photos of one electrode after the second test campaign; c) Magnification of the electrode surface under an optical microscope (photos taken with a mobile phone through the ocular).

diameters (40 , 50 and 60 mm) are sufficient to reproduce the E-field trend of the driver with a relative difference of $\pm 10\%$ for the gaps of interest.

2.1.6 Development and test of Caesium Ovens

In the SPIDER beam source fresh Cs has to be injected in a controlled way by means of 3 Cs ovens. Since the Cs ovens are embedded in the source, their design has to be vacuum and high temperature compatible, and include remote operation.

Design and Design Review were completed successfully in 2016 and Procurement of SPIDER oven prototype was started.

To test the SPIDER ovens, support the experiments and develop MITICA/HNB-relevant design modifications a test stand, the Caesium Test Stand (CATS), was designed in 2017, to be realized on PRIMA site, see Fig. 2.1.50. The facility was installed and commissioned for the thermal tests on the oven prototype, preparations for caesium campaign are ongoing see Fig. 2.1.51, Fig. 2.1.52. The thermal tests were carried out (see Fig. 2.1.53,) with successful results: the oven behaviour, and in particular of the heating systems, is now known, and transfer functions between input power and effective temperature distribution can be positively applied.

Several tools are already in place to manage the next experiments, as the glove box (see Fig. 2.1.54), plus several specific diagnostics, like the Surface Ionization Detector and the Laser Absorption Spectroscopy, which will be also tested in view of the utilization for SPIDER experiments.

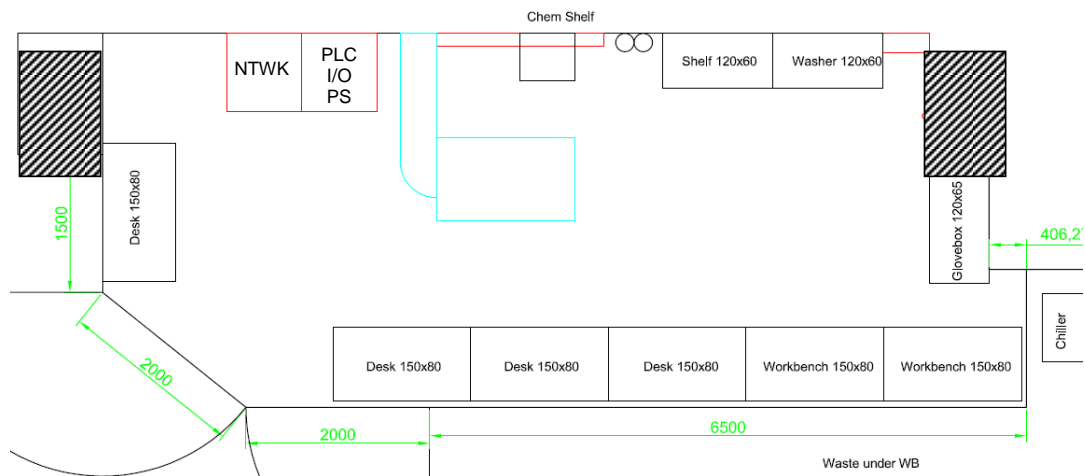


Fig. 2.1.50 Layout of the Cs-oven test bed site.

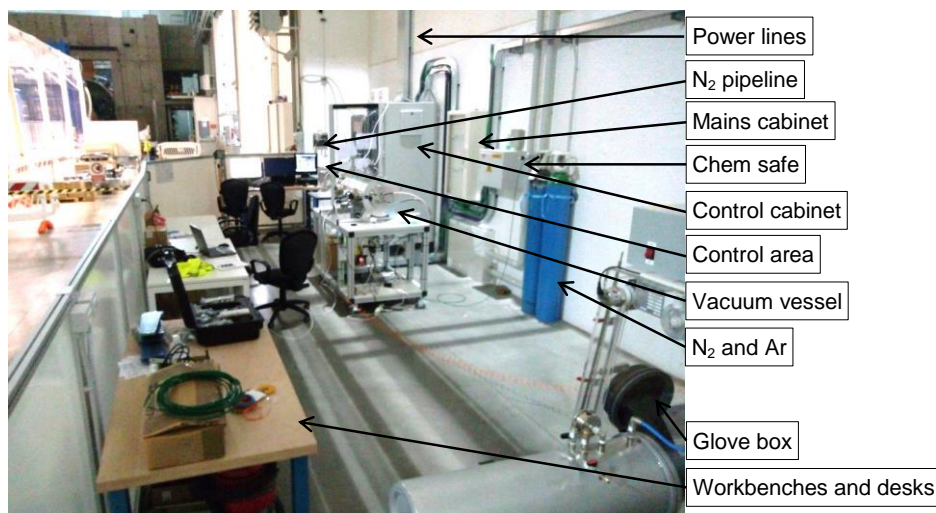


Fig. 2.1.51 Implementation of the Cs-oven test stand site.

2.1.7 Host Activities

During 2017 significant resources were invested on activities for construction supervision and coordination, both concerning buildings completion, with their auxiliary systems, and installation of experimental plants.

Particular effort was required to manage interfaces between buildings and experimental plant units: in fact, most of the latter are now fully assembled and tested or in advanced procurement phase. Also the management of the interfaces between plant units themselves required large effort: specifically to this end, the interface management structure, run by RFX personnel, worked in a coordinate way with the aim of reducing as much as possible clashes during installation of plants being able to define in real-time the modifications required in any of the plants.

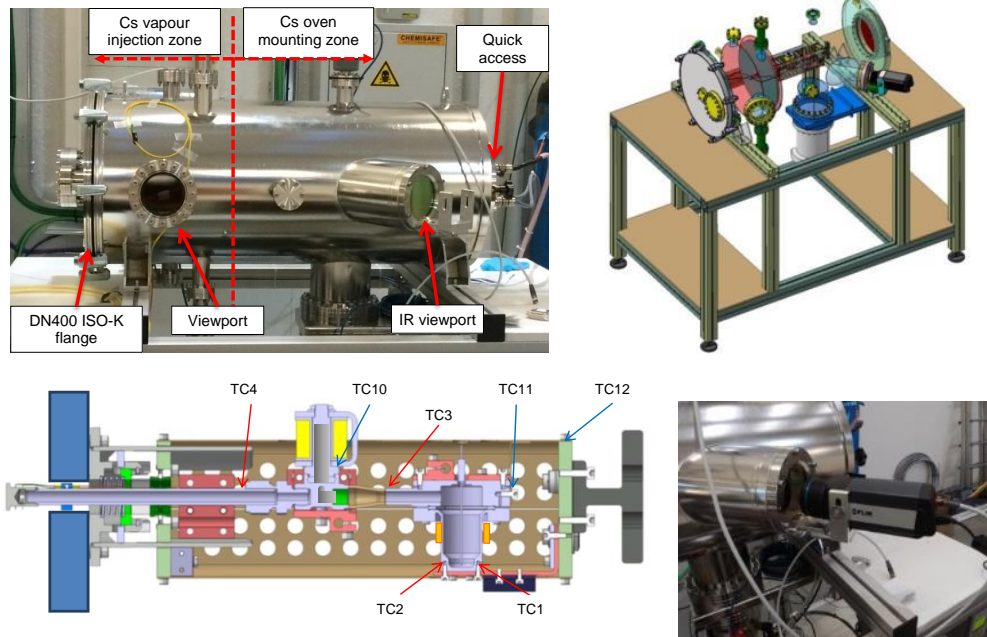


Fig. 2.1.52 CATS vacuum vessel and internal components, in particular the oven and the thermal camera.

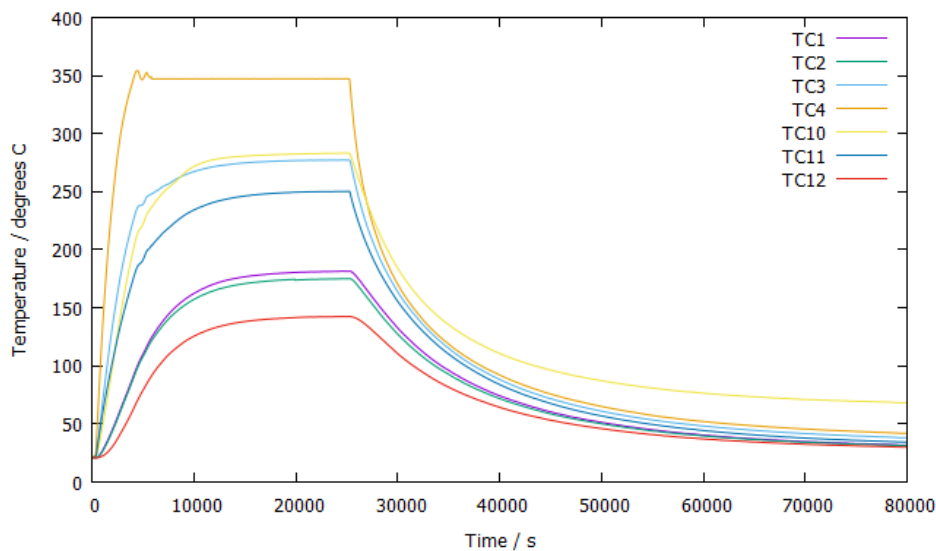


Fig. 2.1.53 Example of results for characterization of oven temperatures.

The support to F4E and the other Domestic Agencies for the management of the Construction-Erection All Risks insurance contract for the NBTf (CEAR), directly managed by Consorzio RFX, continued. A flooding event in building #2, happened in November the 13th, was claimed to the insurance (still under evaluation).

The NBTf-site management, with reference to “Titolo IV of D.Lgs. 81/08” (Health and Safety on-site), whose structure had been set up through the Implementation Agreement, continued in 2017: the Responsible of Works and the Safety Coordinator continuously monitored and periodically reported the state of the site. Significant resources were spent

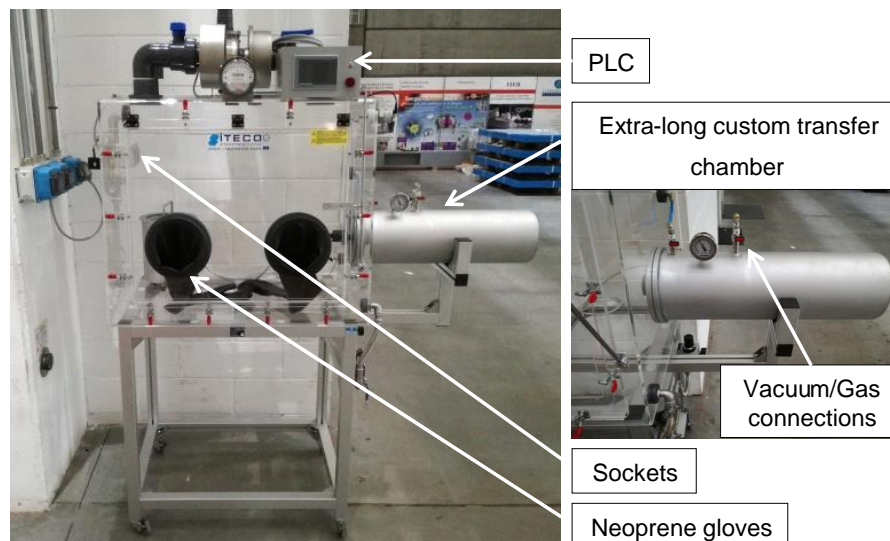


Fig. 2.1.54 Glove box for caesium handling.

to assist F4E, in particular, by the Safety Coordinator who is in charge for the issue of all the Plans for Safety and Coordination (called PSC documents), being the latter an essential part for both the procurement call for tenders and contracts management. RFX personnel (contract Liaison Officer-LO and Deputy Liaison Officer-DLO) closely collaborated with the Safety Coordinator to this end.

With the support of the Coordinator of the Directors of Works (namely CDL) the time schedule for MITICA on-site activities was prepared and discussed among Consorzio RFX and all involved Domestic Agencies during the year: it has not been frozen yet because of uncertainties on some procurement contracts. Furthermore, as a coordination method, more than 40 weekly Site Progress Coordination Meetings (SPCMs) have been held, and the minutes distributed and uploaded in F4E IDM. The SPIDER time schedule has been also managed by preparing, discussing and verifying weekly the activity plan with a visibility of one week, 3 weeks and 3 months.

Several site inspections were performed by nearly all of the Companies and Domestic Agencies that were operating.

General follow up activities were performed for all the companies working on-site and all the companies related to the Balance of Plant procurements. Further working activities have come from the companies involved into the three signed Framework Contracts (CODAS-Interlock-Safety, Diagnostics, Assembly).

A very large effort has been given to INDA and its suppliers by the NBTF team concerning the SPIDER AGPS installation and verification works: in particular the review of the design all the documents required several interactions and follow-up activities.

As for the Licence to operate the two experiments:

- for SPIDER the license (Nulla Osta) category A (art.28 D.Lgs.230/95 e s.m.i.) arrived in November 2015 with some prescriptions. The final “Nulla Osta” with prescriptions for SPIDER has been obtained on 15/07/2016 allowing the operation of the test bed.
- for MITICA the preparation of all the necessary documents to be sent to the Italian Authorities progressed with priority given to the radioprotection technical report that is now ready to be submitted.

Metrology on-site activities were performed mainly devoted to the definition of the SPIDER, MITICA and PRIMA networks. CAD-related metrological activities, complementary to the on-site ones, have been also carried out. The full metrology survey of the PRIMA site areas has been completed preparing, for example, the information (absolute coordinate system, reference coordinate systems and reference fiducial points) to be given to the companies “as reference” or “starting point” for the installation/positioning of different components.

Periodical measurements of the positions of the fiducial points were performed to check the motion of the buildings both during their settlement period and during preloading phase (as for transformers areas). In addition, Consorzio RFX metrology team gave large and frequent support to the personnel of the main contractors in charge for metrology activities, or performed activities on behalf of them.

Starting from February, the Transfer for Use of some Items began. The first Item formally transferred was the SPIDER ISEPS: the ownership is now with ITER and CRFX has the responsibility for use, the latter transferred from F4E to CRFX as per Agreement.

The management of the safety and the personnel on roster for the commissioning activities started for the one-to-one commissioning of SPIDER ISEPS, and prosecuted for the commissioning of the Gas and Vacuum System (GVS) and for the Transmission Line.

2.2 ITER Modelling

In 2017 the contribution to the ITER modelling activities were mainly carried on with studies and analysis on existing devices. In particular validation studies of the M3D code on the JET device and studies related to magnetic topology reconstruction in AUG have been done.

These activities are presented in some more details in the next two paragraphs.

We mention also that Consorzio RFX contributed to the future ITER modelling and analysis system. This important activity regarding the ITER Integrated Modelling and Analysis Suite (IMAS) has been devoted in 2017 to the development of a new data access layer for supporting the data model of the infrastructure, extending the former model used in the Integrated Tokamak Modelling (ITM) initiative. In particular, two layers (backend) are being developed, one based on MDSplus data access and the second one providing memory caching functionality. The use of memory caching speeds execution, since temporary data handled by the simulation programs is only maintained in memory and not written back to disk, and it proved to represent a key factor for the optimization of workflows.

2.2.1 *M3D code validation on JET data*

The M3D code has been used in the last few years for studying disruptions and hot Vertical Displacement Events (VDEs). Despite the code had been already applied to ITER equilibria, a code validation on actual experimental data was still missing and it was considered very urgent. Therefore in 2017 the code was used to simulate a JET case and a careful comparison between code predictions and experimental results has been done. In Fig. 2.2.1 the comparison between experimental macroscopic quantities and code predictions are shown.

The analysis confirms a good correspondence between the model results and the halo fraction and forces as measured in JET. In particular also the Noll⁶ formula, which relates the horizontal force in non-axisymmetric VDEs to the vertical current moment M_{iz} is well confirmed by the simulations.

6 V. Riccardo et. al., Nucl. Fusion 40, 1805 (2000)

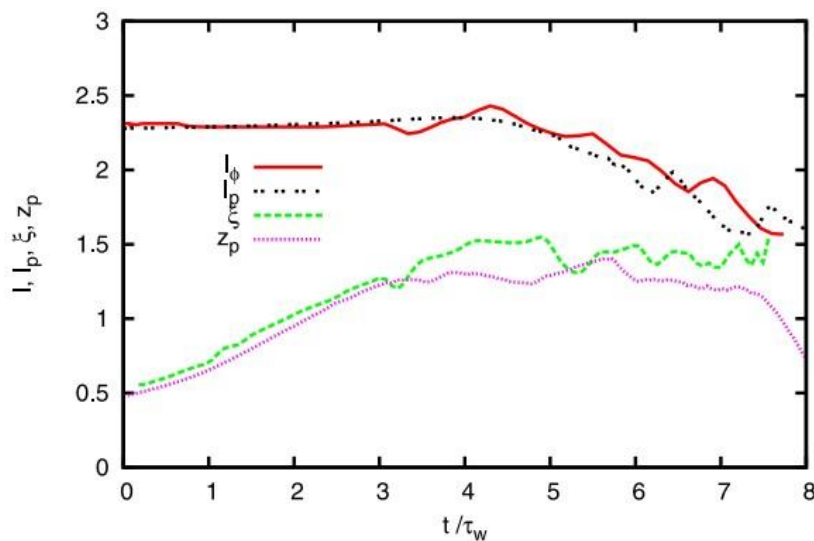


Fig. 2.2.1 Plasma current and vertical position vs. time (normalized to the wall magnetic field penetration time) (black dots and magenta are experimental traces).

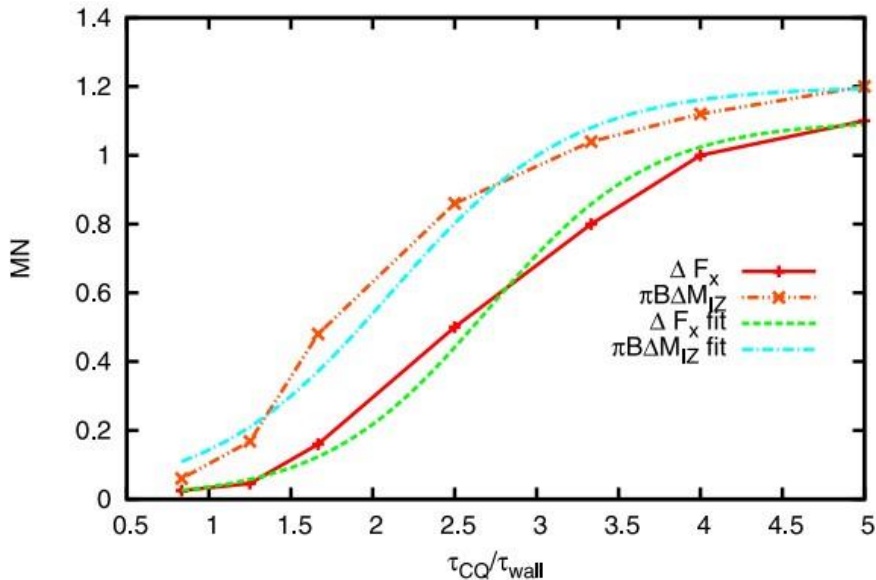


Fig. 2.2.2 Simulation results for JET force (MN) and the Noll's factor vs. time (normalized to the wall magnetic field penetration time).

An important result of this work is shown in Fig. 2.2.2, where the forces are estimated as a function of the current quench time normalized to the wall penetration time starting from the analyzed JET case. It is seen that when this ratio decreases (the actual ratio for JET is around 8-10) the forces also decrease. Since in ITER the current quench is estimated in the order of 50 to 150 ms while the wall penetration time is of the order of 300 ms the forces are expected to strongly decrease and according to this, may be that the ITER forces will be not much different from those measured in JET. Obviously this prediction

based on the JET simulations should be confirmed by new ITER simulations that are presently under way.

2.2.2 *Magnetic topology reconstruction*

During year 2017, the study of the magnetic topology of an L-mode density limit discharge prior to a minor disruption in AUG, via the code ORBIT⁷, has been continued. This scenario is a current topic in the MST-1 EUROfusion program⁸ and in the ITPA-PEP19 program. These disruptions in AUG are believed to be dominated by stochastization due to the superposition of many high- m harmonics ($3 \leq m \leq 5$) coupled

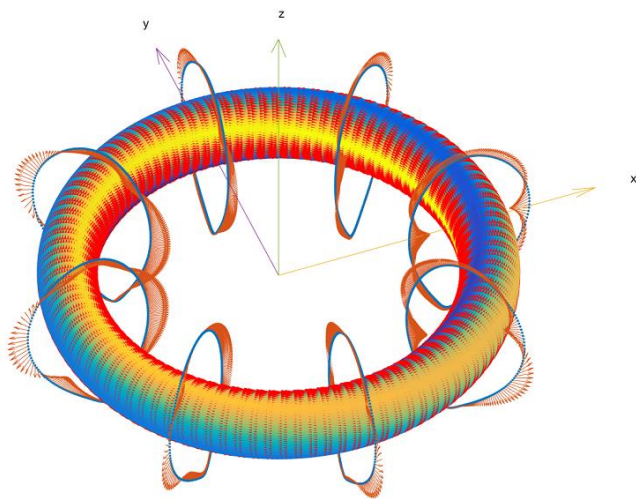


Fig. 2.2.3 Reconstruction of the current due to a 2/1 TM in AUG. The contour is the amplitude of the general current scalar field W on the resonance $q=2$ (yellow=large W , blue=small W), the red arrows representing the resonance currents of the TM. On the LCFS (blue contours at 8 different toroidal angles), we calculated the perturbation fields.

to a dominant $m=2$, $n=1$ tearing mode (TM), which is braking and increasing in amplitude near the final phase of the disruption⁹. Since high m harmonics are considered, a study of the role of passive structures, mainly the poloidal stabilization loop (PSL) has been undertaken¹⁰. The main idea is to use the “step-current” approximation (vacuum eigenfunction) to evaluate the current at the resonance of each $m=2-5$, $n=1$ mode, and insert this value in two very similar codes, which solve eddy-current problems on general polyhedral meshes: these latter codes are CAFÉ and VINCO¹¹.

To this purpose, a general current representation has been developed, to connect the amplitude of the TM eigenfunction, expressed in ORBIT as $\delta\vec{B} = \nabla \times (\alpha\vec{B})$, to the TM current, expressed in CAFÉ as $\vec{j} = \nabla W \times \frac{\nabla\psi}{|\nabla\psi|}$. In this way, for a given amplitude α (in ORBIT-units) it is possible to calculate the 3D magnetic field, in any position in the

7 White, R. B., & Chance, M. S. Phys. Fluids, 27 (1984), 2455.

8 Maraschek, M. et al Plasma Phys. Control. Fusion, 60 (2018), 014047

9 Igochine, V, Nucl. Fusion, 46 (2006) 741-751.

10 Schittenhelm, M., & Zohm, H. Nucl. Fusion, 37(1997), 1255.

11 Bettini, P., & Specogna, R. IEEE Transactions on Magnetics, 52 (2016), 7203104.

machine: in Fig. 2.2.3 the result is shown, for a 2/1 mode and $\alpha = 1$. In particular, it is possible to calculate δB_θ at the location of the in-vessel pick-up probes, and calculate the response matrix (complex coefficients) $B_{\theta,coil} = \vec{M}\alpha_{m,n}$. The result for $\omega=0$ should match the simple calculation, already done in 2016 with the Meskat eigenfunctions¹², while the calculation for $\omega>0$ should give new, interesting insight into the mechanism of toroidal coupling before tokamak disruptions.

2.3 ITER Diagnostics

2.3.1 ITER core Thomson scattering

The activity of RFX in the design of the ITER core Thomson scattering (TS) system continued in 2016 in the framework of the IO/16/CT/4300001320 contract, whose expiration date has been extended by IO from 16/06/2017 until 31/12/2017. The research activity has been carried out in close coordination with the CCFE and IPP Prague partners, through regular VC meeting held every two weeks. Our main contributions to the contract work have been:

- 1) The performance analysis, including the effect of plasma light^{13 14}.
- 2) A complete assessment of the feasibility of polarimetric TS measurements^{15 16}.
- 3) The analysis of dual-laser TS measurements.
- 4) Revision and update of calibrations techniques^{17 18}
- 5) Revision and update of alignment techniques¹⁹.

For 1) a specific code has been developed for the calculation of the plasma light background detected along each Thomson scattering observation chord that determines the expected plasma emissivity from realistic models of T_e and n_e distributions in the plasma deduced by ITER scenarios available in IDM. The effect of line radiation and of the light reflected by the ITER wall has been included using data obtained by CCFE with the CHERAB code, and validated by measurements in JET.

12 Meskat, J. P. Plasma Phys. Control. Fusion, 43, (2001) 1325.

13 R. Scannell, M. Maslov, G. Naylor, T. O’Gorman, M. Kempenaars, M. Carr, P. Bilkova, P. Bohm, L. Giudicotti, R. Pasqualotto, M. Bassan, G. Vayakis, M. Walsh and R. Huxford, "Design advances of the Core Plasma Thomson Scattering diagnostic for ITER" JINST 12 C11010 (2017).

14 "Performance Analysis" ITER_D_UG2AFL

15 L. Giudicotti, "Polarimetric Thomson scattering for high Te fusion plasmas", JINST 12 C11002 (2017).

16 "Depolarization measurements in ITER Core Plasma TS", ITER_D_UD7YKR,

17 "Alignment Systems" ITER_D_PVKNRU

18 O. McCormack, L. Giudicotti, A. Fassina, and R. Pasqualotto, "Dual-laser, self-calibrating Thomson scattering measurements in RFX-mod", Plasma Phys. Control. Fusion 59, 055021 (2017).

19 "Calibrations" ITER_D_Q5U6YP

For 2) a modification of the conventional layout of the detection system that integrates in the same spectrometer the polarimetric and the spectral analysis has been developed and analyzed, showing that this new scheme may improve the performances of the CPTS system in the $T_e \geq 25$ keV range.

For 4) studies on the dual-laser calibration techniques with a secondary laser operating at $\lambda = 1320$ nm have also been completed. In support of these advanced TS techniques an experiment for the measurement of the TS depolarization effect has been successfully performed in JET ²⁰ and RFX participated to an experiment of dual-laser, self-calibrating TS in the LHD stellarator.

2.3.2 Diagnostic systems Engineering Services

During 2018 two Task Orders have been launched as part of the Framework Contract on “ITER Diagnostic Systems Engineering Services”:

- TO#05 – “Engineering and coordination for the Outer Vessel Steady-state Sensors, PBS 55.A5/A6”:
- TO#06 – “Update of the design description and requirement documentation of the ITER magnetic diagnostic”.

The aim of the first Task is to support the ITER Project Team in the finalization of the design of the Steady State magnetic sensors system, presently conceived to be installed on the outer surface of the ITER Vacuum Vessel. In addition to this, the scope was to participate in the development of a novel in-vessel (in-port-plug) steady state sensors system to be installed in the ITER Diagnostic Shield Module (DSM), to achieve the neutron fluence comparable to that expected outside the DEMO vacuum vessel.

In order to qualify the reliability of such diagnostic system, an experimental test of Hall sensor prototypes in the WEST tokamak has been proposed (Fig. 2.3.1)

²⁰ L. Giudicotti, M. Kempenaars, O. McCormack, J. Flanagan, R. Pasqualotto and JET contributors "First observation of the depolarization of Thomson scattering radiation by a fusion plasma", submitted to Nuclear Fusion.

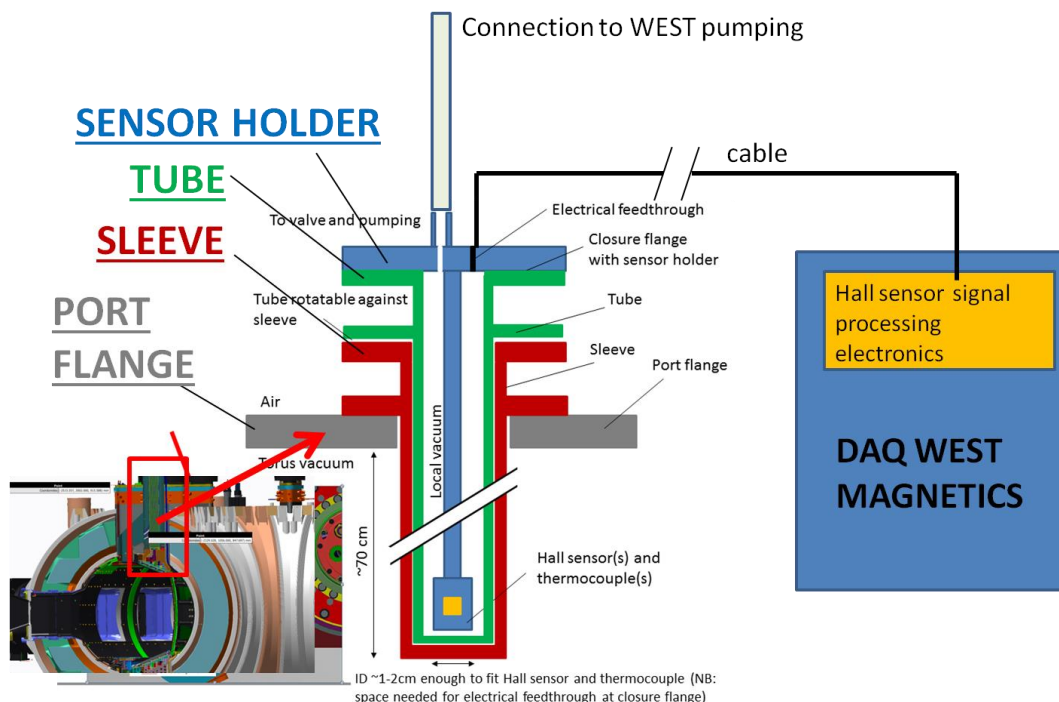


Fig. 2.3.1 Layout of the experimental setup for Hall sensor prototype tests in WEST

To this end a detailed design of an integrated diagnostic system has been developed in collaboration with the Institute of Plasma Physics in Prague, which developed the Hall Sensors, and the CEA Team, for the interfaces in the WEST device. The complete sensor system assembly (Fig. 2.3.2) is composed of a 1.5 m long stainless steel tube, to be inserted in the WEST cryostat from an available top aperture, with dedicated pumping system and pressure gauges (to provide a separate vacuum environment with respect to the main WEST vessel) and suitable connections for instrumentation and heating control wiring. The design of the whole support system has been developed by means of suitable thermomechanical and electromagnetic FEM analyses²¹ up to the complete CAD modelling, manufacturing drawings and issue of technical specifications for the procurement of the components²².

The system is presently under manufacturing phase and the experimental tests are expected to be performed by 2018. Besides, a conceptual design of a support system for the ITER 'in-port-plug' sensor assembly has been carried out as well and its detailed design is expected to be completed by 2018.

²¹ M.Brombin, et al., ITER_D_UFYC6D
²² P.Agostinetti, et al., ITER_D_UFYD7M

The aim of the second Task Order is to support the ITER diagnostic team in the review and update of the documentation relative to the design of the entire ITER magnetic diagnostic system, with particular focus on the system performance assessment and on the definition of interfaces with the diagnostic sub-systems “Plant Controller”, “Bespoke Electronics” and “Scientific Software” developed by F4E. The main activity performed during 2017 was a complete revision and issue of an updated version of the magnetic diagnostic ‘Design Description Document’²³. The Task is presently in progress and it is expected to be completed by the first half of 2018.

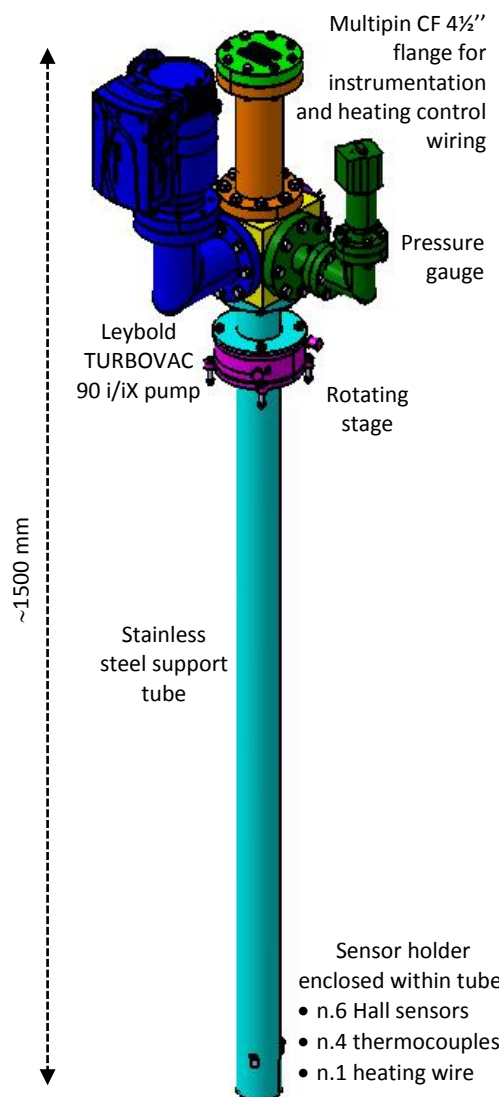


Fig. 2.3.2 Hall Sensors support system assembly

²³ N.Marconato, ITER_D_UX43KT

3 EUROfusion Programme

3.1 RFX-mod: experimental, modeling activities and upgrades

3.1.1 Introduction

The RFX-mod experiment is in a shut-down phase. A proposal for funding an upgrade of the device has been submitted to the local authority in October 2017, applying to the call *Regione Veneto project for the innovation of the local companies*. Therefore, while no experiment has been carried out on the device during 2017, activities related to the design and exploitation of the upgraded RFX-mod (dubbed RFX-mod2) progressed. They include the design of the modified components of the machine (including diagnostic developments), and further data analyses from the last RFX-mod campaign. The latter are important as a preliminary step towards the definition of a scientific programme for RFX-mod2. Indeed in Spring the discussion on the main missions and operational scenarios of the modified device was started, including the possibility of operation at high current and high density with stationary helical states, preparation of proper control tools for the new magnetic front-end, optimisation of the first wall material, scenarios opened by an increased current threshold for spontaneous rotation of tearing modes, Oscillating Pulsed Current Drive scenarios, necessary advancements in modelling tools and diagnostics.

A new activity has also started related to conceptual studies of hybrid fusion-fission reactors based on a RFP fusion module.

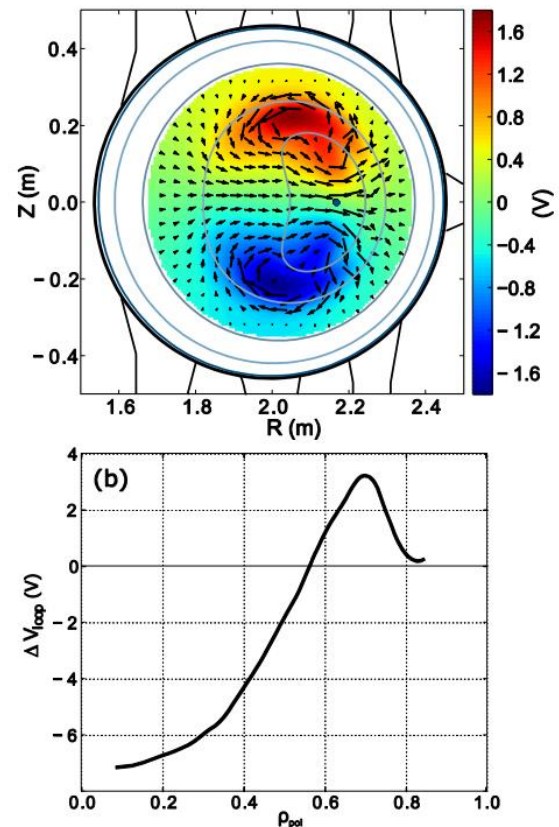


Fig. 3.1.1 Calculation of the dynamo electrostatic potential for a 3D equilibrium reconstruction of a helical RFP state by the V3FIT/VMEC code; (a) helical flux surface (blue contours), electrostatic potential (color contours), $E \times B$ helical flow (arrows); (b) effective dynamo loop voltage as an average of dynamo parallel electric field over axisymmetric flux surfaces

3.1.2 Helical states

The study of helical states induced by external perturbations has been extended in 2017, in particular with a more detailed analysis of experimental data to be related to non-linear MHD simulations²⁴ and more systematic magnetic equilibria reconstructions by VMEC+V3FIT. In particular a statistical analysis of the time behavior of the temperature profiles in a set of plasmas with a $m/n=1/6$ perturbation externally applied has been carried out. It has been found that when $n=6$ is the dominant helicity centrally flatter profiles compared to the $n=7$ case are observed, with a less dynamic behavior. Preliminary indications from the toroidal magnetic analyses by means of the Flit code²⁵ (to be consolidated next year) show a good correspondence between magnetic field structure and temperature profiles.

The RFP helical states have been compared to DIII-D plasmas characterized by an helical core (see sec. 3.2)²⁶. Indeed stationary 3D equilibria can form in fusion plasmas via saturation of MHD instabilities or stimulated by external 3D fields. In these cases the current profile is anomalously broad due to magnetic flux pumping produced by the MHD modes. Such flux pumping is believed to play an important role in hybrid tokamak plasmas, maintaining the minimum safety factor above unity and thus removing sawteeth. It has been shown that in RFPs helical equilibria are maintained by an MHD dynamo emf. Both for Tokamak and RFP, the effective MHD dynamo loop voltage has been calculated for experimental 3D equilibrium reconstructions, by balancing Ohm's law over helical flux surfaces and also by nonlinear MHD simulations. An example referred to a RFX-mod plasma is shown in Fig. 3.1.1. The comparison between the two experiments has indicated an underlying physics common to tokamak and RFP: a helical core displacement modulates parallel current density along flux tubes, which requires a helical electrostatic potential to build up, giving rise to a helical MHD dynamo flow. A specific study to investigate the existence of ohmic helical equilibria in RFP plasmas has been carried out²⁷; in the framework of the developed model the ohmic constraint is found to be approximately satisfied, while the convergence to a real ohmic stationary state is not reached.

²⁴ M. Veranda et al., Nucl. Fus. 57 116029 (2017)

²⁵ P. Innocente et al., Plasma Phys. Contr. Fus. 59 045014 (2017)

²⁶ P. Piovesan et al., Nucl. Fus. 57 076014 (2017)

²⁷ R. Paccagnella "From single Helical axi-symmetric relaxed states to helical equilibria", in preparation

3.1.3 Transport studies

The analysis regarding the reconstruction of the geometric properties of the helical fields and their impact on instabilities and transport has been extended in 2017 (invited presentation at the International Stellarator-Heliotron Workshop in Greifswald, 2017). In particular, it has been found (GENE simulations) that in 3d geometry the ITG growth rate is higher, due to less effective Landau damping and decreased FLR stabilization; ITG modes have helical ballooning structure with higher growth rate where the magnetic surfaces are densely packed. Non-linear calculations have shown enhanced turbulence in 3d geometry, with fluctuations mainly localized along the helical ridge, weaker zonal flows and instability threshold comparable with the experimental temperature gradients (Fig. 3.1.2). However, the effect of 3d geometry on instabilities is not universal: other modes, e.g. microtearing modes, are less affected. Also the effect of a helical geometry on impurities, though described with a simplified treatment not fully 3D, shows small effects²⁸.

A calculation based on a genetic approach has been applied to determine the impurity transport coefficients in RFX-mod. A genetic algorithm is based on the principle of natural selection: a population of individual solutions is repeatedly modified, at each step the

algorithm randomly selects individuals using them as parents to produce the children for the next generation. Over successive generations, the system evolves towards an optimal solution. By the application of this technique in a transport code the convergence towards the values allowing a good reconstruction of the radiation pattern is faster and the full exploration of the parameter space is guaranteed.

In view of the application of Tracer Encapsulated Pellets (TESPEL) in RFX-mod2, aiming at depositing impurities up to the plasma core, the process of TESPEL ablation has been simulated, for velocities of 100m/s and 200m/s and radii of 450 μm and 175 μm . In this first calculations only a full polystyrene case was considered (pellet filled with metals not considered yet). Anyway, the pellet has been found to be fully ablated at $r/a \sim 0.7$ (an

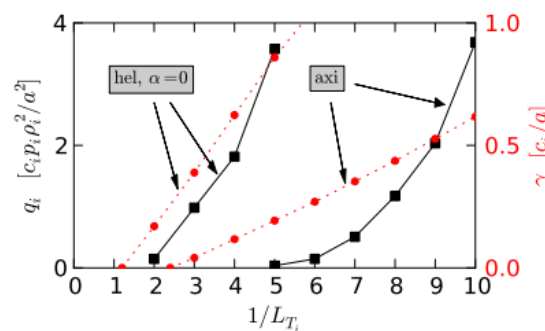


Fig. 3.1.2 Comparison of ion heat flux and ITG linear growth rates in axisymmetric and helical geometry

²⁸ M. Gobbin et al., Plasma Phys. Contr. Fus. 59 055011 (2017)

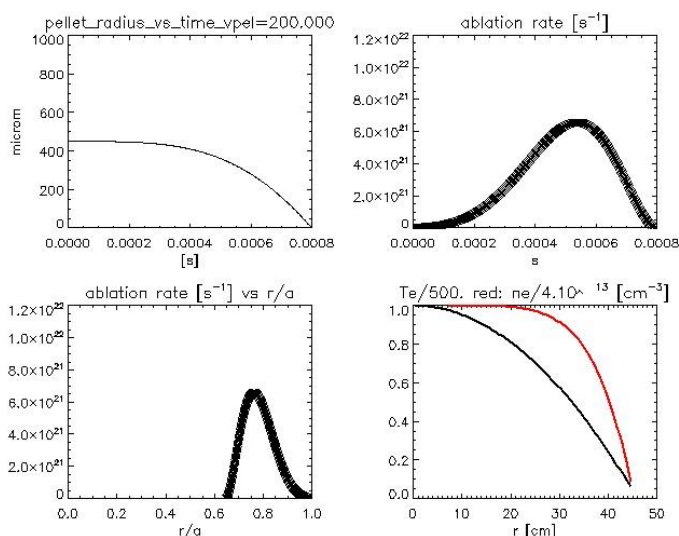


Fig. 3.1.3 Simulation of the ablation process for a polyethylene TESPEL; top: time evolution of pellet radius (left) and ablation rate (right); Bottom: radial profile of ablation rate (left) and of assumed temperature and density profiles (right)

example in Fig. 3.1.3). In order to allow a better penetration in the core spheres with 1mm diameter have been recently purchased.

A study on a unified model able to describe the high density limit in different magnetic configurations, started in past years, has been advanced²⁹. The model is based on a novel 1-dim version of the power balance model, including radiation from light impurities only and coupled to Ohm's law.

A scaling law almost identical for the RFP and the ohmic Tokamak has been recovered. For tokamaks with additional heating, a further term depending on power ($P^{0.4}$) is included. In the case of the Stellarator, the scaling approaches the semi-empirical Sudo law and is well consistent with LHD edge density.

3.1.4 Fast particle dynamics studies

The analysis of Runaway Electrons (RE) experiments in RFX-mod operated as a Tokamak has been completed in 2017, including numerical simulations with the relativistic guiding centre code ORBIT³⁰. Main experimental result was that the amount of RE both during the flat-top and in the post-disruption phase of low density discharges decreases when a magnetic perturbation is externally applied. The reconstruction of the RE orbit space by ORBIT shows that magnetic perturbations generate a layer of stochasticity, mainly at the edge of the plasma, which is responsible for RE losses.

A collaboration with MST RFP (Madison, Wisconsin) has begun to study the behaviour of neutrons and γ rays on that device. A new diagnostic system has been designed, to be applied in 2018 to MST (and to RFX-mod2 in future years), able to measure along several LOS with high time and spectral (for γ rays) resolution.

²⁹ P. Zanica et al., Nucl. Fus. 57 056010 (2017)

³⁰ M. Gobbin et al., Nucl. Fus. 57 016014 (2017)

3.1.5 MHD and magnetic equilibrium active control

The efforts made in last years of operation of RFX-mod for the optimization of the output magnetic field of the active control system has been reviewed carefully, in particular with regard to the sensor/actuator decoupling techniques³¹. This will be useful to implement future tools for the RFX-mod2 device.

The analysis of MHD mode data from RFX-mod tokamak campaign has also progressed: the amplitude and frequency of tearing modes have been calculated using data from the ISIS system (Integrated System of Internal Sensors).

Results allowed the validation of a simple two fluid cylindrical MHD model of tearing mode rotation, based on Newcomb's equations, schematizing the magnetic boundary by two thin shells, with ideal copper shell.

Data have been found to be consistent with the model and it has been shown that the dominant contribution to island rotation is the diamagnetic rotation. An example is given in Fig. 3.1.4. Above a critical density, amplitude and frequency of tearing modes show a characteristic evolution, with a path in the frequency-amplitude space (limit-cycle). Such behaviour has been correlated with the sawtooth activity, see Fig. 3.1.5.

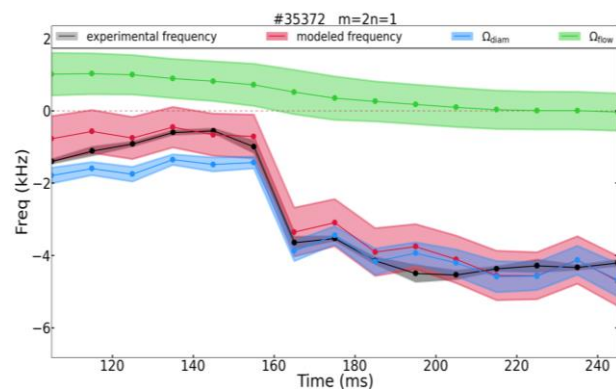


Fig. 3.1.4 Comparison of tearing mode frequency as obtained from ISIS sensors with a two-fluid MHD model

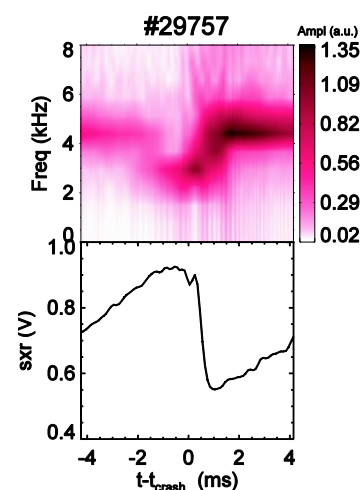


Fig. 3.1.5 (top) frequency and amplitude time evolution of (2,1) TM; (bottom) ST behaviour from SXR signal . Time normalized to the ST crash

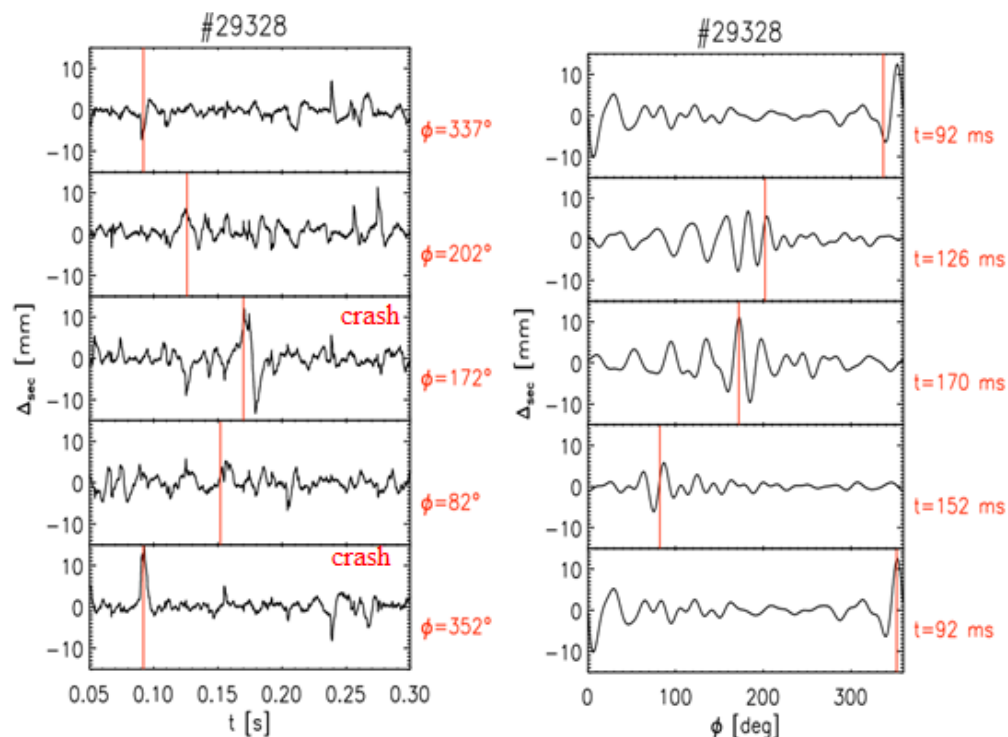
³¹ L. Pigatto et al., IEEE Trans. on Nucl. Science, vol.64,n.6 (2017)

New linearized plasma response models have been developed to improve the accuracy of plasma shape reconstruction and control in tokamak configuration, based on the MAXFEA and CREATE-L codes and on an iterative procedure. A better performance of the vertical position control tool has been obtained thanks to more realistic assumptions on high order dynamics³².

3.1.6 *Plasma-wall interaction*

PWI in RFX-mod has been deeply analysed comparing locally the dominant and secondary $m=1$ mode amplitude with the results obtained by several different diagnostics, including a fast CCD camera, hydrogen and impurity influxes, radiated power, Gas Puffing Imaging, floating potential, electron density, spectroscopy.

The analysis shows that, even in the phases of the RFP pulse with a well developed QSH, corresponding to reduced chaos in the core, an edge region where secondary modes are phase and wall locked is present, which is observed as an enhanced signal from one of the diagnostic systems along the torus. This locking can be seen as a “soft



13

Fig. 3.1.6 Time evolution (left) and toroidal distribution (right) of the horizontal shift of secondary modes at different toroidal locations. Vertical red lines in the left panels indicate the times when the diagnostic at the same toroidal angle shows an increased signal, indicating enhanced PWI. Indicated in the panels are the correspondence of an increased shift with a crash of the Quasi Single Helicity phase. Red vertical lines in the right panels reports the angle where the enhanced shift is observed

locking”, as it corresponds to a shift $\leq 10\text{mm}$, while the shift corresponding at the QSH crash always exceeds 10 mm. An example is reported in Fig. 3.1.6. The occurrence of such soft locking, associated to a local decrease of the connection length of the field to the wall, was in some cases compatible with the development of electron internal transport barriers.

3.1.7 Edge physics, new analysis and developments

The edge response to a magnetic perturbation has been studied, deepening the observation (already mentioned in 2016 activity report) that also in presence of a $m=1$ perturbation, with negligible amplitude of $m=0$ and $m=2$, the edge topology has a more complex structure³³. Indeed, the plasma edge does not exhibit the same helicity as the dominant mode. This has been correlated with the behaviour of the magnetic field connection length to the wall, which is related to the $m=1$ and $m=0$ interaction and features a poloidally non-monochromatic structure (Fig. 3.1.7). Basically, in presence of a magnetic perturbation, toroidally coupled sidebands (for RFX-mod, especially the (0,7) mode) are as important as the dominant mode in determining the details of plasma pressure and floating potential at the edge. The interpretation by the ORBIT code indicates two causes: the presence of a stochastic layer separating the (1,7) and (0,7) resonances and the field line orbit behaviour around the (0,7) O-point. In addition, a new method based on Poincare recurrence time confirms that the main structures determining transport in the edge are the stochastic layer with long recurrence times (>100 toroidal turns) and the O-points of the (0,7) islands, with shorter recurrence times (of the order of 1 toroidal turn)³⁴. This result can be a caveat also for Tokamak, where ELM stability is directly dependent on plasma pressure.

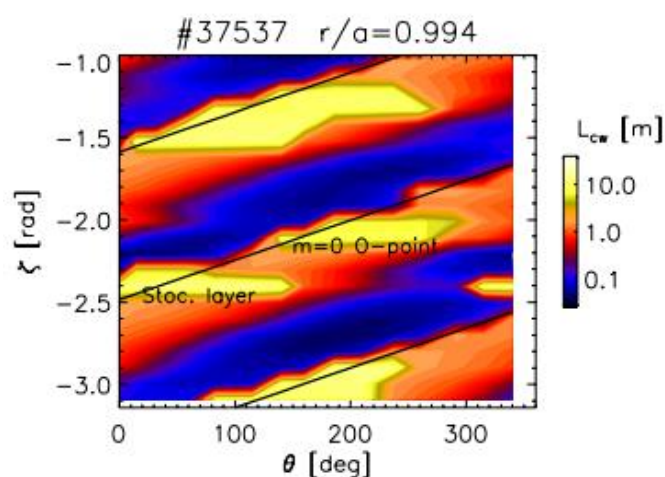


Fig. 3.1.7 Connection length to the wall at $\psi=0$ on the (θ, ζ) plane. Black lines follow the maximum; black line corresponds to the O-point of the (1,7) island. It is clear that a strong non-helical component due to $m=0$ modes is present

³³ M. Agostini et al., Nucl. Fus. 57 076033 (2017)

³⁴ G. Spizzo et al, Nucl. Fus. 57 126055 (2017)

The analysis of edge turbulent structures observed in RFX-mod tokamak discharges in H-mode, started in 2016, has progressed. The ELM-like structures in $D\alpha$ signals have been found to be filamentary fragmented structures. Such structures appear as vortices rotating in the cross-field plane. A detailed analysis of the time evolution of edge profiles led to the reconstruction of a cyclical process, with strong edge gradients followed by expulsion of clusters of filamentary fragments (ELM)³⁵.

3.1.8 *Plasma-beam interaction studies*

Isotopic effects on beam-plasma interaction on RFX-mod have been studied. The work continued the study carried out in 2016 and presented at SOFT 2016³⁶. The isotopic effects have been studied by injecting H/D particles on H/D bulk plasmas. With D injection the losses (shine-through and first orbit losses) have been confirmed to be lower. Due to a change in the critical energy while using D, the power deposition to ions is slightly increased and this effect is enhanced at higher densities. Using scaling laws for L-H transition³⁷ the H mode could be reached only with D bulk plasmas.

3.1.9 *Electrical model of RFP applied to the design of vacuum components in RFX-mod2*

The externally applied loop voltage required to drive current in the RFP can induce currents between the plasma and the surrounding conducting components. An appropriate modeling of the problem can quantify these currents thus constraining the design of RFX.mod2 vacuum components. In 2017, such a model has been developed,

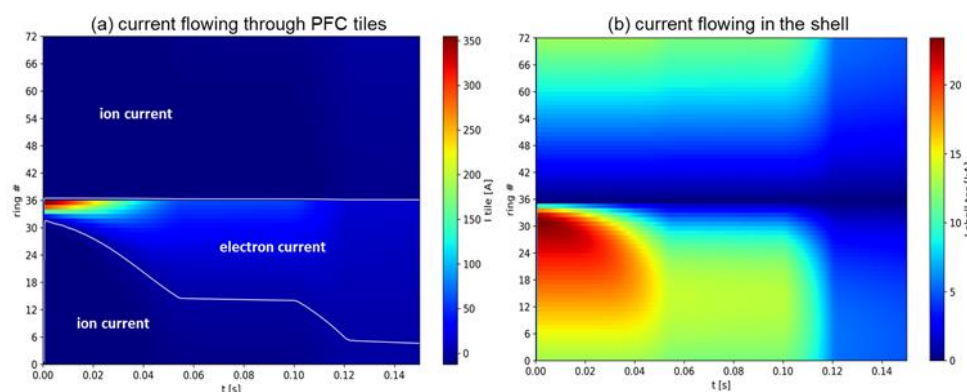


Fig. 3.1.8 Calculated currents flowing through the tiles (left) and total currents flowing in the shell (right)

³⁵ M. Spolaore et al., Nucl. Fus. 57 116039 (2017)

³⁶ Vallar, M., et al. "Requirements and modelling of fast particle injection in RFX-mod tokamak plasmas." FED (2017)

³⁷ Martin YR et al., "Power requirement for accessing the H-mode in ITER", Journal of Physics: Conference Series 123 (1) 012033 (2008)

under simplified assumptions, and combined to specific laboratory tests analyzing the process of arc formation and prevention. As an example, Fig. 3.1.8 shows the currents flowing through the plasma facing graphite tiles and the total current flowing in the shell. The intense tile currents in the gap region correspond to the plasma start-up phase, when plasma loop voltages of 350 V are applied, and the high voltage between the tiles can generate destructive arcs. These results induced a modification of the layout design and a series of ad-hoc laboratory tests (see sec.3.1.11)

3.1.10 *Diagnostic upgrades*

Some new diagnostic systems are foreseen for RFX-mod2. The most urgent to define is the magnetic sensor system, since it impacts on the design of the new magnetic boundary. The ISIS system will not be necessary anymore as it was in RFX-mod, due to the absence of the filtering effect of the vacuum vessel. On the other hand, an increased number of sensors is required to make even more efficient the MHD active control system. The final layout of the system, in terms of number and distribution of sensors, is presently under discussion, the main issues are: the problems entailed by the huge number of associated cables to be fitted in a limited available space and the necessity of optimisation both for RFP and Tokamak. New sensors will be tri-axial probes, allowing the simultaneous measurement of poloidal, toroidal and radial fields.

The design of the Fast Reciprocating Manipulator has been finalized in 2017, and the installation of 2 systems is foreseen.

In the perspective of RFX-mod2, the feasibility of using a direct single channel precision ADC to allow the simultaneous acquisition of dB/dt measurements and the integrated B measurement by means of digital integration has been investigated. The promising result of this study opens the door to a simple, cost-effective and reliable acquisition system, usable for real-time control and scalable from tenths to thousands channel scale, applicable to RFX-mod2 and to a broad class of pulsed plasma experimental devices.

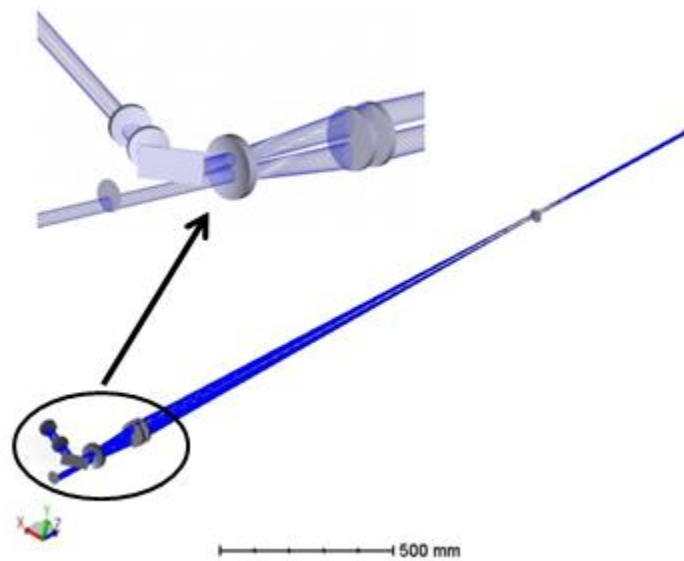


Fig. 3.1.10 Upgraded Thomson scattering system. The incoming beam is the lower one, the reflected beam is the upper. The reflected beam is injected in a second cylindrical telescope.

Upgrades in the design phase also for several diagnostic systems already operating in RFX-mod. Among them, launching and reflecting optics to allow a double laser passage for the Thomson scattering system, thus increasing the signal-to-noise ratio have been designed. With this diagnostic configuration, a manipulator to substitute and align the retroreflector is also necessary. By such retroreflector, the laser beam will be also re-injected towards the edge Thomson scattering optics, placed at a different toroidal angle. A schematic of the system is sketched in Fig. 3.1.10. Tests have been carried out on a new sensor, Multi Pixel Photon Counter (MPPC), to be used in RFX-mod2 for the Gas Puffing Imaging and Thermal Helium Beam diagnostics instead of the usual

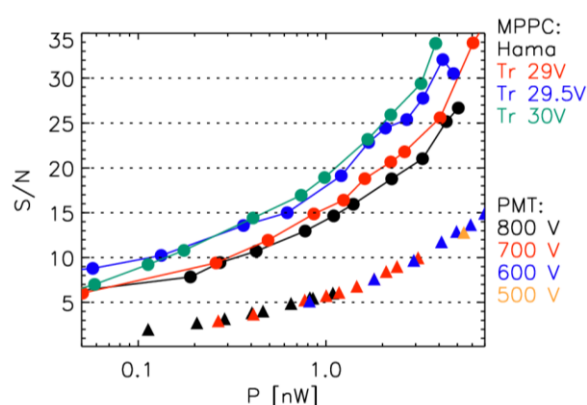


Fig. 3.1.9 Signal to noise ratio versus incident light power: comparison among MPPC from Hamamatsu (Hama), MPPC from AdvanSid and conventional PMTs at various voltage supplies.

photomultipliers (PMT). The motivation of such change relies on the possibility of obtaining a better signal to noise ratio by sensors not sensitive to stray field, and therefore placed close to the machine. Specific tests have been made, comparing MPPCs from 2 factories (Hamamtsu and Advansid, Trento) and conventional PMTs in terms of dark noise and signal to noise ratio (see Fig. 3.1.9).

3.1.11 *Design of machine modifications*

During 2017 the design of the modifications of the machine load assembly progressed with significant variations in the technical solutions with respect to the conceptual design previously proposed.³⁸

During the conceptual design phase the integration of the 22 equatorial ports on the outer boundary of the Vacuum Toroidal Support Structure (VTSS) was considered compatible only with the pre-assembly of two halves of the toroidal complex and the final welding of the two poloidal gaps of the VTSS. This assembly sequence would have excluded the possibility of overlapping the insulated gaps of the Passive Stabilizing Shell (PSS), as adopted in the present RFX-mod configuration to minimize radial magnetic field errors with respect to the 'butt-joint' configuration.

This issue in principle could be compensated with the use of a dedicated active control system of local magnetic field at the PSS and VTSS poloidal gaps³⁹; nevertheless the implementation of such a system, together with the realization of welded VTSS joints based on metal-ceramic brazed structures, were considered too risky both for technical and economic reasons. Therefore the final design focused on a solution compatible with the original assembly sequence of the RFX machine, in which the PSS can be fully assembled with overlapped joints and then vertically inserted between the bottom and top halves of the VTSS, finally bolted at the equatorial gaps (Fig. 3.1.11).

One of the most critical aspects in the new VTSS assembly is the requirement to guarantee vacuum tightness and electrical insulation at the poloidal and toroidal gaps. The new proposed concept of the vacuum-tight electrical-insulated crossed joints is described in Fig. 3.1.12.

Two VTSS quarters (lower and higher) are firstly horizontally tight joined by means of the existing stud bolts with interposed PEEK spacers acting as "half gaskets"; vacuum tightness is provided by proper "CF knife-edge" manufactured on the two surfaces of the mating VTSS quarters.

³⁸ S. Peruzzo, et al., Design concepts of machine upgrades for the RFX-mod experiment, Fusion Eng. Des. (2017)

³⁹ P. Bettini, et al., Modeling of the magnetic field errors of RFX-mod upgrade, Fusion Eng. Des. (2017)

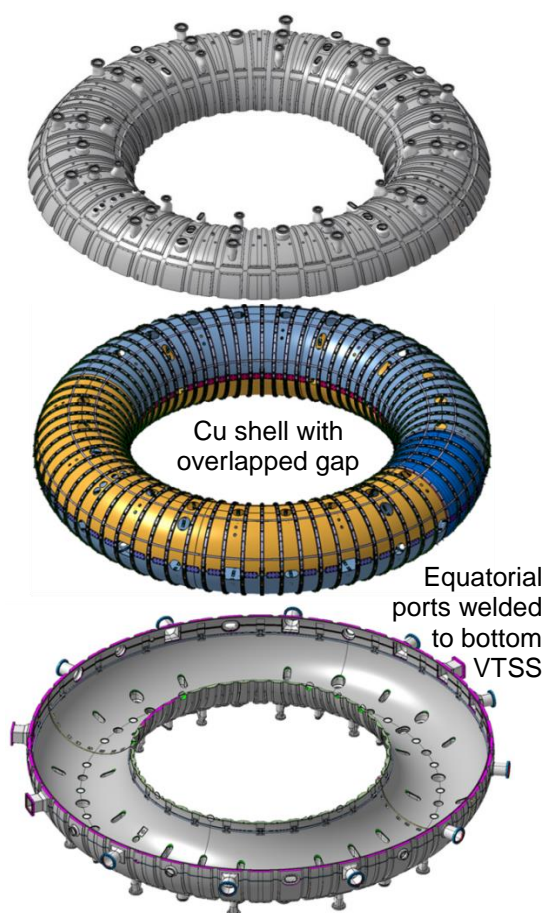


Fig. 3.1.11 New proposed top-down assembly sequence RFXmod2 PSS into VTSS

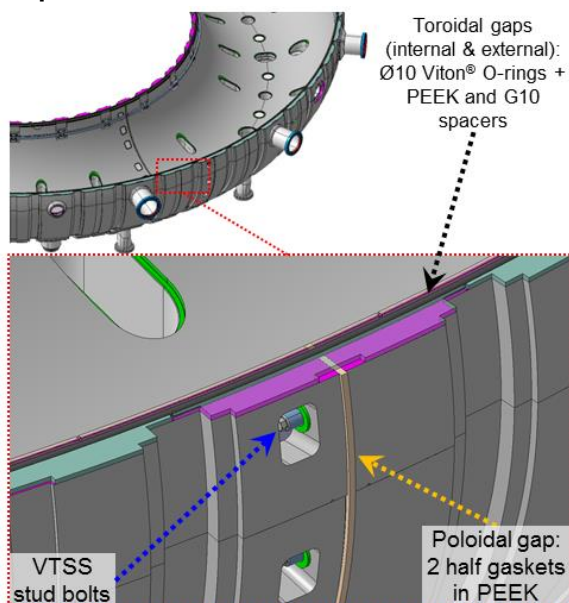


Fig. 3.1.12 The vacuum-tight electrical-insulated crossed joints of the VTSS

The two VTSS halves are then vertically joined (after insertion of the PSS as indicated in Fig. 3.1.11) with interposed standard Viton O-rings (for vacuum tightness) and suitable PEEK and G10 fiberglass spacers (for electrical and structural function). The crossing of the horizontal and vertical joints, which could be source of potential leakage, has been designed with a novel concept combining a particular geometrical shape and a selection of compatible materials.

To verify the reliability of the VTSS crossed joints a mock-up vacuum chamber has been manufactured and tested. Fig. 3.1.13 shows the bottom part of the mock-up cylindrical chamber made of 4 segments, joined at the mid vertical and horizontal planes by means of spacers equivalent to those designed for the VTSS. The mock-up was successfully tested with a helium leak detector that revealed a leak rate $<5 \times 10^{-9}$ mbar·l/s, that is considered acceptable for the operation of the RFXmod2 vessel.

The final design of the PSS for RFXmod2 was focused on the careful definition of the electrical topology of the in-vessel components, to minimize the risk of arcing which could occur during over-voltages induced in standard or abnormal operating conditions (plasma start-up or fast termination).

Fig. 3.1.14 shows the insulating elements made of thermoplastic material (Torlon® PAI) implementing the overlapped gap: bushing at each tile clamping (to keep the 2 overlapped surfaces at the nominal distance of 2 mm) and spacers along the edges of the overlapped surfaces (to avoid the penetration of ionized gas in proximity of sharp edges of the shell, where the increase of the electrical field could initiate a discharge).

A further requirement was imposed on the electrical insulation of the First Wall (FW) with respect to the PSS and simultaneously the electrical connection of all the FW tiles to a resistive grid in order to smooth and distribute evenly the electrical potential of the plasma facing components. Fig. 3.1.15 shows the solution implemented to fulfill the requirement of insulation between tiles and PSS, obtained with an insulating pad made of torlon interposed between the tile locking bushing and the PSS. Fig. 3.1.16 shows the resistive grid connecting all the tiles, realized with stainless steel thin sheets which provide the prescribed global electrical resistances $> 700 \mu\Omega$ and $> 50 \text{ m}\Omega$ along the poloidal and toroidal direction respectively. The status of the design of machine modifications has been presented at the 13th International



Fig. 3.1.13 Mock-up realized to test VTSS vacuum-tight electrical-insulated crossed joints

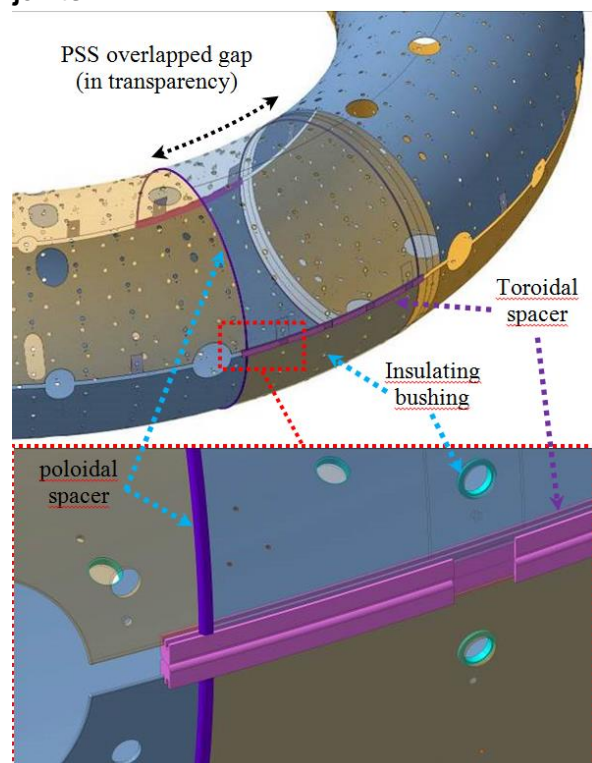


Fig. 3.1.14 Implementation of the overlapped poloidal gap of the PSS

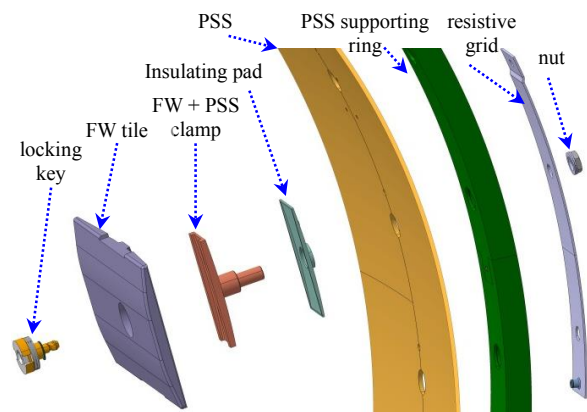


Fig. 3.1.15 Exploded view of FW + PSS clamping system.

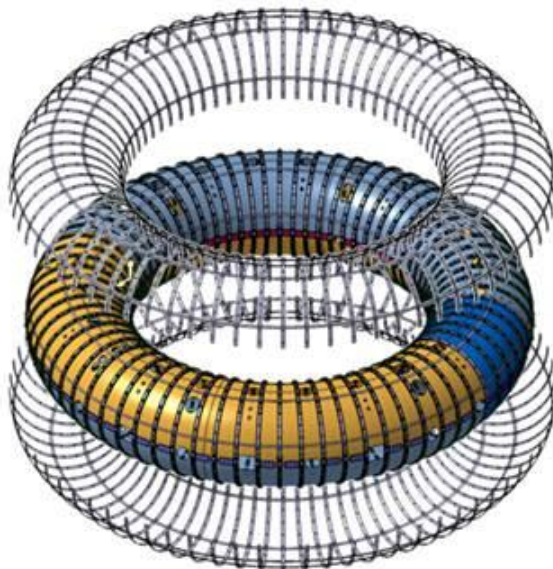


Fig. 3.1.16 Exploded view of the resistive grid connecting the array of 72x28 FW tiles

Symposium on Fusion Nuclear Technology⁴⁰⁻⁴¹. The completion design is expected to be completed by 2018 with contribution of some manufacturing Companies involved in a joined proposal for industrial innovation project partially funded by 'Regione Veneto'.

3.1.12 *RFP as neutron source for a fusion-fission hybrid*

The fusion reactor remains one of the long term, ultimate solution of energy production. This requires to control fusion reaction with an energy gain $Q > 30 - 40$. The tokamak configuration is nowadays the most investigated path to this goal.

Meanwhile a proposed interim carbon-free solution, with the merit of nuclear waste transmutation, is the hybrid fusion-fission reactor, in which sub-critical fission is activated by fast neutron generated in a fusion reactor. In this case fusion could be produced in a device with lower Q , roughly of the order of one.

The Reversed Field Pinch (RFP) is an alternative configuration to tokamak and stellarator for the fusion reactor. Its disruption-free configuration, the much weaker toroidal magnetic field and the capability of reaching thermonuclear temperatures without additional heating, are its most significant advantages in a commercial reactor.

⁴⁰ S.Peruzzo et al, Detailed Design of the RFX-mod2 Machine Load Assembly, presented at 13th ISFNT, submitted to Fusion Eng. Des. (2017)

⁴¹ R.Cavazzana et al, Design constraints on new vacuum components of RFX-mod2 upgrade using electrical modeling of Reversed Field Pinch plasma, presented at 13th ISFNT, submitted to Fusion Eng. Des. (2017)

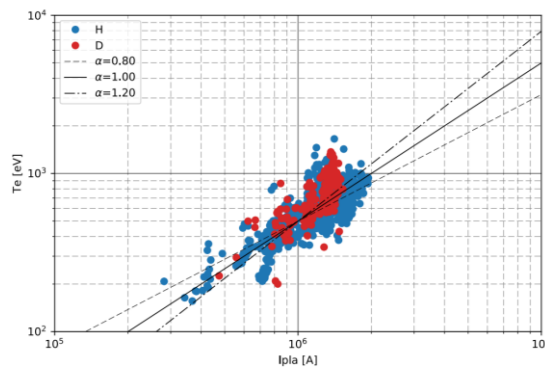


Fig. 3.1.17 Central electron temperature as a function of plasma current in RFX-mod. Red points refer to deuterium plasmas

While RFP plasmas have yet an energy confinement too low for a high Q reactor, reaching Q near 1 might be reasonable for a RFP machine with an appropriate R&D activity. Starting from the present knowledge in RFP configuration, the experimental results from the different machines and the theoretical advancement obtained in the last years, an analysis was done on the

possibility to use the RFP configuration as a fast neutron generator. Advantages of this solution with respect to the tokamak (no disruption, toroidal field coils at room temperature and reduced size with more space for breeding blanket, superconductors limited to the magnetizing coil and no divertor) and the possible issues (steady state operation, for example) have been preliminary analyzed in 2017⁴².

The experimental results of RFX-mod indicate that, at any given current level, the best performances in terms of highest temperature, confinement, QSH duration and lowest resistive loop voltage are achieved in a restricted range of the Greenwald fraction n/n_G between 0.1 and 0.2. Given the ohmic heating nature of the RFP configuration, empirical scaling law relations can be derived from averaged local quantities, like the confinement time $\tau_E = nT/(\eta j^2)$. In particular, maintaining a fixed Greenwald density ratio and assuming energy equipartition and Spitzer-like resistivity dependence, the basic relation $T^{5/2} \sim j \tau_E$ is derived.

On the basis of experimental data, coming from more recent extensive RFX-mod campaign at high current and with Deuterium, it was derived the scaling of temperature vs. the current density (see Fig. 3.1.17) as $T \propto j^{1.1}$. To scale the resistive loop voltage the same criteria are used and a dependence as $E_{\infty} \propto j^{0.65} a^{-1.65}$ was found.

This depicts a situation in between the two classical RFP scalings, the favourable Connor-Taylor and the pessimistic Carreras-Diamond. The initial point for the scaling has been fixed at the RFX-mod attained values: $a=0.46$ m, $R=2$ m, $I_p=1.8$ MA, $T=1.6$ keV, $V_{res}=16$ V.

⁴² R. Piovan, C. Bustreo, R. Casagrande, R. Cavazzana, D. Escande, M. E. Puiatti, M. Valisa, G. Zollino, M. Zuin, "A continuously pulsed Reversed Field Pinch core for an ohmically heated hybrid reactor", ISFNT 13, Kyoto, Sept. 2017. Submitted for publication to Fusion Engineering and Design.

Starting from these plasma performances and scaling with machine size and plasma current level, parametric studies were performed in order to find the necessary magnetic flux (Volt- seconds) as a function of the plasma current level, the burning phase (flat-top) and the current ramp down phase.

It was verified whether the fusion conditions could be reached with feasible RFP machine size. In particular, a wide set of machine parameters (major radius $R = 4 \div 6$ m; aspect ratio $R/a = 4 \div 6$ was considered; in all the explored configurations it was limited the maximum magnetic field below 12 T inside the Ohmic Heating (OH) winding (the highest values are present in the innermost layers of the central solenoid close to the equatorial plane) and the maximum stray field in the plasma region was set not exceeding 10% of the equilibrium field.

Three different plasma current scenarios have been considered ($I_p = 10, 15, 20$ MA). As an example, Table I summarizes the results of three alternative configurations ($R=4m$

Table I - Configurations with different sizes at $I_p = 20$ MA

| | | | |
|------------------------|-----|-----|------|
| R [m] | 4 | 6 | 6 |
| a [m] | 1 | 1 | 1.5 |
| Vs (peak to peak) [Wb] | 350 | 830 | 830 |
| $B_p(a)$ [T] | 4 | 4 | 2.67 |
| V_{loop} [V] | 5 | 7 | 4 |
| Flat-top duration [s] | 10 | 45 | 90 |
| Duty cycle[%] | 62 | 88 | 94 |

$a=1m$; $R=6m$, $a=1m$; $R=6m$, $a=1.5m$) in terms of available magnetic flux swing Vs, poloidal magnetic field at plasma edge $B_p(a)$, resistive loop voltage V_{loop} (as derived from the scaling laws), flat-top duration and duty cycle for the case with $I_p = 20$ MA..

In these conditions, the plasma temperature, from the derived scaling laws, is estimated to 10 KeV and 15 KeV for $a=1m$ and $a=1.5$ m respectively. Under the assumption of energy equipartition between ion and electron, the total fusion power could reach up to 60 MW and the wall neutron load about 0.2 MW/m². These conditions are maintained for the burning-phase duration reported in Table I.

One of the major issue is to sustain the fusion reaction in a continuous way, which requires current drive systems for steady-state operation. Nevertheless RFP can operate

in a continuous pulsed operation in a very efficient way, being the setting up and the plasma current landing much shorter than tokamak. The continuous operation in a pulsed mode is obtained by exploiting the so called “flux double swing” as shown in Fig. 3.1.18.

The dwell time, as reported in Table I can be reduced to about 10% in some cases.

These performances are well adequate for a first prototype of Fusion-Fission-Hybrid-Reactor (FFHR) in which to test an almost continuous neutron production from fusion and the related fission reactions in the blanket, together with the self-consistent tritium generation from lithium.

Scaling from the present RFPs results, such a machine could be realized utilizing the state-of-art technologies and, considering the reduced neutron flux, with the available nuclear material.

Upgrade of RFX-mod machine has been identified which could improve highly the present performances by reduction of magnetic field fluctuations at the plasma edge. As a result, these modifications could make an RFP reactor for FFHR further more attractive and competitive with respect to the other solutions.

3.2 MST1 and ITER Physics Work Packages(Valisa 15p)

For the participation to the EUROfusion work-program Consorzio RFX deployed an overall assignment of around 15 ppy, among whom 10 Scientific Coordinators of experiments within JET and ITER Physics work-packages, one Task Force Leader of MST1, one Task Force Leader for JET1 one Deputy Head in the PMU for JET.

Below a brief description of some of the relevant scientific contributions to the ITER-Physics work-packages is given.

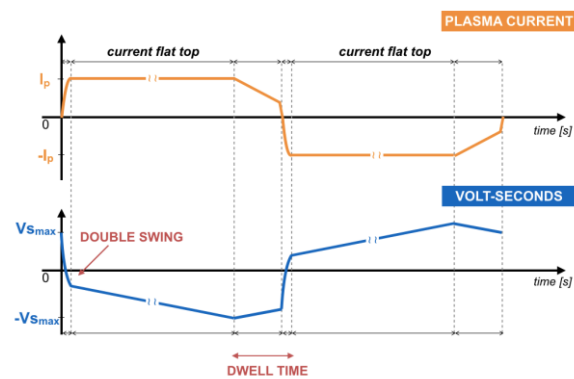


Fig. 3.1.18 Sketch of double swing operations. A short dwell time is required to allow a high duty cycle.

3.2.1 **MST1- Medium-Size Tokamak Campaigns**

3.2.1.1 *Topic 21- Filamentary transport in high-power H-mode and in no/small-ELM regimes to predict heat and particle loads on PFCs for future devices*

Two current scans in L-mode, performed respectively at constant q_{95} and at constant toroidal field B_t , have been performed both in, AUG⁴³ and TCV⁴⁴. In both the machines, the experiment clearly proved that at the same level of fuelling and given toroidal field, at lower currents a flatter SOL profile easily develops, the so called shoulder. In AUG this is also accompanied by a faster increase of neutral density in the divertor region as well as a lower density threshold for target ion flux roll-over. At constant q_{95} , instead, the two machines behave differently, with no shoulder observed in TCV even at high fuelling levels, likely due to the difficulties to reach detachment at lower toroidal fields, mandatory condition to observe any upstream variation on TCV. The H-Mode investigation has been limited to AUG given the difficulties found on TCV to obtain a reliable high density H-Mode scenario with small ELMs and close to detachment condition. On AUG the role of fuelling location and the influence of neutral density, varied by switching on and off cryopumps in otherwise similar discharges, have been investigated. Puffing from either lower or upper divertor does not modify neither the tendency to develop a flat profile in the inter-ELM phases nor the characteristics of the blobs. Instead at comparable fuelling rate SOL profile saturation without the cryopump is clearly more pronounced as seen in Fig. 3.2.1.

3.2.1.2 *Topic 16 Extension of the operating space of fully non-inductive scenarios on TCV towards high β_N and/or stationary or quasi-stationary operation*

The operational space of fully non-inductive single null L-mode plasmas has been explored on TCV. The operational space has been extended towards higher plasma current ($I_p=130\text{kA}$) and density ($n_{e,0} \approx 2.5e19\text{m}^{-3}$). β_N values up to 1.45 have been reached. The experiment has been carried out by carefully scanning Electron Cyclotron (EC) and NB heating and Current Drive (H/CD) radial location. Sensitivity of plasma thermal energy confinement to such location has been found. When on axis EC power is

⁴³ ASDEX-Upgrade

⁴⁴ Tokamak à Configuration Variable

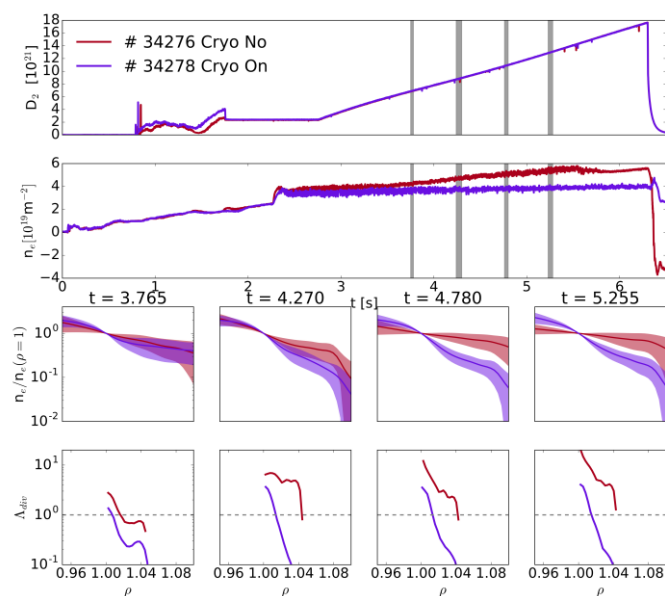


Fig. 3.2.1 From top to bottom: Fuelling rate for two identical shots with and without cryopumps. Edge density from interferometer chord. The 4 panels reports the SOL density as measured by Li-Beam diagnostic at 4 different times, normalized to the corresponding density at the separatrix. The bottom row reports for the same time intervals the values of divertor collisionality

sufficiently high ($P_{EC} > 1.5 \text{ MW}$) the core temperature decreases due to the onset of 3/2 and 2/1 NTMs. The rotation of the 2/1 mode is in counter current direction and is slowed down by co-current NBI. $V_{loop} \sim 0$, high β_N steady-state scenarios have been found to be extremely sensitive to the plasma conditions. NBI can increase/decrease V_{loop} depending on other plasma parameters. The highest β_N does not necessarily correspond to the maximum electron thermal energy because of the Fast Ions strong contribution to the total plasma pressure.

Indeed both ASTRA and NUBEAM modelling predict a large population of fast ions with densities comparable to the bulk ones in these plasmas, while Charge-eXchange (CX) reactions are the main loss channel for the NB heating efficiency. Similar situation was found in circular limiter configuration⁴. Nonetheless, NB current drive efficiency in these diverted fully non-inductive plasmas is observed to be lower despite the expected reduced neutral penetration from the edge. Interpretative TRANSP transport analyses are expected to quantify the role of NB fast ions losses on the NBCD, whose full understanding is crucial for the development of fully non-inductive plasmas. Despite the significant amount of fast ions and related torque neither electron nor ion Internal Transport Barrier have been formed.

3.2.1.3 Topic 9 AUG equilibrium with a helical core and its effects on the plasma

High- β tokamak plasmas are highly sensitive to 3D intrinsic and externally applied error fields. In AUG $q_{min} \sim 1$ hybrid plasmas the plasma response to $n=1$ fields produces an $m=1, n=1$ helical core displacement with an impact on various quantities such as plasma rotation, ion/electron temperature profiles, W impurities and fast ions transport. The study of these effects requires tools that are not constrained to axisymmetry. To this end we used the VMEC code⁴⁵ and the V3FIT code⁴⁶ to reconstruct the actual AUG equilibrium from measurements. To provide a stronger constraint in the core, ECE temperature measurements were used as it had been done in⁴⁷ with MSE data. An example is shown in Fig. 3.2.2 on the left panel where the shaded region shows the displacement between flux surfaces at different toroidal angles. This equilibrium was then used in the NEO-2 code⁴⁸, able to treat neoclassical non-ambipolar transport induced by the helical core. As shown in figure 2 clear effects of the 3D geometry are observed experimentally: both electron and ion temperature profiles are flattened, toroidal flow undergoes a breaking and tungsten concentration is reduced due to expulsion from the helical core. The preliminary modelling analysis with NEO-2 is in accordance with these observations unlike the modelling done neglecting 3D effects and assuming axi-symmetry⁴⁹.

3.2.1.4 Topic 8 Runaway electron beam control

The main aim of these experiments was to advance the study of runaway electron

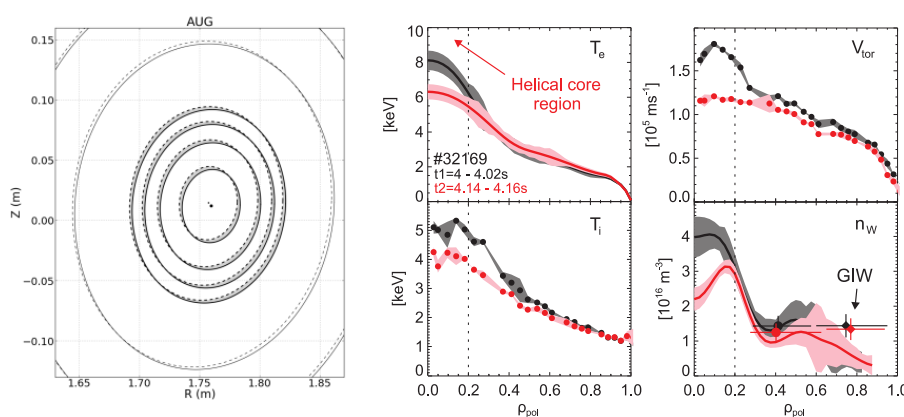


Fig. 3.2.2 Left: example of the reconstructed helical core in AUG: continuous and dashed lines show flux surfaces at different toroidal angles. Right: Experimental evidence of changes in plasma profiles induced by 3D effects (red with and black without helical core).

45 S.P. Hirshman and J.C. Whitson, Phys. Fluids 26 3554 (1983)

46 J.D. Hanson et al. Nucl. Fusion 49 075031 (2009)

47 M. Cianciosa et al., Nucl. Fusion 57 (2017) 076015 (11pp)

48 A.F. Martitsch et al., Plasma Physics and Controlled Fusion 58, 074007 (2016)

49 P. Piovesan et al., 59th APS Conf., 23-27 Oct. 2017, Milwaukee, Wis, USA, UP11.00077

mitigation via applied magnetic perturbations (AUG), control of the Ohmic circuit (TCV) , also exploiting voluntary contribution from non-MST devices (COMPASS, FTU). Experiments and modelling in AUG extended the work started in 2015 and 2016 which showed a reduction of the runaway current when $n=1$ RMPs are applied. MARS-F numerical simulations showed that the most effective phasing of the currents in upper/lower B-coils is the one related with the maximum edge kink response. In 2017 shots the amplitude of the perturbation has been lowered and the time of application of the RMP has been varied. These experiments have shown that the maximum current allowed in the B-coils for a toroidal field of 2.5 T is very close to the minimum threshold required to see any effect on the runaways. Perturbations applied after the disruption do not seem to affect the RE beam evolution but the recurring loss of RE beam position control in these experiments prevents to draw definitive conclusions on this issue. This activity has been presented in an Invited talk at the last EPS Conference ⁵⁰. The results obtained in AUG suggested similar experiments in COMPASS. Such a device is equipped with a set of flexible top/bottom and midplane RMP coils which can be powered with a current up to 3.5kA. The relative phasing of the current in the coils can be varied in four different configurations. Preliminary shots have been executed at the end of 2017. As in AUG, one orientation of the coils is the most efficient in reducing the runaway current. Unlike AUG, the perturbations affect also the fully developed RE beam. Further experiments will be performed next year supported also by MARS-F simulations. TCV experiments have continued those started in 2015-2016 and have been mainly dedicated to obtain a reproducible stable post-disruption RE beam. Several new scenarios have been developed in low density plasmas for future use and for modelling in particular: Low Ip scenarios (120 & 150 kA), 200 kA scenario at higher density, medium pressure argon Mass Gas Injection scenario. A scan in elongation - has been completed in a wide parameter range: no RE beam is found at $k > 1.4$ while for $1.1 < k < 1.3$ RE can be generated also at higher density with respect to $k \sim 1$.

3.2.1.5 Topic 7 Disruption Avoidance

A series of about 10 shots have been performed in AUG applying slowly rotating (5-10 Hz) external perturbations in order to entrain the 2/1 mode, which is the main cause of disruptions in the chosen high beta H-mode scenario. An example of a typical shot is shown in Fig. 3.2.3.

⁵⁰ M.Gobbin Plasma Physics Control. Fusion **60** 014036 (2018).

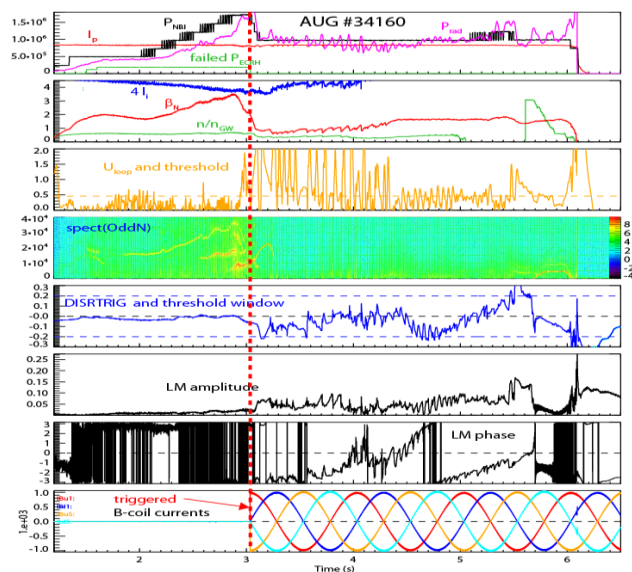


Fig. 3.2.3 Plasma current, NBI power, \square , loop Voltage, $n=1$ spectrum, trigger signal, Locked mode amplitude and phase, B coils currents.

Although interesting from a physical point, since some entrainment of the 2/1 to the external RMP has been observed, these experiments were not conclusive as to the disruption avoidance, since some discharges didn't disrupt even without any applied RMP, while others disrupted with the RMP turned on.

3.2.1.6 Topic 24 and 25

Interpretative simulations with the ASTRA code have been performed in order to evaluate the effect of various divertor configurations (single null,

double null and snowflake) on the core confinement in TCV plasmas, the main question to address being why, increasing the NBI power, the plasma temperature does not increase. Preliminary results suggest that such phenomenology is compatible with an increased NBI shine-through and a larger turbulent transport. Firstly an evaluation of which of the proposed shots was suitable for the analysis was carried out and then some preliminary simulations were performed. Investigation on the reliability of ion temperature measurements, that are typically higher than the electron ones in ohmic discharges is in progress.

On TCV, NBI power ramps have confirmed that the power threshold for L-H transition is higher in Double N null than in SN configuration by about 30% at the same operational regime. In terms of power splitting between up and down strike points a scan in the distance between the two separatrixes has shown that optimum power sharing is not obtained for the exact double null configuration but rather when the two nulls belong to different separatrixes. As for the L-H transition the result depends on the presence of ∇B drifts; edge modeling with SOLEDGE2D-EIRENE on this pulses will allow a direct validation of the drift implementation in the code. Double null pulses have been also analyzed and compared to SN ones in terms of core transport parameters with the ASTRA code. Preliminary results have shown that in similar discharges $\chi_{e,DN} > \chi_{e,SN}$ and $\chi_{i,DN} < \chi_{i,SN}$, in agreement with previous DIII-D results.

3.2.2 *JET1 - JET Campaigns*

3.2.3 *Task 17-02. Development and integration of a real-time state observer for plasma state monitoring*

State observers are well established control engineering tools to merge data from different sensors into one consistent estimate of the state of a system. The objective of this work was the implementation of a real-time state observer for JET based on the control-oriented 1D transport code RAPTOR⁵¹. This code is used as a simulator to provide a model-based prediction of the plasma profile evolution, which is then combined with all the available JET diagnostic data to yield a corrected estimate of the plasma state in real-time.

Raptor has been coupled to the equilibrium reconstruction XLOC/Equinox code⁵², which has been upgraded in order to provide new flux surface averaged quantities and real-time the electron density profile. The upgraded code has been benchmarked with EFIT(K)⁵³ and validated using experimental data.

A new real-time application called FluxMap has been implemented to map a generic diagnostic profile from the geometric machine coordinate (r,z) to the normalized toroidal flux coordinate (ρ_ϕ). The development of synthetic models for the available real-time JET diagnostics, among these the upgraded Electron Cyclotron Emission (ECE) and the upcoming real-time High Resolution Thomson Scattering (HRTS), is underway. The XLOC/Equinox, FluxMap and the state observer RAPTOR codes are going to be integrated in the real-time MARTe framework on JET. Transport modelling activity has been performed within the tasks T17-07 (DT scenario extrapolation) and T17-08 (L-H transition physics).

3.2.3.1 *Task T17-07 DT scenario extrapolation*

Interpretative and predictive simulations using JETTO transport code coupled with PENCIL/ASCOT as the NBI module have been run for the shot 92054 that, besides high q_{95} , low density and high NBI heating power, during the current ramp-up features the development of an internal transport barrier with high ion central temperature and impurity accumulation. The scope of the work was to validate the predictive modelling of

51 F. Felici et al Nucl. Fusion 51 083052 (2011).

52 J. Blum, C. Boulbe and B. Faugeras, "Real-time plasma equilibrium reconstruction in a Tokamak", Journal of Physics: Conference Series, Volume 135, Number 1, (2008)

53 3 D. P. O'Brien et al Nucl.Fusion 32 1351 (1992).4 B. Geiger et al Plasma Phys. Control. Fusion 509 (2017) 115002

this discharge and then make an extrapolation to the highest NBI power in D-T plasma in order to evaluate the neutron yield, in that scenario.

3.2.3.2 Task T17-08 L-H transition physics

Different NBI heated shots have been modelled by interpretative (JETTO+PENCIL/ASCOT) simulations, in order to calculate the power balance at the L-H transition, with particular attention to NB shine-through losses in L mode. In order to evaluate the importance of the heating channel (ion vs electron heating) at L-H transition for different average densities (same I_p , B_t). The Qualikiz transport code has been used to reconstruct with predictive modelling the ion temperature in the core. Power going to the ions at L-H transition will be compared for the 3 different average densities and results will be compared to AUG results.

3.2.3.3 T17-05 3D equilibrium reconstruction with V3FIT/VMEC

Non axi-symmetric configurations are observed in JET on a limited extent during operation with EFCC, when snake structures appear and in extreme conditions during a disruption when the plasma undergoes a global 3D distortion. In order to properly reconstruct some of these configurations (though with the limitation of not being able to model configurations with magnetic islands), among different approaches, the VMEC was considered for computing 3D equilibria for JET and the V3FIT code was considered to solve the inverse problems of equilibrium reconstruction from measurements. A more flexible interface had to be considered in order to connect V3FIT/VMEC to the EFIT++ output since different modelling configurations can be used in JET according to the plasma regime that is being addressed. This involves mostly the modelling of the iron core that has reached a more mature and advanced description. Fig. 3.2.4 shows the diagnostics that were implemented for the JET experiment, where magnetic measurements have been modelled considering local probes (red dots), saddle coils (blue lines) and full flux loops (green lines) as well as some kinetic diagnostics such as

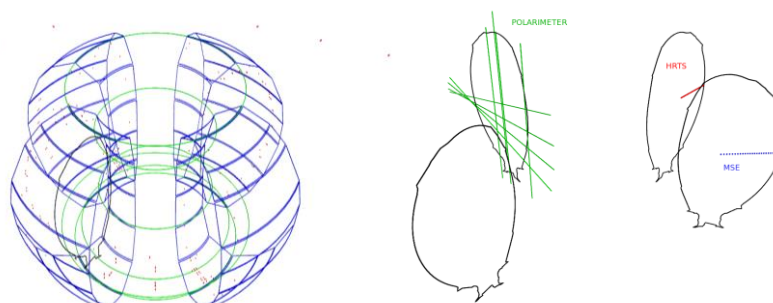


Fig. 3.2.4 Jet diagnostics implemented in V3FIT: magnetics (left) and kinetic (right)

interferometer-polarimeter (green), high resolution Thomson scattering HRTS (red) and partially MSE (blue). Ongoing work is devoted to the benchmark of vacuum shots (including the iron core contribution) and of free-boundary equilibria and it will utilize also information on internal profiles provided by kinetic diagnostics. In this respect different parametrizations will be considered for pressure and current profiles.

3.2.3.4 T7 Core transport modelling with isotopes'

Interpretive TRANSP run aimed at comparing the energy transport in the core of Hydrogen and Deuterium ILW discharges have been performed.

The results confirm that there is a positive isotope effect (in contrast with the gyroBohm scaling) at the edge of L-mode and H-mode plasmas. Such effect propagates through the plasma core of H-mode plasmas via constant critical temperature gradient in conditions where electrons and ions are strongly coupled and/or ion heat transport is stiff. No significant isotope effect has been found in the core of L-mode plasmas. TRANSP interpretive runs aimed at understanding whether the 'confinement scale invariance principle' showed by Cordey valid in the carbon wall case is still valid for the ITER-like wall. The analyses show that in L-mode the invariance principle holds, while it has not been possible to validate it in H-mode shots. This seems to be due to a degradation of the confinement in ILW hydrogen H-mode shots with respect to the CW ones. The effect of fast ions on core confinement of L-mode ILW, NBI heated plasmas is under investigation particularly in order to correlate the un-stiffening of the ion temperature profiles in the core.

Full tritium plasma behaviour has been predicted by means of TRANSP runs regarding in particular neutron yield, particle, heat and momentum deposition and fast ion population.

The main results are that in baseline scenario plasmas the neutron production is

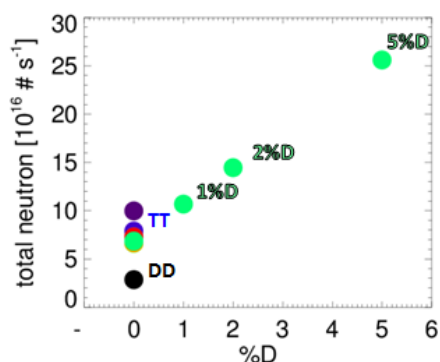


Fig. 3.2.5 Neutron yield foreseen for TT JET plasma with a D contamination

expected to be a factor 3 larger than in D reference cases. As reported in Fig. 3.2.5, the neutron yield linearly increases with D contamination of TT plasma, posing some limit in the JET exploitation at full performance at the very beginning of the T phase.

Because of the lower neutral beam particle velocity in T, the deposition profiles result peaked off-axis. To recover the particle and heat deposition on axis, a 20% lower plasma

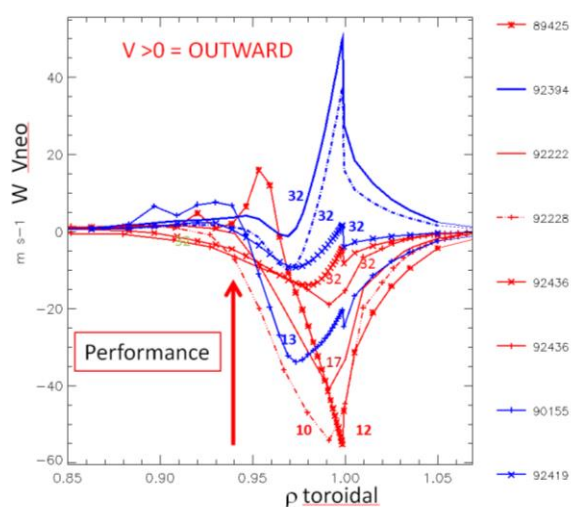


Fig. 3.2.6 Neoclassical convection of W for the series of discharges listed in Table 1. In red the baseline and in blue the hybrid cases. The total power input associated to each curve is indicated in MW.

density is needed, whereas the momentum deposition is less affected (thanks to the larger full energy fraction of the beam in T). On the fast ion population in T two opposite mechanisms are at play: the more external deposition of T beams leads to a degradation of the fast ion confinement. The latter is compensated by the longer slowing down time τ_{SD} resulting from the larger isotope mass and higher particle average energy. In plasma with similar densities, the fast ion particle density results larger in T than in D, confirming that the leading mechanism is the longer τ_{SD} . To recover

the D fast ion population the plasma density have to be 1.25 time higher in T than in D.

3.2.3.5 Task T17-13 DT scenario extrapolation

A modelling activity was carried out on the analysis of some JET discharges and validation of the 3D MHD code M3D⁵⁴. Moreover an activity about the coupling of the M3D code with the 3D electromagnetic code Cariddi is on the way and some results are expected in few months. A weak coupling scheme is used, i.e. the relevant boundary data produced by the M3D code are passed in time to the Cariddi code that calculates the current evolution through the external structures solving a set of standard electromagnetic equations inside the conductors.

3.2.3.6 Task T17-10 particle transport

The inward neoclassical pinch of W associated to the edge kinetic gradients in the inter-ELM phases and evaluated by means of the NEO code coupled to the JETTO-SANCO transport code has been shown to decrease as the total input power in the JET plasmas is increased (Fig. 3.2.6). This type of analyses was suggested by the observation that in high power and high performance discharges the ion temperature gradients at the edge was, in proportion, increasing more than the electron density gradient, indicating that in

⁵⁴ H. Strauss et.al, Phys. of Plasmas 24 (2017) 102512.

the neoclassical convection expression the screening term proportional to the normalized ion temperature gradient was gaining against the unfavourable term depending on the normalized density gradient. One can therefore expect that at moderately higher power JET should eventually reach regimes in which the transport of W at the edge is representative of the one expected in ITER. The analysis of the W content in the selected discharges in order to verify to what extent the reduced pinch velocity was beneficial, is matter of a current analysis based on integrated edge-core analysis.

3.2.3.7 Tasks T17-11

Edge modelling with SOLEDGE2D-EIRENE for JET has been performed for M15-19 and M15-20 pulses with and without nitrogen seeding and flux expansion have been analysed. The final aim of such modelling was the validation of the code to be later used to design future experiments. In the unseeded pulses simulations have shown a relatively good agreement with experimental Langmuir probes data at the inner strike point and less good agreement in terms of n_e and T_e at the outer one. A relatively good agreement has been obtained also in terms of bolometric radiation and Be II lines emissions. Modelling will continue on Nitrogen seeded discharge to compare measured and simulated Nitrogen line emission.

For M15-19 experiment a pulse has been modelled to compute deuterium and nitrogen density and temperature at the whole wall boundary. This is possible with SOLEDGE2D-EIRENE code only, thanks to its ability to extend the fluid mesh up to the wall. The results will be used to evaluate Ammonia formation. After optimization of the transport parameters, a good match of temperature and density profile was obtained at the equatorial plane, while in the divertor region, probably due to the detachment state (very low simulated plasma temperature), a good agreement was possible only in terms of ion saturation current, while a fair agreement was obtained for Bell line emission. Results of previous modelling are presently used by people involved in Ammonia evaluation.

3.2.4 WPS1/2 - Preparation and Exploitation of W7-X Campaigns/Stellarator optimization

3.2.4.1 LHD Campaigns

Participation to LHD first D experimental campaign: in 2017 LHD has started its activity with D as the main gas. The isotope effect on stellarator is a controversial matter, since no strong evidences have been found in past experiments in smaller devices. To study the transport properties in LHD, preliminary cold pulse experiments have been

performed. In particular, a configuration with a 1/1 RMP island has been chosen, to evaluate the transport in the bulk plasma and the effect of the presence of an island. The analyses have been performed with MAxS, highlighting a transport reduction of a factor 10 inside the island with respect to the bulk plasma for the H case. The experiments in D suggest a reduced transport in the bulk plasma. A complete estimate of the bulk/island transport properties is foreseen for 2018, when full NBI power will be available also in D.

3.2.4.2 Support on Data Acquisition

The activities carried out for the Preparation and Exploitation of W7-X have been devoted to the development of a timing board used as generic timing generator in several diagnostics. The activity included the development of a framework for the integration of Zinq FPGA architecture and of specific HDL FPGA programs for the timing functions.

3.2.4.3 WP17-S1-B6

During 2017 the design of the High Resolution Probe head, to be installed on the W7-X experiment was finalized at Consorzio RFX, in collaboration with the IPP Greifswald team. The final version of the build-to print drawing was approved by the IPP Greifswald team.

In particular the aim is to provide information on parallel current density associated to L-mode filamentary turbulent structures as well as on ELMy structures in H-mode^{55 56 57 58}. Furthermore, the possibility to measure the time evolution of radial profiles of flows was considered as an interesting part of the study, given the strong interplay expected between the turbulent fluctuation and the average flows.

Special attention was devoted to the design of a shield for magnetic sensors embedded into the probe head, which would allow the magnetic fluctuation measurements ($f_{\text{meas}} \leq 1$ MHz) and at the same time the shielding from ECRH ($f_{\text{ECRH}}=140\text{GHz}$) used for additional heating. The first version of the shield of the magnetic sensor was experimentally tested at Consorzio RFX. A revised improved design of this shield was then proposed (see Fig. 3.2.7).

⁵⁵ M. Spolaore, et al, Phys. Rev. Lett. 102, 165001 (2009)

⁵⁶ N. Vianello, et al, Nucl. Fusion 50, 042002 (2010)

⁵⁷ Furno I., Spolaore et al., Phys. Rev. Lett. 106, 245001 (2011).

⁵⁸ M. Spolaore et al "*Electromagnetic ELM and inter-ELM filaments detected in the COMPASS Scrape-Off Layer*", accepted on Journal of Nuclear Materials DOI 10.1016/j.nme.2016.12.014

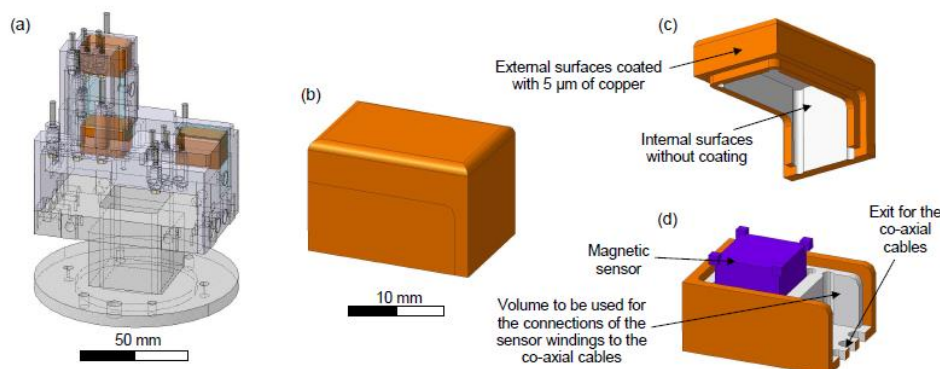


Fig. 3.2.7 Design of the electrostatic shields for the magnetic sensors: (a) position of the three magnetic sensors; (b) magnetic sensor shield; (c) cover part; (d) bottom part and magnetic sensor. The parts in orange with a 5 μm layer of copper

The material necessary for the probe construction was then procured and a company for the different pieces machining was identified.

It was decided to operate the probe head predominantly within **OP1.2b** phase.

A detailed description of the HRP design was presented at the 27th IEEE Symposium On Fusion Engineering 4 – 8 June, 2017 Shanghai, China. The related paper was submitted to IEEE Transaction on Plasma Science ⁵⁹.

3.2.4.4 Advanced Thomson scattering experiments in JET and LHD

In 2017 two experiments to test advanced Thomson scattering (TS) techniques of interest to ITER have been performed in JET and LHD. The purpose of the JET experiment was to measure for the first time in a fusion device the depolarization of the TS radiation. This is a relativistic effect at the basis of polarimetric Thomson scattering, a technique complementary to the conventional one that is under consideration to improve the accuracy of the CPTS (Core plasma Thomson scattering) system of ITER in the $T_e > 25$ keV range⁶⁰. The experiment has been successfully carried out in the HRTS system of JET, in close collaboration with the JET TS team⁶¹.

In addition RFX has participated to dual-laser, self-calibrating TS experiments in LHD. This technique, that was demonstrated for the first time in RFX⁶², is also of interest for

59 P. Agostinetti, et al, "Design of a High Resolution Probe Head for Electromagnetic Turbulence Investigations in W7-X" submitted to IEEE Transaction on Plasma Science

60 L. Giudicotti, "Polarimetric Thomson scattering for high T_e fusion plasmas", JINST 12 C11002 (2017)

61 L. Giudicotti, M. Kempenaars, O. McCormack, J. Flanagan, R. Pasqualotto and JET contributors "First observation of the depolarization of Thomson scattering radiation by a fusion plasma", submitted to Nuclear Fusion

62 O. McCormack, L. Giudicotti, A. Fassina, and R. Pasqualotto, "Dual-laser, self-calibrating Thomson scattering measurements in RFX-mod", Plasma Phys. Control. Fusion 59, 055021 (2017)

ITER. In LHD the higher T_e of the plasma allowed to implement TS measurement with a ND:YAG and a Ruby as a main and secondary laser. This resulted in a higher accuracy of the measurement compared to the previous experiment in RFX in which the wavelength difference of the two lasers (Nd:YAG and Nd:YLF) was very small. The RFX contributed to the set-up of the TS system, the data collection and the preliminary data analysis.

3.2.5 WPISA - Infrastructure support activities

The activity carried out in 2017 for the ITER Integrated Modelling and Analysis Suite (IMAS) has been devoted to the development of a new data access layer for supporting the data model of the infrastructure, extending the former model used in ITM. In particular, two layers (backend) are being developed, one based on MDSplus data access and the second one providing memory caching functionality. The use of memory caching speeds execution because temporary data handled by the simulation programs is only maintained in memory and not written back to disk. It proved to represent a key factor for the optimization of workflows.

3.2.6 WPSA - Preparation of exploitation of JT-60SA

3.2.6.1 Detachment Modelling

The low density and high density inductive scenario #2 studied in the JT-60SA Research Plan has been analyzed in term of power exhaust with the SOLEDGE2D-EIRENE edge code. Simulations were performed on pure D and C wall, with a power of 41 MW crossing the separatrix and radially varying transport parameters corresponding to H-mode density and temperature profiles and a SOL parallel heat flux decay length of ≈ 3 mm. Modelling shows that for the low density case ($n_{\text{sep}}=2 \cdot 10^{19} \text{ m}^{-3}$) plasma is attached at both strike points with very high peak powers. Instead, at higher density, $n_{\text{sep}}=6 \cdot 10^{19} \text{ m}^{-3}$ (corresponding to a $n/n_c \approx 0.8$), when carbon from the wall is self-consistently included in the simulation, plasma detaches at both strike points with a peak power load lower than 10 MW/m^2 .

3.2.6.2 MHD Modelling

MHD stability and control studies aiming at preparing the scientific exploitation of JT-60SA continued in 2017 with their main focus on RWM stability and active control. RWM stability was studied including kinetic effects in simulations with the 2D MHD code MARS-F/K. A detailed analysis of the available Scenario 5.1 equilibrium allowed to identify the presence of a possible stability threshold corresponding to the crossing of $q_a=7$ (limiter plasma with truncated x-point).

A research period has been spent at General Atomics, collaborating with Dr. Yueqiang Liu. Part of the work with MARS-F/K on MHD stability of high beta plasmas has been then applied to JT-60SA.

Ongoing work is devoted to expanding the parameters scan for better understanding of this threshold. MARS-K computations of kinetic RWM stability will be then reconsidered depending on the new position of the target plasma with respect to the ideal wall limit. A 3D model for active RWM control studies was refined in 2017 and results allowed to significantly evolve the proof-of-principle feedback control obtained in 2016. A complete dynamic simulator has been developed and applied to a Scenario 5.1-like plasma. A mode control scheme has been implemented, allowing the identification and closed-loop simulation of the $n=1$ most unstable eigenmodes.

A number of time simulations allowed to identify the purely proportional gain required for the stabilization of the $n=1$ mode (in purely fluid description)

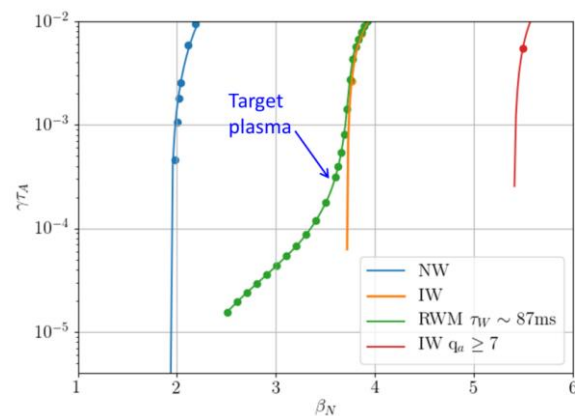


Fig. 3.2.8 Pressure scan showing ideal kink (no-wall & id-wall) and RWM

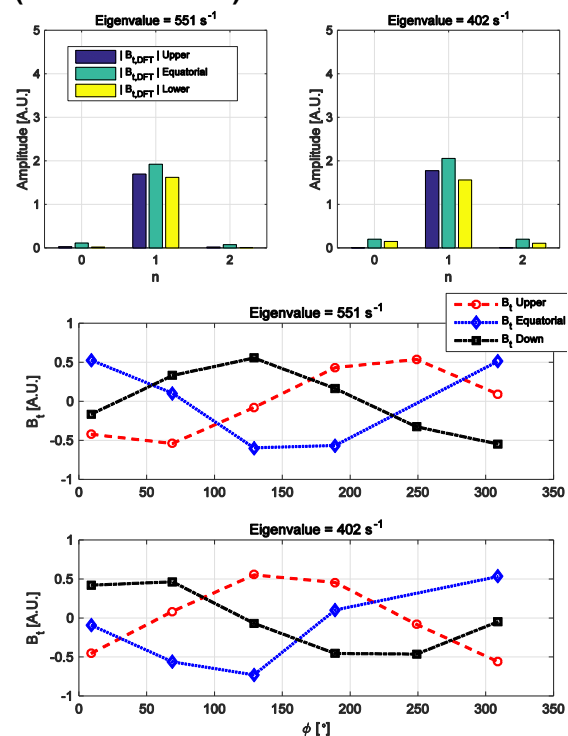


Fig. 3.2.9 Image of the two most unstable eigenmodes on each sensor array (top). Harmonic content of the two eigenmodes (bottom)

3.2.6.3 Neutral Beam modelling

JT-60SA is a device that will rely on neutral beams as primary source of additional power and current drive. ASCOT⁶³ is a orbit-following Fokker-Planck equation solver and it has been used to simulate different scenarios, in order to evaluate the performance of NBI in such plasmas. Furthermore, parametrical studies on beam energy and plasma composition have been accomplished.

3.2.6.4 WPDTT1

Assessment of alternative divertor geometries and liquid metals PFCs The alternative divertor configurations proposed for available DEMO equilibrium have been modelled with the SOLEDGE2D-EIRENE edge code. Modelling started for the Snowflake plus and minus (SFP and SFM) and Super-X divertor (SXD) configurations and stationary results have been obtained for (SFM and SXD).

Results have been compared with those obtained with the Single Null (SN) standard configuration. It was the first time that modelling was performed with a fluid code coupled to the EIRENE Montecarlo code for neutrals treatment and for configurations like the Snowflake. Previous modelling was done with the SOLPS code coupled to a fluid code for neutral treatment and only on configurations with just one null inside the vessel.

Simulations were performed on pure D with a power of 150 MW crossing the separatrix and transport parameters ($D_{\perp}=0.42 \text{ m}^2/\text{s}$ and $\chi_{\perp}=0.18 \text{ m}^2/\text{s}$) corresponding to a parallel heat flux decay length of $\approx 3 \text{ mm}$. With these parameters no configurations show plasma detachment at both strike points for a peak power load lower than the maximum allowed of $10 \text{ MW}/\text{m}^2$ for $n/n_G < 1$ (or $n_{\text{sep}} < 5 \cdot 10^{19} \text{ m}^{-3}$). The SXD only provides plasma detachment at the other strike point at all densities (see Fig. 3.2.11) and with a peak power lower than $10 \text{ MW}/\text{m}^2$ for densities above $4 \cdot 10^{19} \text{ m}^{-3}$ (see Fig. 3.2.12) .

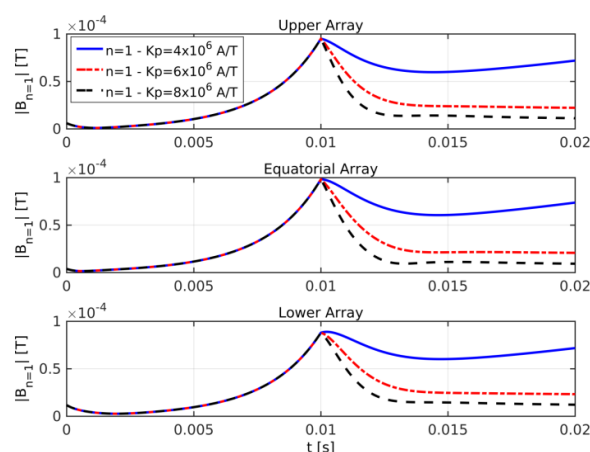


Fig. 3.2.10 Time evolution of $n=1$ component with different proportional gain in closed-loop control

⁶³ E. Hirvijoki et al., Comput. Phys. Commun. **185** (2014)

As expected SXD does not provide any advantage at the inner strike point with respect to the SN configuration, instead the snowflake solution provides at both strike points temperature similar to the SN one (see Fig. 3.2.11) but it is much better in terms of a lower peak power (see Fig. 3.2.12).

3.3 ITER NBI Physics activities and accompanying program

3.3.1 Operation of NIO1

The operation of NIO during 2017 started with a test of an alternative magnetic configuration of the filter field. The polarity of a couple of permanent magnets forming the multi-cusp confinement field was reversed, in order to produce an additional 14 mT B field in the source, to enhance the electron cooling in the proximity of the extraction area, and consequently the extracted negative ion current. This improvement, together with the optimization of the source bias allowed to achieve a negative ion current density up to about $j=10 \text{ A/m}^2$, at a voltage of 1.4 kV and relatively low power ($P=1.2 \text{ kW}$). This result was in line with the scaling to achieve a 200-300 A/m^2 beam when the full power (2.5

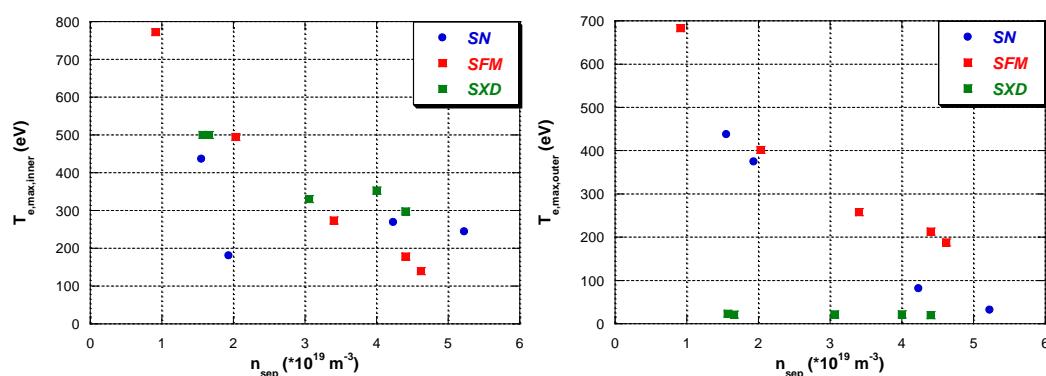


Fig. 3.2.11 Electron temperature at the inner and outer strike points for the SN, SFM and SXD divertor configurations versus electron density at the separatrix.

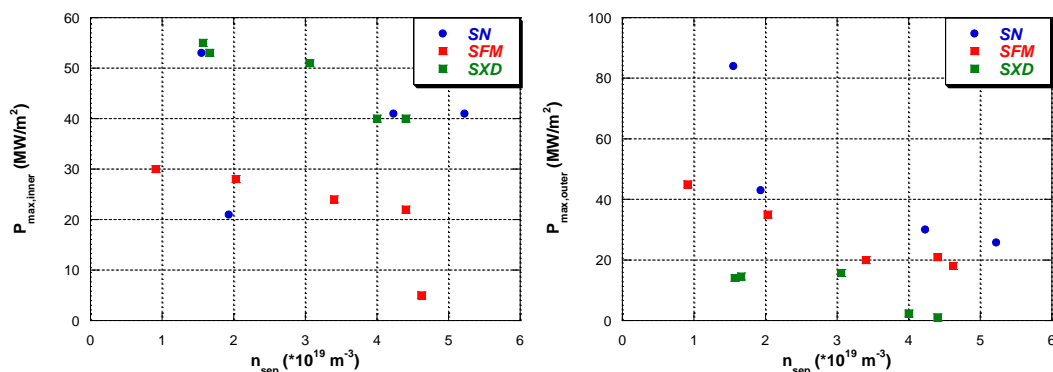


Fig. 3.2.12 Peak power at the inner and outer strike points for the SN, SFM and SXD divertor configurations versus electron density at the separatrix.

kW) will be and the caesium injected in the source. A major shutdown was done during April-May, in order to replace the extractor and the magnets there embedded. From the accelerator point of view this modification was expected to significantly improve the beamlet optics, by reducing the beam divergence and the deflection induced by the previous magnetic configuration, whose B field was too high. Unexpectedly after the restart of operation, a significant increase in the electron current was observed, accompanied by a reduction in the H⁻ current ($j < 3 \text{ A/m}^2$). A full characterization of the new configuration with respect to voltages, pressures, power and source biases, confirmed this behaviours. A possible explanation is that the reduction of the B field in the accelerator, also affected the plasma confinement in the source region. A new set of magnets, with intermediate intensity will be installed soon to verify this hypothesis. In spite of this difficulties in increasing the ion current, during the second half of the year the experiment was enriched by new diagnostics and auxiliary systems. In particular, a cryogenic pump was installed on the diagnostic tube of NIO. This gave a huge increase in the pumping speed of H₂ with respect to the basic system based on turbo-molecular pump, and allowed reaching baseline pressures in the order of 0.02 Pa, when a pressure of 0.6 Pa is applied in the source. This represents a tenfold decrease of pressure, resulting in a huge suppression of the stripping losses along the accelerator and the diagnostic tube.

The beam emission spectroscopy diagnostic reached a full maturity, and real time evaluation of beam divergence and average angles are now possible. A new power supply allowed exploring the biasing of the PG with respect to source vessel, in a large range of voltages. Moreover, the installation of a pair of 2D CCD sensors to monitor the beam drift region appeared to be a valuable source of information on the beam optics: a thorough analysis of the light emission profiles could be used to estimate beam pattern on intermediate plan, in view of the complete beam tomography, to be installed in near future. The first measurements with a retarding field energy analyzer (installed on an axial actuator) probe were also collected.

3.3.2 Development of alternative ion source (Enabling Research)

A first code has been developed: it consists of Monte Carlo(MC) gas model has been developed [1-2] to implement the H₂ chemical kinetics in HT: vibrational and electronic excitations, dissociation, dissociative ionization and ionization are described in [1-2], while [1-2] highlight the relevance of electron-induced and ion-induced dissociation according to the vibrational excitation of H₂. With a 2D axially symmetric geometry, a

prescribed electron density and temperature profiles (Fig. 3.3.1a), calculated for the HT SPT100 ($L=25\text{mm}$) with Xe as propellant, were used as input parameters. Results, reported in Fig. 3.3.1b-c-d, show a peak of atomic density and temperature 0.9 cm from the exit plane. At this distance, there are also a maximum of electron density and an optimal electron temperature for electron-induced dissociation, that is, 10 eV [1-2]. A second more detailed code was developed. It consists of the implementation of the Particle-in-Cell / Monte Carlo Collision (PIC-MCC) methodology [1-2] to represent the plasma dynamics in a neutral fixed background. The model is three-dimensional in cylindrical coordinates (r, θ, z) and simulates an angular sector of the discharge channel. As for the previous MC model, the axial domain extends from the anode to the exit plane where the cathode condition ($\phi=0$) is forced to occur. Poisson's equation is solved by PETSc software package [1-2]. The equations of motion are solved with the CYLRAD Boris leap-frog type algorithm [1-2]. Finally, the MC method [1-2] is used for both volumetric collisions and secondary electron emission from the lateral walls. Hybrid parallelization techniques (MPI mixed with OpenMP [1-2]) were implemented. To validate the code [1-2], the HT SPT20 configuration with $L=28\text{mm}$, $D_{\text{out}}=20\text{mm}$ and $D_{\text{in}}=10\text{mm}$ [1-2] was studied as first case. A run using Xe was launched before to study the H₂ case was studied.

Fig. 3.3.2 shows the three-dimensional structure of electric potential $\phi(\text{V})$ and electron density $n_e (\text{m}^{-3})$ for both Xe and H₂. It is evident how the working gas macroscopically affects the structure of the acceleration channel. Using Xe, the acceleration region is confined to the last 6 mm of the channel length, in good agreement with experimental measurements [1-2]; on the other hand, with H₂ the potential drop extends by 18 mm.

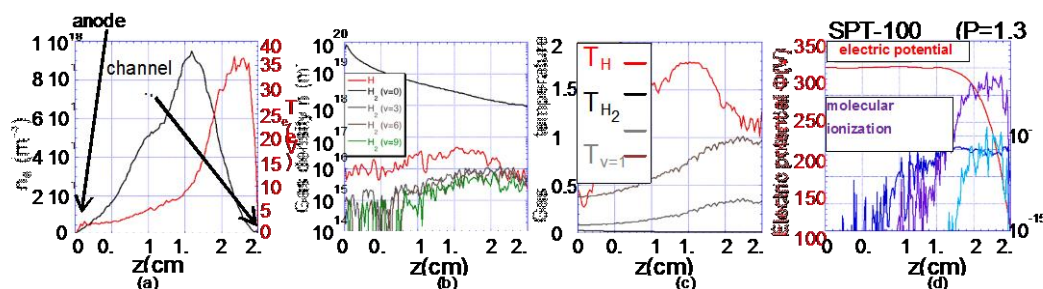


Fig. 3.3.1 (a) Electron density and temperature axial profiles inside the SPT100 channel. (b) Gas density corresponding to (a). v is the vibrational level of the molecule. (c) Gas temperatures corresponding to (a). (d) Profiles of electric potential and reaction rate coefficients of some relevant reactions involving electron-induced H₂ collisions corresponding to (a).

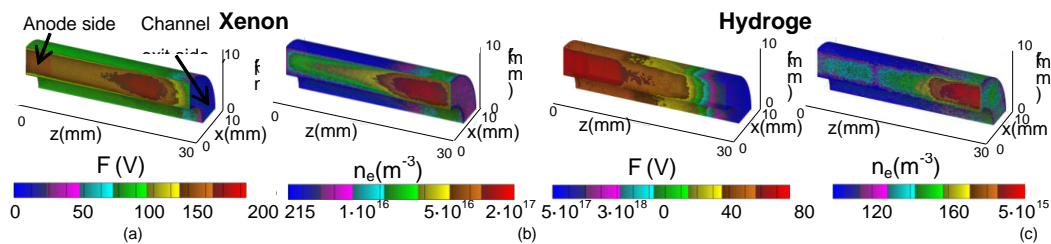


Fig. 3.3.2 Three-dimensional electric potential $\phi(V)$ (a and c) and electron density n_e (m^{-3}) (b and d) maps of SPT20 discharge channel using Xe (a and b) and H_2 (c and d) as propellant. A discharge voltage $V_d=160$ V, a discharge current $I_d=0.75$ A, a neutral propellant mass flow rate of $\dot{m}=0.1$ mg/s and a maximum magnetic field $B_{r,max}=350$ G were used for all cases.

This large extension has major impacts on the thruster performances due to the high rate of ion loss on lateral walls. In addition, the presence of competing channels, such as vibrational excitation and dissociation, to the ionization causes the plasma density to be lower in the H_2 case. In fact, the maximum n_e reaches $8 \cdot 10^{17} m^{-3}$ for Xe, while it is three times smaller for H_2

3.3.3 *Magnetic configuration*

In ATHENIS (Alternative Thruster Hall Effect Negative Ion Source), the magnetic field has an important role in the thruster efficiency. Instead of coils, permanent neodymium magnets generate the field due to the small size of the device. Moreover, the thruster is modular both along the radius and z-axis, that is, it is composed of rings with a thickness of 8mm. The external rings are made of aluminium and each of them hosts 15 magnets. The mid-internal set of rings is made of ferromagnetic material in order to lower the intensity of the magnetic field.

Then there is the internal cylinder, which is made of ferromagnetic too. Each component is electrically isolated by cylinders of glass or PEEK. The aim was to obtain a radial component of the magnetic field such as the one in Fig. 3.3.3 With permanent magnets, the best fit obtained is shown in Fig. 3.3.3b: the ring facing towards the anode is without magnets otherwise the magnetic field obtained was not acceptable (Fig. 3.3.4). The double peak should not compromise the dissociation but only the ionization efficiency inside the channel, which is not our objective.

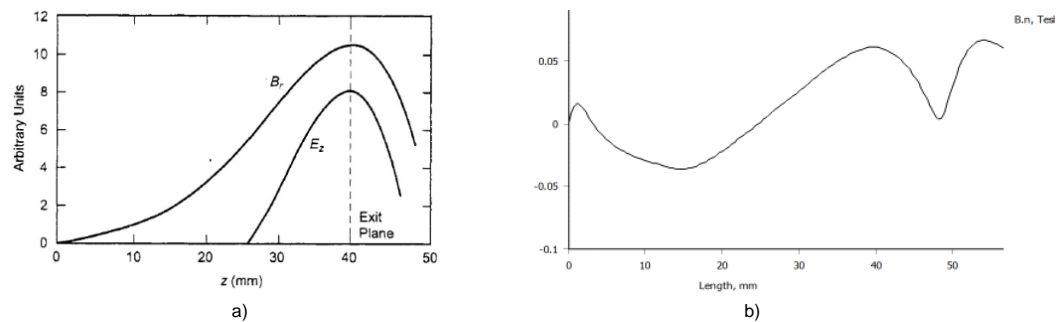


Fig. 3.3.3 ATHENIS magnetic configuration. (a) Ideal radial magnetic field and axial electric field along the channel. (b) Real radial magnetic profile for ATHENIS.

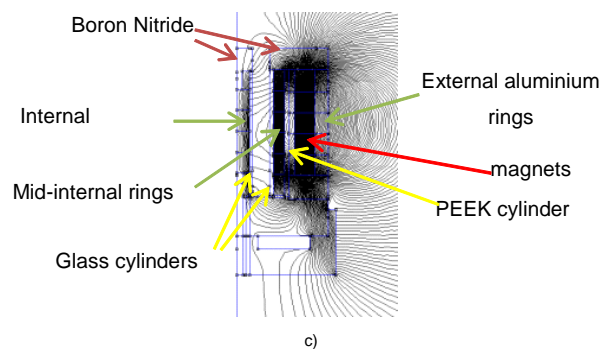


Fig. 3.3.4. Magnetic field contour plot for ATHENIS.

3.3.4 Pressures, flux and final configuration

The experiment will take place in a vacuum environment (Fig. 3.3.5). A TURBOVAC 1000C and a TRIVAC D 65B are the vacuum pumps available. The vacuum systems laws used in the simulations to determine a first geometry of the device are $Q = C(p_{\text{Hall}} - p_{\text{ch}})$, $\frac{dp_{\text{ch}}}{dt} = \frac{Q - p_{\text{ch}} S_{\text{eff}}}{V_{\text{ch}}}$ where Q is the total flow of Hydrogen injected, $C = 3.81 \frac{(D-d)^2(D+d)}{l} \sqrt{\frac{T}{M_{\text{H}_2}}} K_f$ is the conductance of the Hall channel, p_{Hall} , p_{ch} are the pressures inside the Hall channel and outside the device respectively, V_{ch} is the chamber volume and S_{eff} is the real pump velocity of the vacuum pumps since all the conductance of the test facility are considered in this term. In the first attempt, the simulation considered $p_{\text{Hall}} = 1.5\text{Pa}$ at the anode section, changing the geometry of the device in order to find a suitable Hydrogen flow which could be pumped away by the vacuum devices. Once got the geometry, the simulation considered the Hydrogen flow fixed and therefore it was possible to determine the real pressures inside the Hall thruster and inside the vacuum chamber. It is impossible to keep p_{Hall} constant along the channel, indeed, the pressure at the channel exit is equal to p_{ch} . A trade-off between these 2

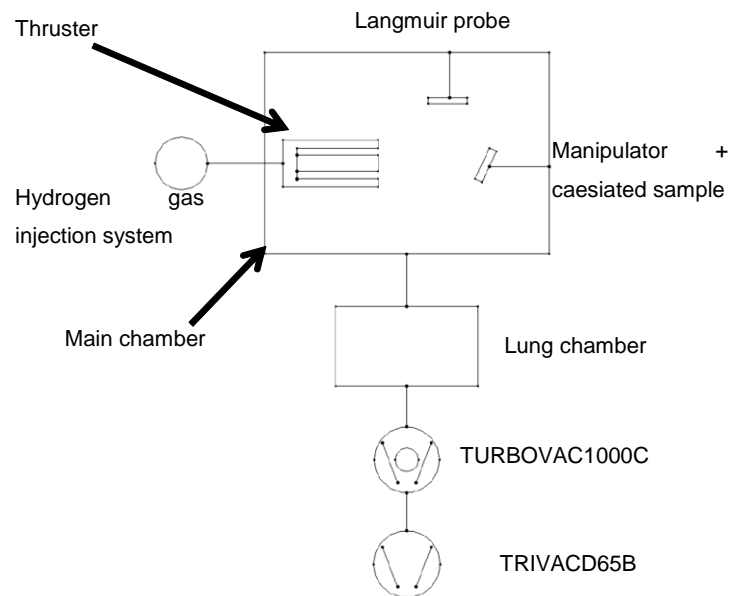


Fig. 3.3.5 Scheme ATHENIS test facility

pressures is necessary: p_{Hall} should be high enough to guarantee the discharge along the channel, while p_{ch} should be low enough to obtain certain free path of the Hydrogen atoms derived by the dissociation.

Through Serway's approach, the mean free path of an Hydrogen atom through a background of Hydrogen molecules is $\lambda = \frac{KT}{\sqrt{2}\sigma^2 p_{ch}}$, where the cross section corresponds to $\sigma^2 = \pi d_{H_2}^2$ and d_{H_2} is the Hydrogen molecule diameter. Keeping $p_{Hall} \approx 1.5Pa$, the mean free path lower limit is $\lambda_{lim} = 0.113m$, enough space to install the last part of the experiment at the exit of the Hall channel without problems. This component consists of a caesiated sample which will be mounted on a z-translator manipulator, hence movable along the device axis.

To determine an approximate range of the sample positions, the particles at the exit of

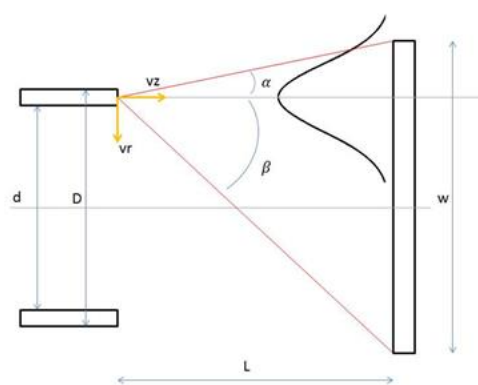


Fig. 3.3.6 Sample position scheme

the Hall channel are supposed to have a Maxwellian velocity distribution. Therefore, the radial velocity has a Gaussian profile which depends on the distance L of the sample (Fig. 3.3.6). The α, β angles limit the integral with which we determine the particles impact probability on the sample $P = P_\alpha - P_\beta$, with $P_\alpha = \frac{1}{2} \left[1 + \operatorname{erf}\left(\frac{v_{r\alpha}}{v\sqrt{2}}\right) \right]$, $v_{r\alpha} = v \frac{D-d}{2} \frac{w}{L}$, $v =$

$\frac{\varphi}{An}$. We consider the flux φ as $\varphi = \frac{1}{4}n\sqrt{\frac{8k_bT}{\pi m_H}}A$, where n is the Hydrogen atom density, A is the exit section, T is the energy of the atom and m_H is the atomic mass of the Hydrogen.

Thanks to these considerations, the final configuration of the device is represented in Fig. 3.3.7. The important parameters are $D=25\text{mm}$, $d=12\text{mm}$, $L=56.5\text{mm}$, $\dot{m}_{H_2}=0.03\text{mg/s}$, $p_{\text{Hall}} \approx 1.1\text{Pa}$, $p_{\text{ch}} \approx 0.15\text{Pa}$.

It is possible to change the pressures modifying the conductance among the chamber and the rest of the vacuum system; moreover, the design of the thruster allows to decrease the length of the channel in order to test other configurations. Finally, if we expect an Hydrogen atomic density at the exit of the channel of $n_H=10^{15}\text{m}^{-3}$, following the hypothesis cited previously and considering a conversion factor of 12%, that is, the probability of negative Hydrogen ions released after the impact of atoms on the caesiated surface, we expect a negative ionic current in the order of μA .

3.3.5 Numerical simulation including space charge compensation

Numerical activities were carried out in order to optimize the filter field component in the source region. An extensive study of the balance among the B field generated by the magnetic bars of the cusp magnets surrounding the source, allowed to found a configuration minimizing the vertical component of the field, so that the filter field becomes completely perpendicular to the co-extracted electron B field, and no mutual interference among the two are possible. From the beam transport point of view, a novel tool was made available to simulate the extraction and acceleration of multiple beam from the plasma. The code exploits the set of numerical libraries of "IBsimu", which were implemented in a 3D iterative self-consistent ray tracing code. A validation of the code

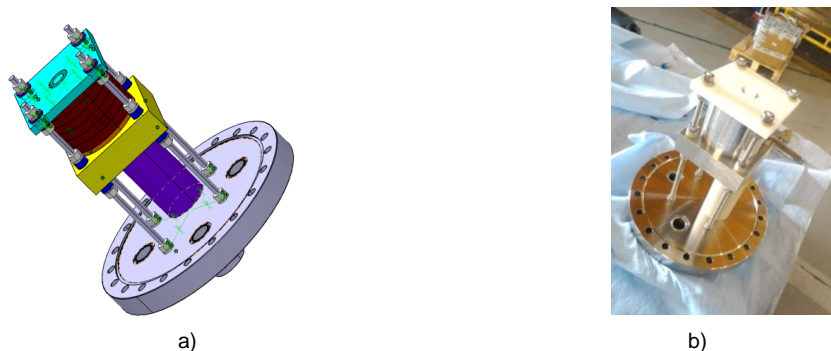


Fig. 3.3.7 ATHENIS design. (a) CATIA CAD. (b) Real prototype

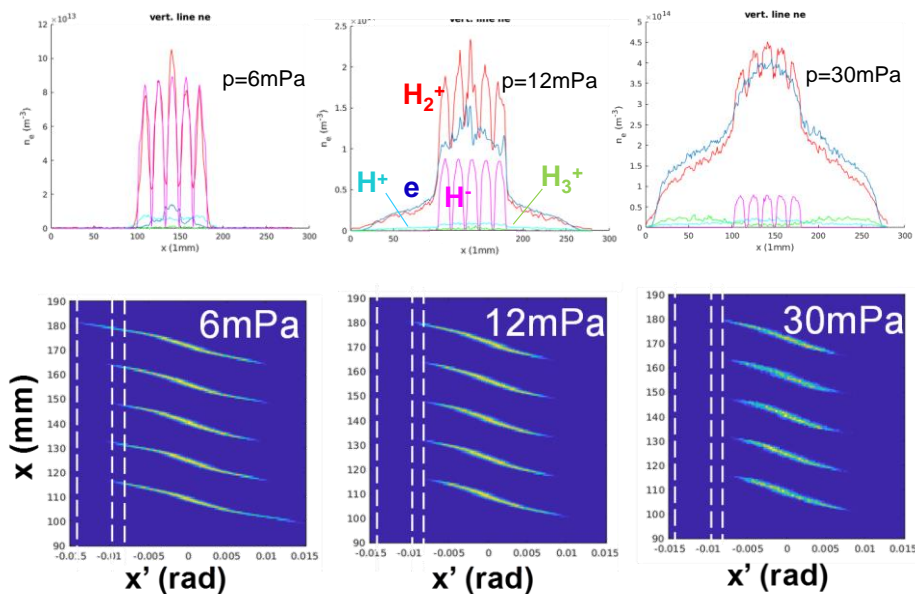


Fig. 3.3.8 Simulation results at different pressures: (TOP) - calculated density profiles along transverse direction for the 5 charged species; (BOTTOM)-, calculated total emittances including the 3 beam species (H-, H0, H+). Notice the growth of transversal velocities at reduced pressure, in particular for the edge beamlets.

against analytical estimation of the beam perveance and a comparison with the SLACCAD code in use at RFX gave satisfactory results. The tool is a valid alternative of the OPERA 3D code, and has some advantages over it, as a more sophisticated model for the negative ion extraction, and the fact that is developed in a open-source environment, allowing for include further physics effect as the interaction with the residual gas.

During 2017, a Particle In Cell-MonteCarlo Collision (PIC-MCC) code based on GPGPU was improved to include up to 26 collisional processes with differential cross sections, and it was applied to the beam plasma formation in NIFS Test Stand in which experimental measurements of the compensation plasma are were performed. The dependence on the background gas pressure was studied, as reported in Fig. 3.3.8. The density profiles at steady state for the five charged species (H0 is not shown) show a marginal compensation of the beam space charge at low pressure, while a denser secondary plasma is grown at relatively high pressure. The effect on the beam is a change from defocusing to focusing effect when increasing the pressure.

As shown in Fig. 3.3.9, the trend of plasma potential calculated with the PIC-MCC and the experimental measurements are in agreement. The study showed that the space-charge compensated beam potential is determined by the calorimeter bias voltage and the secondary electron emission at the calorimeter.

3.3.6 Plasma characterization by Energy Analyzer on NIO1

The beam plasma has been studied by experimental measurements and numerical modelling. The beam plasma permits the propagation of an ion beam by neutralizing the ion space charge; the level of compensation influence the single beamlet optics and the multibeamlet focusing. During 2016, a 4-grids Retarding Field Energy Analyser (RFA) was built (Fig. 3.3.10a); the probe designed to operate in very low density plasmas, was installed and used in the R&D Negative Ion Test Stand of National Institute for Fusion Science (NIFS), in Toki, Japan; the subject of the experimental campaign was the effect of gas pressure on space charge compensation and beam plasma parameters.

During 2017, the 4-grid RFA probe design was improved and a Langmuir probe was integrated in the system; an upgraded electronics for control and acquisition was also

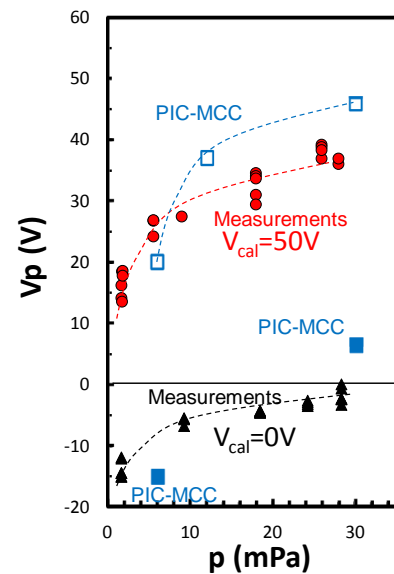
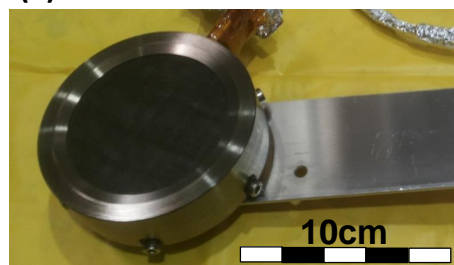
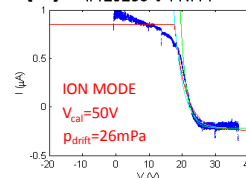


Fig. 3.3.9 Comparison between measured plasma potential as a function of gas pressure with RFA in NIFSR&D test stand (red circles and black triangles), and results of the PIC-MCC simulation (blue empty and solid squares).

(a)



(b)



(c)

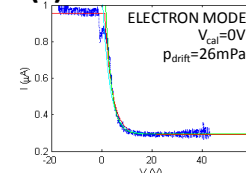


Fig. 3.3.10 a) the 4-grids Retarding Field Energy Analyser; example of ion (b) and electron (c) characteristics measured at NIFS for 2 different biasing voltages

prepared. The new system was installed and used again in the NIFS R&D Negative Ion Test Stand in November 2017. The RFA and LP characteristics were obtained for different beam energies and background gas densities. The effect of beam optics on the beam plasma and the plasma parameters have been studied in the absence of a carbon calorimeter at short distance: this latter study is important to scale the results to the case of SPIDER and MITICA. Examples of the current voltage characteristics are shown in Fig. 3.3.10 (b) and (c), for the use in ion-mode and electron mode.

The probe was also installed in NIO1 and measurements of the beam plasma were performed, also varying the distance from the beam axis thanks to the use of a axial manipulator as shown in Fig. 3.3.11.

3.3.7 *International collaborations*

In 2017 the collaboration with NIFS has continued, with purpose of characterizing the features of the beam generated by the newly installed plasma grid and of investigating the beam plasma characteristics. Two segments make up the plasma grid; in each half grid, two complete rows (15 apertures each) are open after masking together with 3 more apertures, not close to each other, in a further row. Several beam diagnostics were in operation: NIFS beamlet monitor made of two CFC tiles (to record the 2D beam pattern by the RFX thermal camera and to measure the electrical current by RFX and NIFS circuitries), Retarding Field Energy Analyzer (RFEA, provided by RFX, measuring the electron and the ion energy distribution functions), Langmuir probe (supplied by RFX to

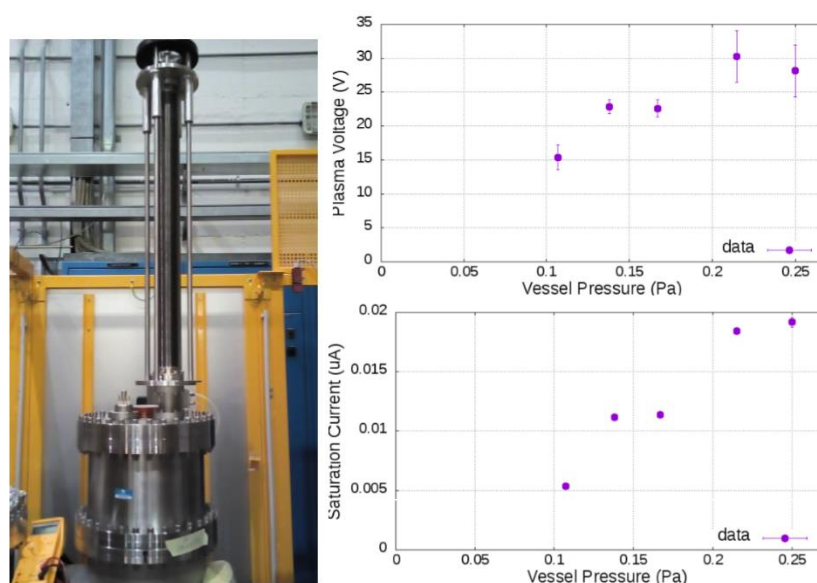


Fig. 3.3.11 (left hand side): the 4-grids Retarding Field Energy Analyser installed in NIO1, on a movable system to vary the distance with respect to the beam axis; (right hand side), example of measurements as a function of the vessel. pressure.

measure the electron properties; mutually exclusive with respect to the RFEA), the Beam Emission Spectroscopy (BES, provided by NIFS to measure the beam divergence), a CCD camera provided with H_{α} filter (supplied by NIFS to observe the beam). BES and visible camera cannot operate when the beamlet monitor intercepts the beam.

The activity at NIFS involving RFX personnel lasted 5 weeks in November-December 2017; the first 3 weeks were devoted to the installation of RFX diagnostics in the beam drift region (drift tube), of the beam source and of the hydrogen gas injection system for the drift tube; then operation started with source conditioning while RFX personnel tested the diagnostic systems and developed the software for acquisition and analysis of the CCD camera. The last week was fully dedicated to the characterization of the beam. Several campaigns were performed: with beamlet monitor, scan of arc power, acceleration voltage and pressure in drift tube; with BES and CCD camera, scan of drift tube pressure and at fixed pressure scan of arc power and acceleration voltage; in all cases either the RFEA or the Langmuir probe were also operating. As the data collection ended on 8 December, the data will be analyzed in the next months. Preliminarily

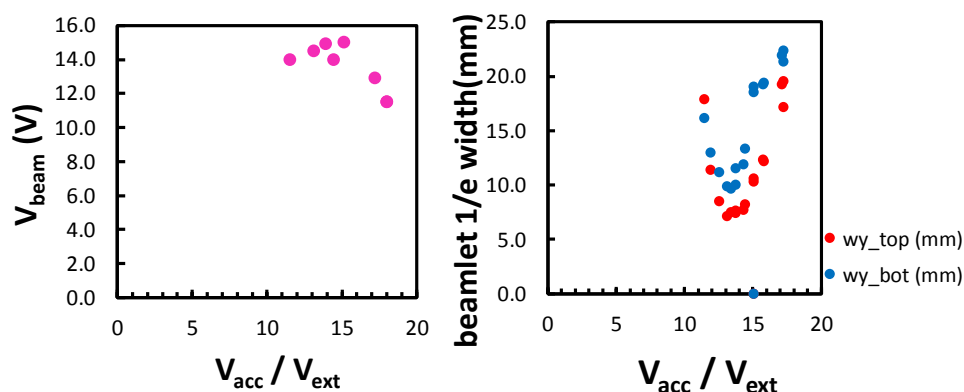


Fig. 3.3.12 Beamlet width (left) and beam potential (right) vs acceleration voltage

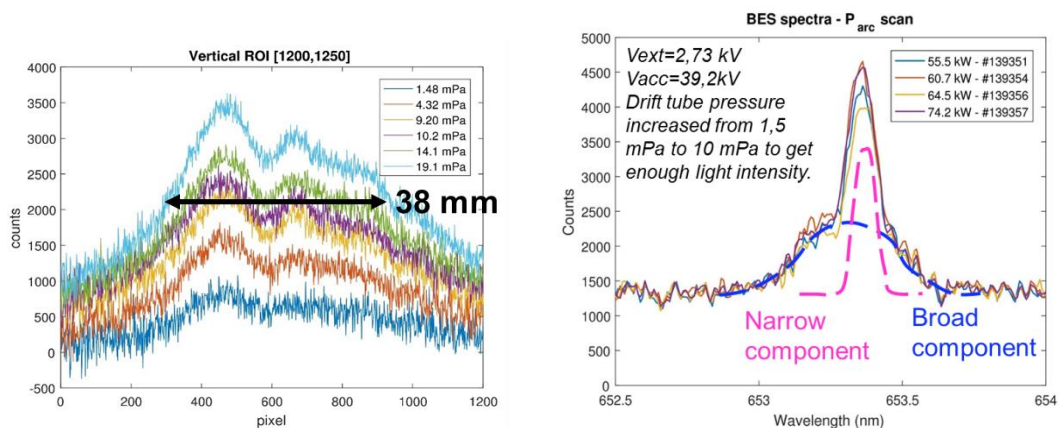


Fig. 3.3.13 Beamlets viewed by 2D CCD camera as function of drift region pressure (left) and an example of BES signal exhibiting two components (right)

examples of the beam characterization are given in the following Fig. 3.3.12 and Fig. 3.3.13.

3.4 PPPT Projects

In 2017 further modifications of the DEMO reference design have been proposed by the design team, mainly consisting in the reduction of the number of toroidal field coils from 18 to 16. The resulting parameters from a new run of the PROCESS code have been issued by in July 2017, thus part of the work in all the packages has been addressed to verify the relevant impact on the different subsystems.

3.4.1 WPHCD - Heating and Current Drive systems

The injection of high energy neutral beams is one of the main tools to heat the DEMO plasma up to fusion conditions. A conceptual design of the Neutral Beam Injector (NBI) for the DEMO fusion reactor is currently being developed by Consorzio RFX in collaboration with other European research institutes. High injector efficiency and RAMI (Reliability, Availability, Maintainability and Inspectability), which are fundamental requirements for the success of DEMO, must be taken into special consideration for the DEMO NBI.

During 2017, the following activities have been carried out:

- A novel design of the beam source for the DEMO NBI has been developed featuring multiple sub-sources, following a modular design concept, capable of increasing the reliability and availability of the system.
- A full comprehensive suite of models, featuring a self-consistent magnetic-electrostatic-ion particle tracking, an electron tracking and a thermo-mechanical model, has been set up and used as the main tool for the development of the extraction/acceleration system for the DEMO NBI. The suite of models can take into account all the main physics and engineering aspects (beam optics, co-extracted and stripped electrons, heating power deposited on the grids, working temperature of the grids and related stress and deformations) at the same time and in a self-consistent way.
- The suite of models described at the previous point has been applied to investigate the current conceptual design of the extraction/acceleration system for the DEMO NBI, featuring grids having a decreasing number and increasing size of the apertures from the entrance to the exit of the system.

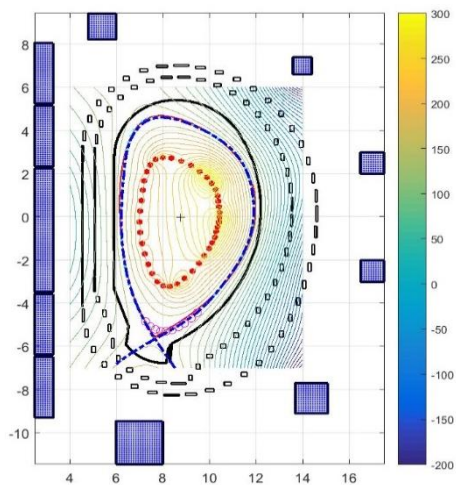


Fig. 3.4.1 reconstructed boundary (dashed blue line) and equilibrium code reconstruction (red line)

cavity has been put under operation and it has demonstrated the possibility to achieve stable optical configurations. These activities have been carried out in collaboration with LOS (Laser Optical Systems St Petersburg).

- Regarding the studies on the energy recovery, during 2017 the first circuit prototype of the high voltage inverter at the input stage of the energy recovery circuit was constructed and tested.

3.4.2 WPDC – Diagnostic and Control

A broader effort is underway to develop a plasma position and shape control system for DEMO, where in-vessel magnetic measurements will be not available due to the high neutrons flux and long pulse operations. At RFX, in 2016, an alternative plasma boundary reconstruction algorithm based on a purely geometrical approach and relying solely on reflectometric measurements has been developed and numerically tested for a DEMO reference equilibrium. This approach allows a reasonable estimate of the macroscopic plasma parameters such as the plasma cross-section area, elongation and triangularity. The robustness of the algorithm has been also tested against a reduced set of reflectometric measurements and the experimental measurement error. This analysis allowed defining a minimum number of reflectometer per poloidal section (15) needed to accommodate plasma shape and position control requirements. In 2017, the algorithm has been complemented with a more accurate treatment of the reconstruction of the X-

- The DEMO NBI conceptual design has been discussed with the interested working groups of EUROfusion, working on the main related issues (physics, integration, breeding blanket, remote maintenance, neutronics).

- Photoneutralization is regarded as one of the most interesting alternatives to stripping neutralizers in NBI systems. R&D activity on photoneutralization at Consorzio RFX involves the construction and test of a non-resonant cavity for second laser harmonic trapping, fed by a pulsed Nd-Yag laser. During 2017, the

point region⁶⁴. The new algorithm version, thus, included the information of the currents flowing in the plasma and in the poloidal field coils. Fig. 3.4.1 (dashed blue line) shows the final boundary reconstruction with respect to the equilibrium code boundary (red line): the agreement is fairly good.

A second part of the activity concerned a statistical assessment of the algorithm reconstruction: different tests confirmed the reliability of the method even if the reconstruction of the X-point amplifies the error in the reconstruction based solely on reflectometric measurements (purely geometrical approach). Also in the light of this consideration, a reduced set of measurements appears not suitable for a correct plasma shape reconstruction. These results, however, suggested further improvements in the algorithm to be implemented in 2018.

3.4.3 WPPMI - Plant Level System Engineering, Design Integration and Physics Integration Plant Electrical System Design

In 2017, the awareness has increased of the need of studies on the Plant Electrical System both to face some issues related to power peaks, reactive power demand and generator operation and to better consider RAMI, size and cost of the plants. To improve the confidence of the preliminary design, two new activities have been launched, that have also been the themes of two master degree thesis.

The first one was the development of a simplified zero-dimensional linear model of the poloidal circuits of DEMO, on the basis of the available geometry of the poloidal magnets and vacuum vessel (referred as DEMO 1 reference design before the last modification in July). This model accounts for the magnetic coupling among the coils and the vessel, allows integrating the power supplies, besides requiring very low computational resources. The model can be used to reproduce the circuits operation in normal and anomalous conditions, thus identifying possible overcurrents end/or overvoltages. An example of application is given in Fig. 3.4.2, showing the currents in the poloidal magnets and in the vacuum vessel in case of central major disruption, with a linear decay of plasma current in 74 ms starting from $t = 0$. The simulation allows evaluating the level of overcurrents that can occur in the coils in this specific operating condition; these overcurrents in some cases could cause an exceeding of the nominal value. Thus, this

⁶⁴ G. Marchiori, G. De Masi, R. Cavazzana, A. Cenedese, N. Marconato, R. Moutinho, A. Silva and the EUROfusion-IM Team, "Study of a plasma boundary reconstruction method based on reflectometric measurements for control purposes", 27th IEEE Symposium On Fusion Engineering 4 – 8 June 2017 Shanghai, China, submitted for publication on IEEE Transactions on Plasma Science.

tool can help to achieve a better definition of requirements of the sub-systems, useful for the design phase.

The second main task line launched has been focused on studies of advanced technologies for the power converters, capable to solve some of the issues under consideration. One of them is the huge reactive power demand to the grid network by the poloidal base converters. The study has been organized as follows: firstly, considering a traditional design approach based on thyristor rectifiers, the reactive power has been estimated with a comprehensive model, including circulating mode and sequential controls, assuming coil voltage and current profiles provided by CREATE Consortium. Then, a possible reactive power compensation system has been tentatively outlined, in analogy with ITER. Finally, alternative solutions for the converters, and in particular those based on the Active Front End (AFE) technology, have been considered. Their suitability for DEMO has been verified with a dedicated model, and their impact on the reactive power demand, reliability and space occupancy has been studied; the work is still in progress and will continue next year.

In parallel, work on the other task lines has been continued with further analysis of the electrical system configuration and circuits of the pulsed power supply system, ratings of the main converters, discussions and contributions to the definition of realistic operative

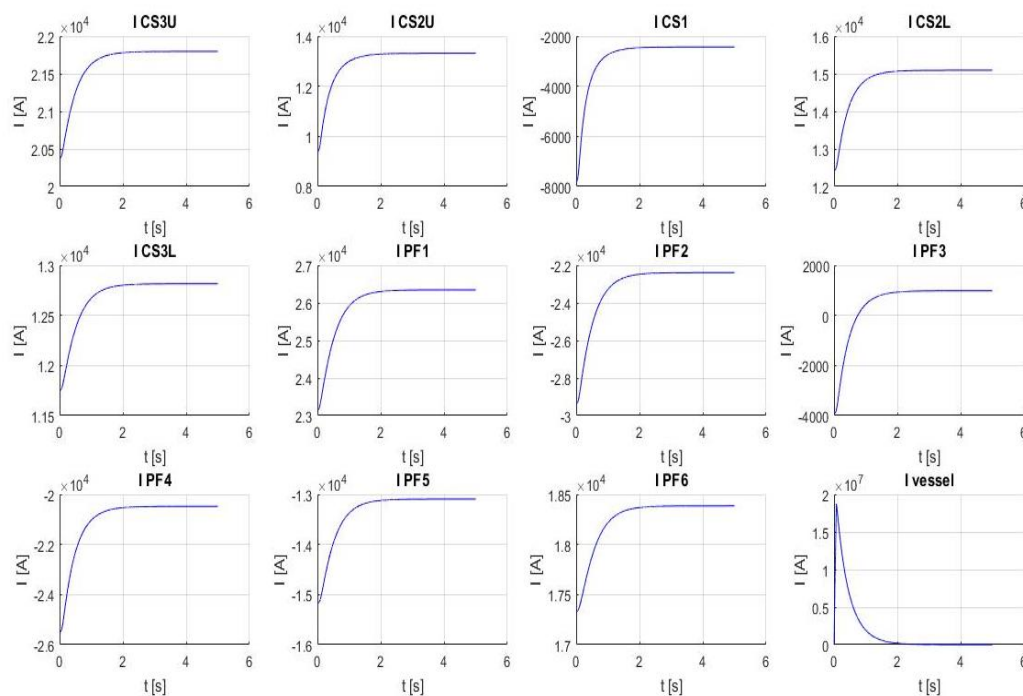


Fig. 3.4.2 Currents in the poloidal magnets and in the vacuum vessel in case of central major disruption (linear decay of plasma current in 74 ms starting from $t = 0$)

scenarios, update of the Plant Breakdown Structure and Electrical Load List.

3.4.4 WPMAG - Magnet system

In 2017, further studies has been carried out on the DEMO TF circuit topologies to explore the possibility to decrease from 18 to 9 the number of Quench Protection Circuits (QPC), Current Leads (CL), busbars and penetration into the tokamak buildings, which can produce benefits in terms of cost reduction and efficiency increase. Some evaluations on the impact of the possible modification from 18 to 16 TF coils have also been done. The studies on TF circuit topologies have been carried out with the aim to estimate the maximum voltage applied at the coils terminals with respect to ground, the voltage across each coil and the equivalent time constant for the discharge; this year the work continued evaluating the reduction in the voltage peaks achievable by adopting temperature dependent resistors.

In addition, first analyses on the poloidal field circuits have started, using the model developed in the frame of the PMI2.1 task; an example is given in Fig. 3.4.3, showing the the currents in the poloidal circuits in case of a fast discharge which allows the evaluations of discharge times and I^2t levels in the coils.

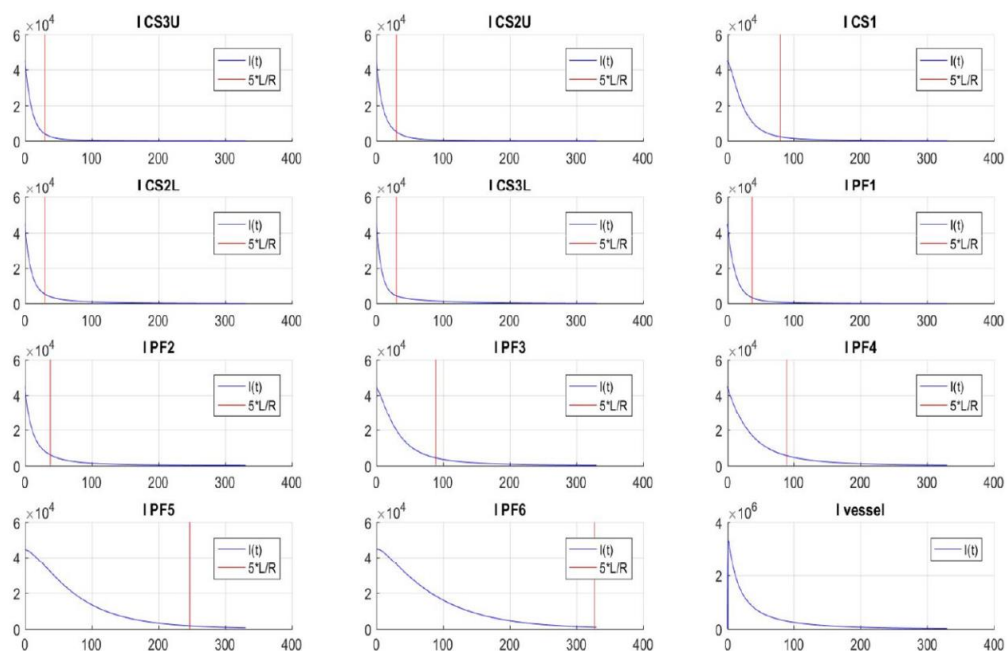


Fig. 3.4.3 Currents in the poloidal magnets and in the vacuum vessel in case of

3.4.5 WPTFV Tritium, Fuelling and Vacuum

Large Non-Evaporable-Getter (NEG) pumps were proposed for fusion applications in Neutral Beam Injectors (NBI) as an alternative to cryosorption pumps. In order to demonstrate the scaling of relatively low-size NEG commercial pumps for the use in NBI vacuum systems, in the framework of the WPTFV a

mock-up pump is being designed. During 2017, this conceptual design activity has been carried out, and the detail design phase was started. In the conceptual design phase, the number of disks, heating system, multi-disk pattern and overall pump geometry were defined in collaboration with SAES.

At the same time, the experimental characterization of NEG disks continued at SAES in close collaboration with RFX researchers: the characterization focused on the regeneration phase, essential to determine the duty cycle for the pump sorption/desorption phase and the maximum gas load with respect to the number of the disks. These experimental activities aimed performed on getter assemblies of increasing size (see Fig. 3.4.4) had a fundamental role in the strategy to the development of a large size mockup pump: the conceptual design of the NEG mockup pump, up to date the biggest NEG single pump ever built, is based on the use of numerical models that were validated in these experimental characterizations (see). In the present design, the mockup pump has a pumping speed of 10000 l/s.

In the same framework of the WPTFV, the gas flow simulations of the present DEMO injector design were performed with Avocado, in order to preliminarily evaluate the gas density profile and related beam losses for different pump configurations (see Fig. 3.4.6).

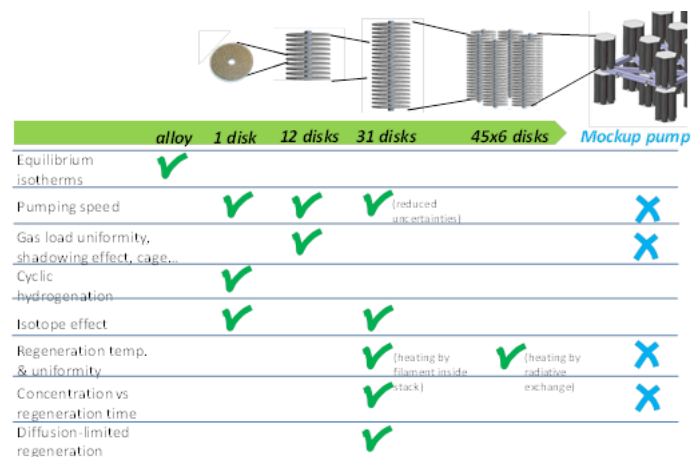


Fig. 3.4.4 R&D strategy to the development of a large NEG pump: the fundamental properties are studied characterizing getter assemblies of different sizes

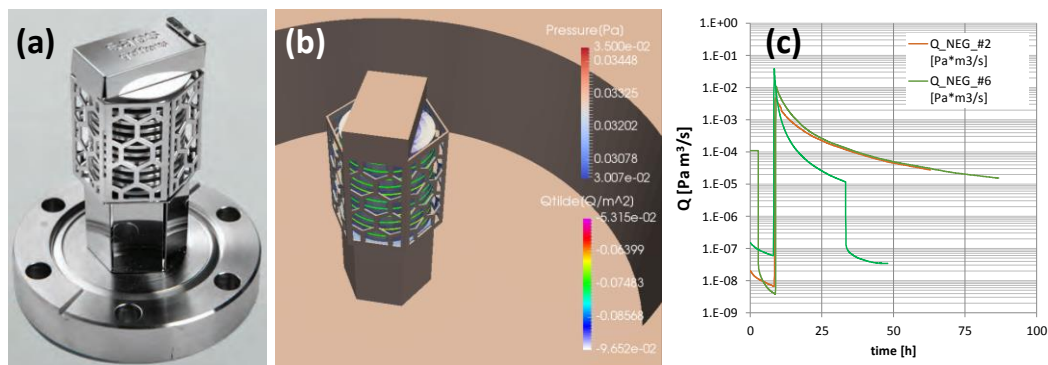


Fig. 3.4.5 (a) one type of SAES commercial pump used for the experimental characterization; (b) numerical simulation in Avocado code; (c) hydrogen desorption during regeneration of a 31-disks NEG pump

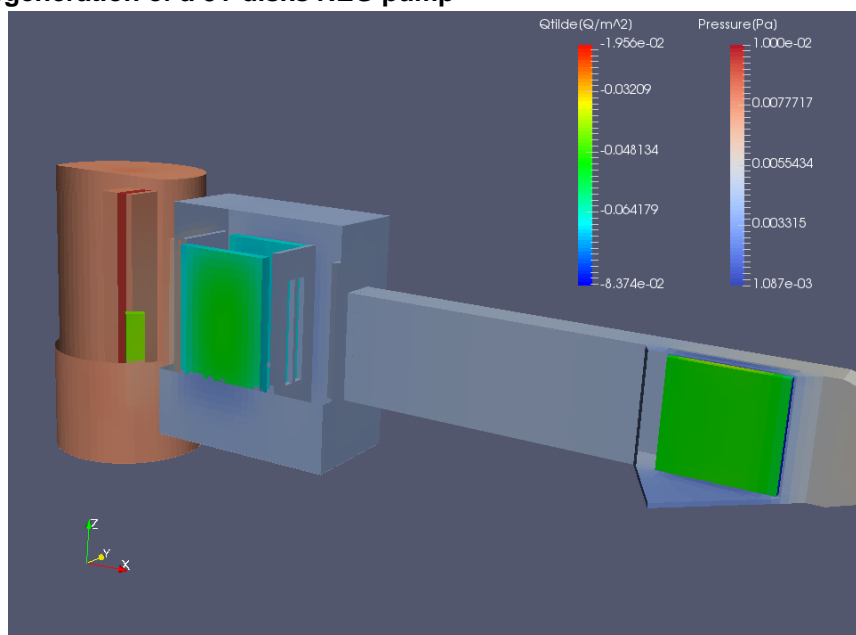


Fig. 3.4.6– 3D view of the vacuum domain, colours in log scale

3.4.6 WPSSES - Socio Economic Studies

3.4.6.1 Fusion power plant assessment studies

Shortage of relevant new information about costs from ITER and industries formally involved in EUROfusion activities on fusion cost estimation did not allow for updates of the economic model of FRESCO. On the other hand, a small task under WPPMI has been carried on cost sensitivity studies with PROCESS code for 1) the identification of the most cost-critical components/materials in the model, 2) and the sensitivity of overall costs to variations in those factors. According to the current cost model, the direct power plant costs generally account for ~60% of total plant capital cost while the rest is indirect, contingency and interest during construction costs. Among direct costs, the magnets, the cryogenic system and the reactor building are those with the greater weight. The activities

will be continued in order to identify alternative possible strategies for deriving cost estimates of the most cost-critical plant components.

3.4.6.2 The role of fusion in long term energy scenarios

The resources allocated on WPSES (Socio Economic Studies) have been invested on both the project management and research activities.

According to the 2017 Annual Work Plan, the ETM model (which now stands for EUROfusion TIMES model) has been revised after a first debugging. Special attention was paid to regional results of the energy scenarios being the major interest of the general public. Efforts were spent for reviewing the external costs of fusion as compared to the other electricity generating technologies. Compatibly with the available data and considering the whole life cycle analysis, the external cost of fusion exceeds only those of wind and hydro power stations and the current generation of fission power plants. Due to the limited literature, advanced nuclear fission generation (GenIII+ and GenIV) could not be included in the comparison. First work has been carried out with ENEA to couple ETM with PLEXOS, a dispatch model generator. The activity aims at estimating the storage capacity required in Europe to cope with an increasing share of electricity from renewables and assessing the effect of different fusion power plant operative mode (steady state or pulsed) on the electric grid. Finally, a first contribution has been given to the implementation of an energy game for the Fusion Expo that will be based on the energy scenarios generated by ETM under WPSES activities.

Besides, activities for the enhancement of the COMESE code (*COsto MEdio del Sistema Elettrico*) have been carried out. The code can now assess the sustainability of the energy scenarios according to the resources availability and technical constraints (e.g. limits on the installable wind or solar capacity); estimate the storage capacity required to meet the energy demand on a hourly basis; assess the economic viability of alternative strategies for electricity generation and demand management.

3.4.6.3 Surveys on visitors' reaction to fusion labs

In 2017 the activity on improving visits' feedback to fusion labs developed in collaboration with JET and IPP within the Socio-Economic Studies and FuseCOMM teams. Data collected on visits to labs, by the FuseCOMMs, have been investigated to elaborate useful line guides for visits improvement. The results have been published and presented to the FuseCOMMs for discussion.

4 Broader Approach

In the context of the Remote Experimentation Centre (REC) activity and in particular , within the F4E OPC566 contract, in 2017 the scheduled tasks have been finalized producing the final document about the exploitation of the MDSplus data system for remote data access. In June 2017 the site acceptance test has been carried out in Rokkasho, and the ability of the developed tools to effectively display remote signals has been demonstrated.

4.1 Contribution to the JT-60SA tokamak

In 2017 Consorzio RFX team mainly continued working on the second system to be procured for JT-60SA: the “Power Supplies for the in-vessel sector coils for RWM control”. In parallel, participation in the JT-60SA international Project Team activities has continued; this year, in particular, more specific discussions have started regarding the integration of the power supply systems and more in general the JT-60SA integrating commissioning and first operation.

4.1.1 **Power supply system for in-vessel sector coils for RWM control**

This power supply system is devoted to feed the 18 in-vessel sector coils of JT-60SA, aimed at controlling a set of plasma instabilities called Resistive Wall Modes (RWM). This system is composed of an ac disconnecter, a step-down transformer, an ac/dc conversion system and 18 power amplifiers. The power amplifiers (300 A, 240 V each) constitute the most innovative part; their final design has been the result of an R&D task aimed at proving the feasibility of the fulfilment of stringent dynamic requirements (bandwidth of 3 kHz and latency between output voltage and reference lower than 50 μ s), which were beyond the standard industrial performances, adopting a simple H-bridge topology. A prototype, based on hybrid Si-SiC IGBTs (Isolated Gate Bipolar Transistors) recently available in the market, has been developed and widely tested in 2013-2014. Considering the very successful results, the final design for the whole system has been based on the same technology. This is the first PS system in fusion experiments adopting SiC semiconductors.

In 2015 the Agreement of Collaboration and the Procurement Arrangement for the full system were signed. The call for tender was launched at the beginning of 2016 and the contract has been awarded to the company E.E.I. The First Design Report has been issued in the end of 2016. As shown in the scheme of Fig. 4.1.1, the system is split in two

Power Conversion Cabinets (Fig. 4.1.3), each with its own ac/dc converter and distributed dc-link capacitor bank and fed by a separate transformer secondary winding.

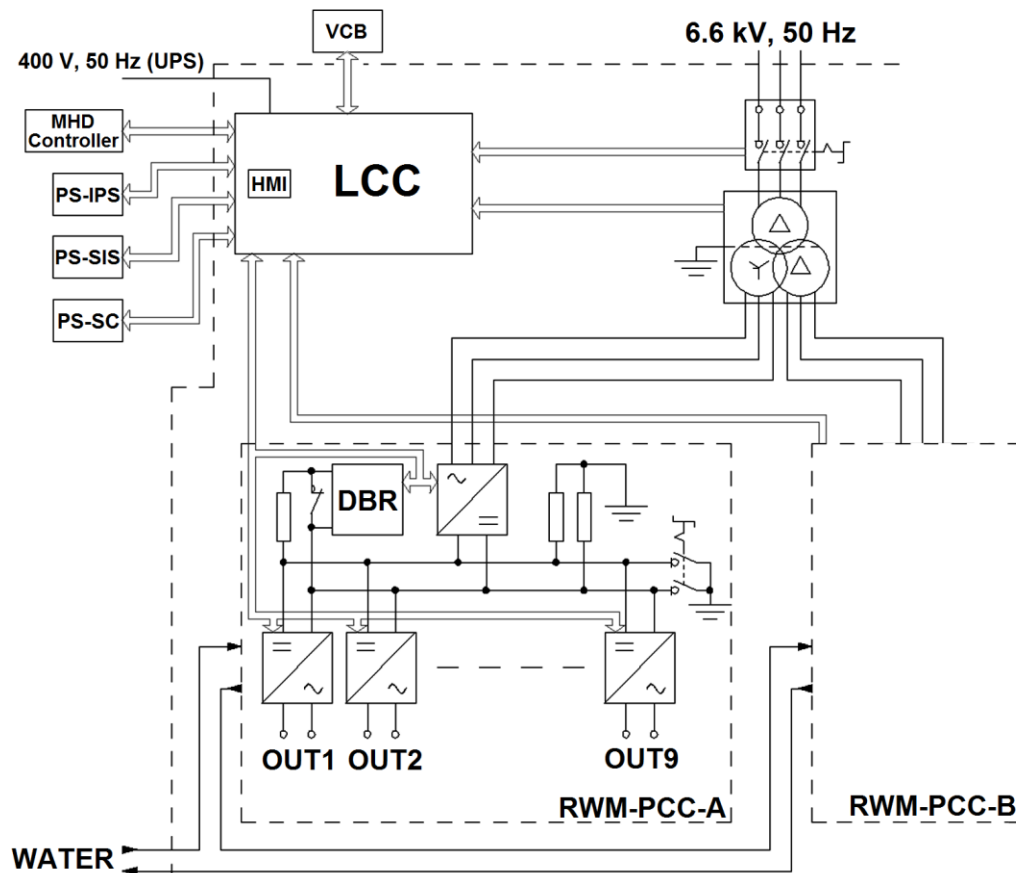


Fig. 4.1.1 - Scheme of the full RWM-PS system

The whole prototype for the Type Tests was completed in June 2017 (Fig. 4.1.2); it includes: one cubicle with the fast power amplifier provided with a new advanced digital control board, one cubicle with one ac/dc rectifier and the Local Control Cubicle with the necessary boards. Also a cubicle with the entire dc-link capacitor bank of 9 inverters has been realized, for testing purpose only. After preliminary ones, the official Type Tests have been conducted in factory in August and September 2017, according to the agreed schedule. The results have been very good proving the compliance with the specifications and in particular with the dynamic requirements, already verified with the first prototype and fully confirmed. A Design Review Meeting with F4E and QST has been held in Padova on October 2017, to discuss the Type Test Report. Additional tests on the output filters have been performed in November, to gain more confidence on the suitability of their thermal design and dedicated software protection, under anomalous input reference conditions.

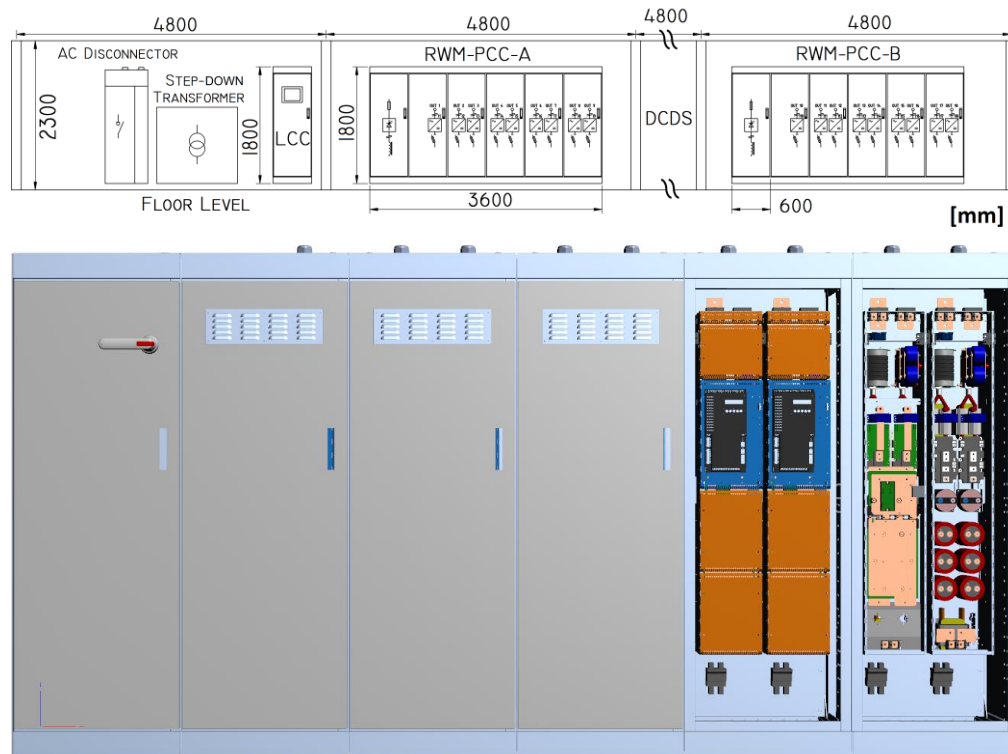


Fig. 4.1.3 - Top: overall view of the RWM-PS. Bottom: Power Conversion Cabinet, with the details of two fast inverters and their internal components on the right

This year, besides the usual contractual follow-up activities, proper management of the technical interfaces and monitoring of type test campaigns in factory, a lot of follow-up effort has been addressed to the introduction and testing of further improvements, focused in particular on: the thermal performance of the differential output filter, the suitability of the common mode output filter in reducing the EMI on the delicate



Fig. 4.1.2 - RWM-PS system prototype for the Type Tests

diagnostics in the tokamak building, the optimization of the dynamic current limiter (which avoids the permanent stop of the inverter in case of plasma-induced overcurrents), and the study of the switches “dead-time” compensation to improve the quality of output voltage. Regarding this last point, an example of the achieved

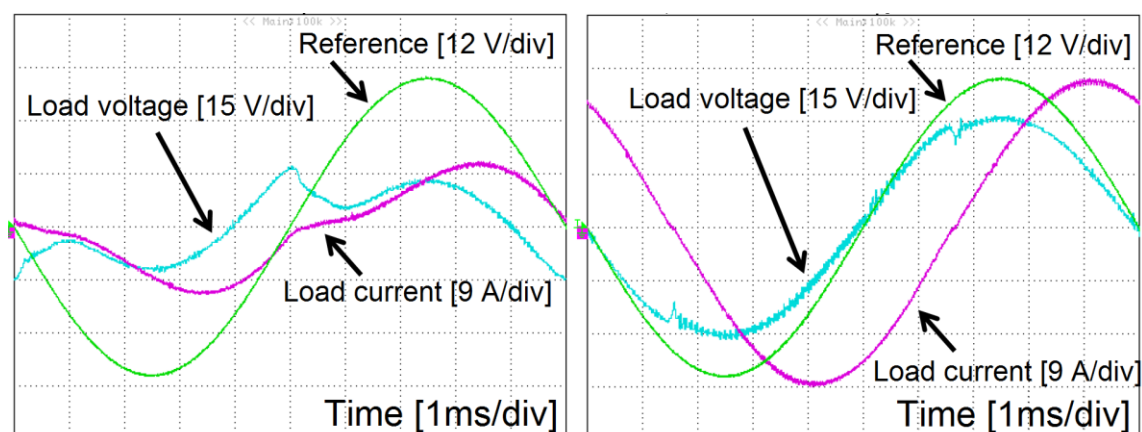


Fig. 4.1.4 - Load voltage and current without (left) and with (right) dead-time compensation, measured on the first inverter prototype in VCM.

performance is given in Fig. 4.1.4.

The manufacturing of the entire system is in progress, with the plan to deliver it in Japan in September 2018.

An oral presentation of the system design and features⁶⁵ has been given at the 27th IEEE Symposium On Fusion Engineering in Shanghai.

4.2 Remote participation

In the context of the Remote Experimentation Centre (REC) activity and in particular , within the F4E OPC566 contract, in 2017 the scheduled tasks have been finalized producing the final document about the exploitation of the MDSplus data system for remote data access. In June 2017 the site acceptance test has been carried out in Rokkasho, and the ability of the developed tools to effectively display remote signals has been demonstrated. .

5 Industrial Collaborations

5.1 Model for the electrostatic design a new VCB prototype

In February 2017 the contract with Siemens has been concluded. The Final Report has shown that the fully 3D version of the Voltage Holding Predicting Model VHPM works in a very satisfactory way in terms of fast convergence to the true solution. In fig. xx is shown the pattern of the trajectories calculated for the contact of the VSG24-1-25 tube (nominal voltage 24 kV - pure 3D geometry of the contact); in warmer colours are also indicated

⁶⁵ A. Ferro, et al., "Design and manufacturing of the SiC-based Power Supply system for Resistive-Wall-Mode control in JT-60SA", IEEE Transactions on Plasma Science, in press

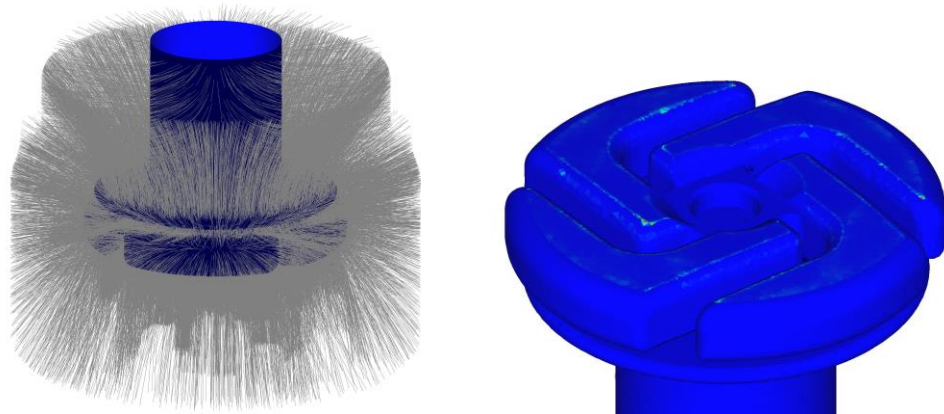


Fig. 5.1.2. Left: trajectories of particles emitted from the cathode. Right: in warm colour the areas with the higher breakdown probability.

the contact areas with higher breakdown p.u. probability to be the origin of the voltage breakdown.

The comparison of the prediction made by VHPM with the measured voltage breakdown distribution was actually not satisfactory. Detailed analysis has shown that there were inconsistencies in the measured data: for example, the voltage breakdown measured of the 24 kV tubes resulted –surprisingly– higher than the 36 kV tube. Other controversial points regarded the quality of the statistical distribution, which deviated in non-negligible way from the expected Weibull one: this was deemed to be the consequence of a not achieved voltage conditioning.

For this reason, Consorzio RFX has proposed to Siemens to continue the cooperation, using, instead the test lab in Berlin, the HV test lab at the Department of Industrial Engineering of the Padova University. The proposal has been accepted by SIEMENS; this agreement was under finalization in December 2017.

5.2 Biomedical plasma applications

The area of applications of low-temperature, atmospheric pressure plasma technology in medicine (also known as “plasma medicine”) is experiencing a steady growth, with new research groups entering the field each year. The expertise gained by the RFX plasma medicine group is proving precious to keep the pace of

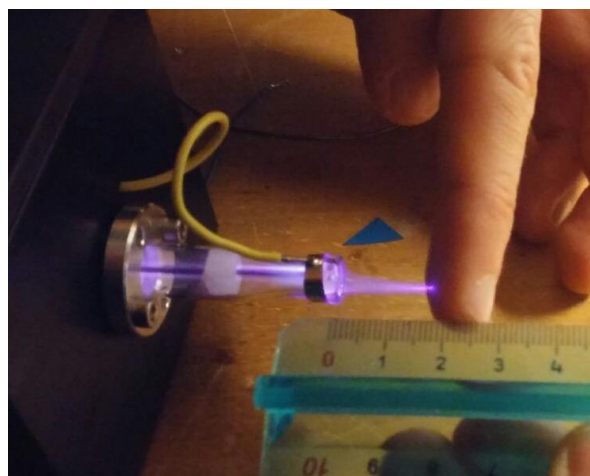


Fig. 5.1.1 Helium plasma created by the DBD plasma jet.

the increasingly accelerating science and innovation in the field.

In 2017 a remarkable effort has been devoted to the improvement of the array of plasma sources available for this kind of research. In the past, all the activities were performed using a radiofrequency (RF) plasma source for indirect treatments, originally developed for disinfection within the context of corneal keratitis. During the course of the year, a new plasma source based on the principle of the Dielectric Barrier Discharge (DBD) plasma jet has been developed and tested. The source hosts a high voltage electrode and a grounded electrode, separated by a dielectric layer, required to prevent the onset of an electric arc. The high voltage electrode is driven by a specifically developed power supply, creating a voltage waveform with an amplitude of 6-8 kV and a frequency of the order of 10 kHz. The power supply unit uses an Arduino Leonardo microcontroller to drive a coil mounted on the source head, which produces the required high voltage. As shown in the figure, a plasma jet having a length of the order of 2 cm is produced, having a gas temperature low enough to allow a direct non-damaging treatment of living tissues. Several versions of this source have been built, improving the design with experience, with the last one being a reliable and carefully designed tool with all the required properties for the use in a biological laboratory. The source can use helium or argon as working gases. The development was carried out in the framework of the 3-year research project which Consorzio RFX is carrying out in collaboration with University "Magna Graecia" of Catanzaro and AIST-Tsukuba, on the topic of non-thermal plasma driven blood coagulation, with funding from "Fondazione con il Sud".

The project on non-thermal coagulation mentioned above, following the plasma source development phase, has started to produce the first results. Indeed, the use of the DBD plasma jet on blood samples obtained from patients following an anticoagulant therapy has shown the ability of the helium plasma to accelerate the coagulation process. The coagulation of treated samples required in these first tests about 15% less time than that of control ones, for a duration of the plasma treatment of one minute. However, it should be mentioned that there is still ample space for optimization of the process. In this respect, a spectroscopic characterization of the plasma properties has been started, with emphasis on the identification of active chemical species which can be the origin of the coagulation acceleration. Some preliminary tests performed on rats have also shown an accelerated coagulation following a one-minute treatment with the plasma jet.

The effort in the improvement of the array of available plasma sources has also led to the construction of a prototype of surface discharge source, a type of DBD source operating

in air. The source has been driven by one of the prototypes of the power supply built for the DBD jet, and has been used in collaboration with the Department of Chemical Sciences within a project on the use of plasma for food disinfection. The first results obtained with this source have been encouraging, showing a remarkable disinfection power, stimulating a refinement of the design and further tests to be carried out in 2018.

Meanwhile, the work on selective killing of cancer cells using the RF plasma source has been continued, yielding new results and improving the statistics. The experiments, performed on primary cells of lung and laryngeal cancer obtained from surgical samples, have confirmed the ability of the plasma to induce apoptosis in cancer cells with a higher rate than in healthy ones, and the primary role played in this process by intracellular Reactive Oxygen and Nitrogen Species formed as a consequence of the plasma action. Furthermore, the selective effect can be enhanced by the synergic effect of a molecule which is known to increase the ROS level within the cells.

The problems encountered with the power supply of the industrial-grade RF source being developed jointly by Consorzio RFX and by the company holding the patent license were solved in the course of 2017, and new biological tests were performed in collaboration with the company, confirming the good disinfectant properties, and paving the way to the start of the clinical trials on the treatment of corneal infections, which will be organized by the company in the course of 2018.

6 Education, Training and Information to the public

6.1 Education and Training

6.1.1 *International Doctorate in Fusion Science and Engineering*

In 2017 the *Joint Research Doctorate in Fusion Science and Engineering* by Padua University (Università di Padova), Lisbon University (Universidade de Lisboa) and Naples University (Napoli Federico II) has been operating under the coordination of the University of Padua and Consorzio RFX. Twenty PhD students enrolled from academic year 2013/14 (XXXIX cohort) to academic year 2016/17 (XXXXII cohort) within this framework (two belong also to the Erasmus Mundus Fusion-DC programme, within international co-tutelle agreements between the Universities of Padua and Ghent and the Universities of Padua and Carlos III de Madrid UC3M) have been performing their study and research activities at Consorzio RFX, under the supervision of experts belonging to the University of Padua and Consorzio RFX.

In 2017, 4 PhD students successfully defended their PhD thesis (April 2017) and obtained their degree. One of them is now working at Consorzio RFX, two moved to different Laboratories (INFN Legnaro and IPP GRCHING) and one went back to China.

Moreover, 8 PhD students (XXIX-XXX cohort) have completed their three-year programme and have been admitted to the PhD thesis defence that will take place in 2018.

It as to be mentioned that in 2017 the Universities of Padua and Gent, on the basis of the successful experience in running two international leading programmes (the Padua-Lisbon-Munich initiative and the Erasmus Mundus Fusion Doctoral College), have implemented a Joint Doctorate Programme in “Fusion Science and Engineering” aiming at the continued formation of a suitable number of doctoral students at the highest level of excellence. As a result, from academic year 2017/18 (i.e. from 1 November 2017), 4 PhD students enrolled within this new framework have started their activities at Consorzio RFX under the supervision of experts belonging to Padua-Gent Universities and Consorzio RFX.

Two advanced courses on “Plasma Diagnostics and Control” (Padua, May 2017, 6 ECTS) and “Fusion Technology” (Padua, November 2017, 6 ECTS) have been organized by Consorzio RFX and offered to PhD students belonging to the Joint Research Doctorate and Network.

6.1.2 Other education and training activities

The other educational and training actions carried out at Consorzio RFX have continued as usual, with tutoring of Master/Bachelor students, with internships of master students and with summer stages of high school students.

Also the educational activity for the RFX staff continued with an advanced course on MDS Plus dedicated to our scientists.

Moreover the following 7 regular courses on Plasma Physics, Fusion Technology and Industrial Applications of Plasmas were held by teachers from Consorzio RFX at Padua University:

- Basic principles of Plasma Physics (6 ECTS, 1st Level Degree, Physics)
- Physics of Nuclear Fusion and Applications of Plasmas (6 ECTS, 2nd Level Degree, Physics)
- Fluid and Plasmas Physics (6 ECTS, 2nd Level Degree, Physics)
- Fission and Fusion Nuclear Plants (9 ECTS, 2nd Level Degree, Engineering)
- Energy Technology and Economics (9 ECTS, 2nd Level Degree, Engineering)

- Thermonuclear Fusion (6 ECTS, 2nd Level Degree, Engineering)
- Industrial Applications of Plasmas (6 ECTS, 2nd Level Degree, Engineering).

6.2 *Information to the public*

The public information activity developed in continuity with the tasks opened in 2016 and in collaboration with ITER IO and F4E communication offices and EUROfusion Public Information network. Within this framework of collaboration, on 22-23 May 2017, Consorzio RFX participated in the 3rd EUROfusion FuseCOMM meeting in Madrid: a specific topic in the agenda was dedicated to the presentation of the main social and economic objectives and results in energy scenarios research, with the Consorzio RFX contribution.

On 5 May 2017, the II^o meeting on the NBTF visibility project was held in Barcelona among IO, F4E and the Consorzio RFX responsables of the communication to check the progress of the activity and coordinate future actions.

The information activity developed along two main lines of activities:

- production of information content;
- outreach and communication initiatives.

6.2.1 **Production of information content**

In 2017 Consorzio RFX accurately recorded in pictures and documented in video clips the major activities carried out on the NBTF and RFX-mod sites. In particular two professional reportages were produced by Enrico Sacchetti, New Scientists photographer, and the Overfly team, with clicks and video by drone.

Two time-laps cameras were installed in MITICA, to record the progress of MITICA HVBA assembly (the footage was shared on the Dropbox™ platform) and of MITICA assembly inside the bio shielding. The material was made available and shared among the partners involved, on the common digital platforms.

The NBTF timeline schedule was translated into a communication timeline and a new brochure on the NBTF projects was produced and finalized, together with posters of SPIDER and MITICA components and 2 posters on NIO1 experiments.

Concerning the RFX-mod activity, a significant contribution was provided for the participation to the action 1.1.4 "Call for support for research and development projects developed by Regional Innovative Networks and Industrial Districts" promoted by the Veneto Region in the framework of POR FESR 2014-2020, the European funding

scheme for regional development, in view of a financial support to the RFX-mod2 improvements.

6.2.2 *Outreach and communication initiatives.*

The activities were coordinated within a science and society programme including tours and visits to the facilities, round tables, open days and events which got a significant public response.

Great effort continued to be dedicated to schools: 1008 students (see Fig. 6.2.1) visited the laboratory in 2017, receiving a preliminary introduction into energy scenarios and fusion as a possible energy option for the future. The "Porto la fusione alla maturità" ("I bring fusion to maturity") project developed into a citizen science project; a poster was presented at the 1st Italian Citizen Science Conference in Rome ⁶⁶

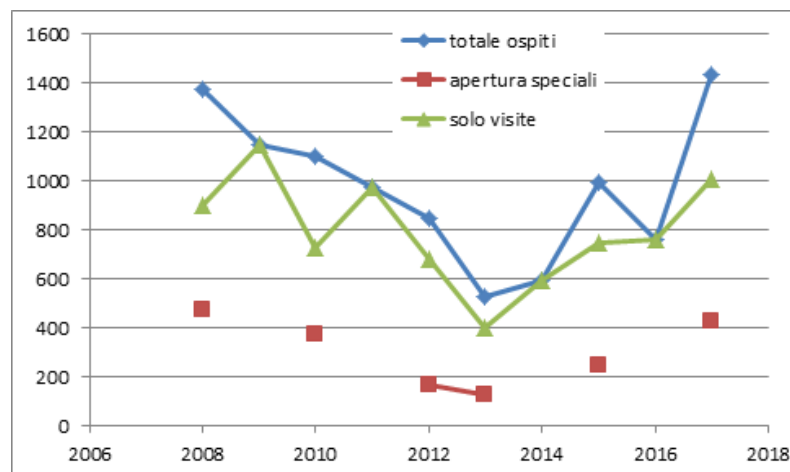


Fig. 6.2.1 Distribution of visitors to Consorzio RFX 2008-2018

The activity for the Consorzio RFX new website could start only in June. In July the technical specifications for the call for tender were finalized and the call was launched soon after. Due to the Summer holiday period, no offers arrived in time and a second call was launched in September.

The evaluation of the offers is underway.

Socials media were implemented: in particular in *Facebook*TM the average number of visualizations is increasing and today is around 500 per post and the number of followers has significantly increased up to 425 in 6 months activity. Please note the post "Bake off on fusion" which got 1155 visualizations. The followers in *Instagram*TM are around 70 (in few months): much effort will be put in order to contact the young.

⁶⁶ R. Piován, F. Auriemma, M. Dalla Palma, MT. Orlando, MG. Romanelli "High school students having the chance to be authors of scientific presentations on nuclear fusion", First Italian Citizen Science Conference, Roma (2017).

6.2.3 *Events and media coverage*

- “Visit of ITER Deputy Director General GS Lee “ - 20 January 2017. The event was covered by Mattino di Padova, and Gazzettino, reported on Facebook, Instagram and Twitter™.
- “Articolo 9 project” – 17 February 2017 (footage produced and published by CNR), article on Gazzettino on 19 February 2017.
- Article on Corriere del Veneto (Imprese) on 13 March 2017.
- “MEMEX” RAI shot on NBTF site and RFX-mod facility – with a 3m video dedicated to NBTF and RFX-mod, available at <http://www.raiscuola.rai.it/articoli-programma-puntate/memex-i-luoghi-della-scienza-padova/37209/default.aspx>
- “Women’s day” , RAI on air on 15 April 2017
- “Galileo Festival” on 11-13 May 2017, promoted by university of Padova and Sole 24 Ore Newspaper.
- Article on Mattino di Padova on 11 May 2017,
- <http://mattinopadova.gelocal.it/regione/2017/05/11/news/iter-rfx-sogno-da-15-miliardi-asse-con-francia-1.15321798?ref=search>
- Article on Avvenire newspaper, to be included in a large publication on fusion research in Padova.
- Article on New Scientist magazine of 3 June 2017
- “European Night of Research 2017” on 30 September 2017 with a round table on radio live streaming among ENEA Frascati, Radio Libera (<https://www.radioliberatutti.it/>) and Consorzio RFX; visits to NBTF of public reaching the site by shuttle buses provided by Consorzio RFX; and participation to the open day of the CNR Area. N.3 RAI shooting during TG Scienza programme
- “ITER Media Day” – live streaming from NBTF site with journalists worldwide convened in ITER.
- “Celebration of the completion and delivery of the Japanese components for the ITER Neutral Beam Test Facility (NBTF)” – with the participation of ITER Deputy Director General GS Lee and Yoichi Ito, Deputy Minister of the Japanese MEXT.
- Delivery of SPIDER Beam Source – end of procurement event on 19 December 2017.